Universidade de São Paulo
Instituto de Física

Aspectos de emaranhamento, caos e complexidade: dos sistemas de muitos corpos aos de altas energias

Daniel Lombelo Teixeira Júnior

Orientador: Prof. Dr. Diego Trancanelli

Diego Trancanelli

Tese de doutorado apresentada ao Instituto de Física da Universidade de São Paulo, como requisito parcial para a obtenção do título de Doutor em Ciências.

Banca Examinadora:
Prof. Dr. Diego Trancanelli - Orientador (IF-USP)
Profa. Dra. Bertha María Cuadros Melgar (EEL-USP)
Prof. Dr. Bruno Geraldo Carneiro da Cunha (CCEN-UFPE)
Prof. Dr. Dmitry Melnikov (IIP-UFRN)
Prof. Dr. Gabriel Teixeira Landi (IF-USP)

São Paulo
2021

FICHA CATALOGRÁFICA
Preparada pelo Serviço de Biblioteca e Informação
do Instituto de Física da Universidade de São Paulo

Teixeira Júnior, Daniel Lombelo

Aspectos de emaranhamento, caos e complexidade: dos sistemas de muitos corpos aos de altas energias. São Paulo, 2021.

Tese (Doutorado) – Universidade de São Paulo, Instituto de Física, Depto. de Física Matemática.

Orientador: Prof. Dr. Diego Trancanelli

Área de Concentração: Física

Unitermos: 1. Física Teórica; 2. Física Matemática; 3. Fisica da Matéria Condensada

USP/IF/SBI-017/2021

Universidade de São Paulo
Instituto de Física

Aspects of entanglement, chaos and complexity: from many-body to high energy systems

Daniel Lombelo Teixeira Júnior

Supervisor: Prof. Dr. Diego Trancanelli

Thesis submitted to the Physics Institute of the University of São Paulo in partial fulfillment of the requirements for the degree of Doctor of Science.

Examining Committee:
Prof. Dr. Diego Trancanelli - Supervisor (IF-USP)
Profa. Dra. Bertha María Cuadros Melgar (EEL-USP)
Prof. Dr. Bruno Geraldo Carneiro da Cunha (CCEN-UFPE)
Prof. Dr. Dmitry Melnikov (IIP-UFRN)
Prof. Dr. Gabriel Teixeira Landi (IF-USP)

São Paulo
2021

Aos meus pais e à minha irmã.

Agradecimentos

O presente trabalho foi realizado com apoio do CNPq, Conselho Nacional de Desenvolvimento Científico e Tecnológico - Brasil, e da Fundação de Amparo à Pesquisa do Estado de São Paulo (FAPESP), processo n^{0} 2017/02300-2. Um duplo obrigado pelo apoio financeiro.

Estruturar o reconhecimento de alguns atores que integraram esta peça intitulada tese de doutoramento neste formato, nesta simples página de texto, é perverter o próprio significado do agradecimento que gostaria de fazer, para além das práticas acadêmicas. Sobre tal colocação, alguém não perderia a oportunidade de recomendar o ensejo de sonhos que aliviem o cérebro dos futuros mortos, quando-onde me incluo. Como quase sempre, devo reconhecer que, nas devidas proporções, me parece uma ótima observação fora de contexto e um péssimo conselho. Portanto, como quase sempre, vou abraçá-lo, junto da impossibilidade em questão, reconhecendo também outra falta: a de palavras que expressem o real agradecimento às pessoas que transformaram o processo de produção destas páginas em uma tarefa menos alienante. Destaco aqui alguns militantes dessa causa que ocupam meu pensamento neste momento:

Pais e irmã: o agradecimento a vocês é atemporal;

Do "cenário IFUSP" – Alex, Caio, Carlos, Diego, Felipe, Gabriel, Gian, Giulio, Laura, Leo, Levy, Márcia e Renato: com quem compartilhei estudos, insultos, bebidas, pesquisas, viagens, filmagens, dilemas, poemas, frustrações, reflexões, diversões, revisões, opressões... e sambas;

Diego que, para além dos enredos acima, atuou também no papel de orientador, sem o qual esta tese não existiria. Aproveito e agradeço a outros colegas/professores que também foram orientadores no trabalho e fora dele: David, Gian e Pramod;

Felipe, pelas conversas intermináveis, delirantes ou não, pela companhia domiciliar, nos cafés de madrugada e nas cervejas de manhã. Nunca esquecerei do seu beijo;

Andresa, pois cicatrizes são coisas passadas que não se foram;

Márcia, pelas sessões não-pagas de terapia. Por ter carregado em espírito, e às vezes fisicamente, a Náusea;

Paula, por ser uma constante nesta tragicomédia que já dura uma década e meia. Quaisquer tentativas de traduzir isso em significantes só resultam em frustrações. Obrigado por nunca ter me perguntado sobre física, por sempre me fazer sentir bem e mal e vice-versa e, obviamente, pelas ótimas receitas de coquetéis;

Lislie, também a última a saltar no barco da neurose durante a irônica trégua no interregno. Obrigado, não sei por quê!

"Cada qual cuide de seu enterro, impossível não há"
(Frase derradeira de Quincas Berro D'água)
— *A Morte e a Morte de Quincas Berro D'água*, Jorge Amado

Resumo

A determinação de estruturas que podem emergir a partir das interações entre os constituintes de um sistema quântico de muitos corpos é uma tarefa fundante da física da matéria condensada. Uma das propostas mais avançadas nesse paradigma, historicamente motivada pelo princípio holográfico e pela correspondência AdS/CFT, é a geração holográfica do espaço-tempo em alguns sistemas caóticos, fortemente correlacionados, com certos padrões de emaranhamento e complexidade quântica. Como parte desse cenário, esta tese é dedicada à análise de alguns conceitos relevantes em tal proposta, onde são aplicados separadamente para alguns modelos com estrutura de rede. Concretamente, o assunto é dividido em três estudos principais: primeiro, o cálculo da complexidade de estados em função do tempo para o modelo de Ising com um campo transverso oscilante, onde estabelecemos a eficácia dessa quantidade na detecção de transições de fase quânticas de não-equilíbrio. Nossos resultados proporcionam pistas para entender como características universais são capturadas pela complexidade quando fora de equilíbrio. Segundo, a derivação de uma cota superior na produção de entropia de emaranhamento para uma classe de circuitos quânticos unidimensionais com dinâmica periódica. Um exemplo de circuito que satura essa cota é composto de portões-SWAP paralelos atuando em pares emaranhados. A partir de desigualdades obedecidas pela entropia, somadas à considerações sobre emaranhamento muiltipartite, indicamos que o efeito de uma dinâmica caótica não pode resultar em um aumento da taxa de produção de emaranhamento. Terceiro, a construção de uma classe de sistemas de muitos corpos supersimétricos utilizando semigrupos simétricos inversos. Para *toy models* particulares gerados com essa estrutura, estudamos algumas questões a respeito de fases supersimétricas, integrabilidade, desordem, propagação da informação quântica e localização de muitos corpos. Por fim, além desses três trabalhos, incluímos um ensaio abordando o problema de espaços holográficos emergentes a partir de teorias de campo conformes em duas dimensões, em que a mediação entre as duas partes é feita utilizando uma estrutura Riemanniana definida no espaço de Hilbert da teoria de campos.

Palavras-chave: Transições de fase quânticas; Complexidade quântica; Caos quântico; Dinâmica do emaranhamento; Geometrias emergentes

Abstract

The determination of structures that can emerge out of the interactions among the constituents of a quantum many-body system is a foundational task of condensed matter physics. One of the most advanced proposals within this paradigm is the holographic generation of spacetime in some strongly coupled chaotic systems with particular patterns of entanglement and quantum complexity, which is historically motivated by the holographic principle and by the AdS/CFT correspondence. As a part of this scenario, this thesis is dedicated to the analysis of some concepts that are relevant to such proposal, where they are separately applied to some lattice models. Concretely, the matter is divided into three main studies: first, the calculation of the time-dependent circuit complexity in the Ising model with a periodically driven transverse field, where we establish the effectiveness of this quantity for the detection of nonequilibrium quantum phase transitions. Our results provide hints for understanding how universal features out of equilibrium are captured by the complexity of quantum states. Second, the derivation of a bound on the maximal rate of entanglement entropy production for a class of one-dimensional quantum circuits with periodic dynamics. An example of a circuit that saturates the bound is composed by parallel SWAP gates acting on entangled pairs. Out of inequalities obeyed by the entropy, in addition to considerations on multipartite entanglement, we indicate that the effect of a chaotic dynamics cannot result in the increase on the rate of entanglement production. Third, the construction of a class of supersymmetric many-body systems using symmetric inverse semigroups. For particular toy models built out of this structure, we study some questions regarding supersymmetric phases, integrability, disorder, spreading of quantum information and many-body localization. Finally, besides those three works, we include an essay addressing the problem of emergent holographic spaces out of two-dimensional conformal field theories, where the mediation between the two parts is performed by means of a Riemannian structure defined in the Hilbert space of the field theory.

Keywords: Quantum phase transitions; Quantum complexity; Quantum chaos; Entanglement dynamics; Emergent geometries

Contents

List of Figures

Introduction

"The ability to reduce everything to simple fundamental laws
does not imply the ability to start from those laws and reconstruct the universe."

— *More is different*, P. W. Anderson

The first experimental observation of the finite relative speed of propagation due to quasiparticle pairs in a quantum many-body system dates to one decade ago [1]. The inaugural experiment realizes a quantum quench in a one-dimensional quantum gas in an optical lattice. It then studies the subsequent spreading of correlations between entangled pairs that emerge at all sites and propagate ballistically in opposite directions. The report on an effective "speed of light" that leads to an upper bound on the propagation of correlations confirms the theoretical conception of an emergent light cone for quantum dynamics, a result that was derived forty years earlier by Lieb and Robinson [2]. Experimentally, the work performed by Cheneau *et al.* [1] can be regarded as an unfolding of the cold atoms experiments initiated by Greiner *et al.* [3]. The latter sets up a turning point on the manipulation and control of atomic systems, where the practical realizations of effectively closed many-body dynamics became feasible, resulting on the actual simulation of models that were once designed to explain low energy physics of highly complex systems. The former represents a gathering of concepts from condensed matter physics and quantum information under an ongoing synthesis that flows to the development of quantum materials together with prospects towards the engineering of quantum computers.

The experimental determination of the Lieb-Robinson velocity is part of a wider movement. In the field of many-body physics, the traditional understanding of phase transitions based on symmetry breaking – at classical [4] and quantum [5] levels – was enhanced by geometrical formulations assimilated from quantum information science. This has opened the door for important discoveries including, for instance, a whole category of order in quantum phases of matter – the so-called topologically ordered phases[1]. In due course, the intertwine of these ideas has also brought to existence new areas of research, such as topological quantum computation [7], which theoretically bypass several problems of stability in the encoding and processing of quantum information. The merge of condensed matter physics and quantum computing that started taking place within the last two decades can be thought of as a prelude for a more general paradigm shift. In the context of high energy physics, the analogous process was sparked by the Black Hole Information Problem [8, 9], however reaching its maturity after the holographic principle [10, 11] and the AdS/CFT correspondence [12]. Some initial representative facts in this direction were the connection between the entanglement entropy in a quantum field theory and the area of minimal surfaces in gravity [13, 14], proposed by Ryu and Takayanagi, and the essays of Van Raamsdonk [15, 16], where entanglement was identified as the glue binding the bricks of spacetime geometry. In the past few years, such developments single out a special quantum mechanical system – the Sachdev-Ye-Kitaev (SYK) model [17] – which is thought to holographically describe quantum aspects of black holes. This is a solvable model, tractable even in its strongly interacting limit, that incarnates the underlying movement we are describing through a link between quantum chaotic many-body systems and quantum gravity.[2]

The conceptual interplay of the areas mentioned above is no longer a tendency only and it has already acquired life of its own. At the front line of this development, it follows the idea that spacetime can be interpreted as a qualitative new emergent phenomenon, holographically generated due to quantitative accumulation of increasingly complex patters of entanglement in chaotic systems. This is under scrutiny not only theoretically, but it has also initiated proposals on the experimental counterpart [21]. The latter is the missing link that can provide a synthesis of all those theories and establish the era of "quantum gravity in the lab".

[1] We refer to [6] for a review both on the entanglement between condensed matter and quantum information theories and on the subject of topological phase transitions.

[2] Some reviews on the SYK model and its relation to black holes include [18, 19, 20].

Organization of the thesis

The thesis is divided into two main parts: a walk-through of the sketchy scenario presented above from a theoretical perspective and a compendium of studies related to the underlying topics.

Chapter 1 is devoted to the first part. It contains the main concepts that will show up in the subsequent chapters. In particular, it can be regarded as a lift (or dive, depending on the point of view) from quantum many-body systems to quantum gravity – in the sense of the AdS/CFT correspondence – crossing conformal field theories.

A word of warning regarding Chapter 1: the large amount of material involving the themes in question reflects a particular choice to proceed in the presentation. Different levels of precision are encountered throughout the exposition, including some disruptions whenever the necessary apparatus becomes more demanding. The great deal of footnotes aims to avoid lots of detours in the main narrative.

The second part is composed by the remaining chapters:

In Chapter 2, we apply the concept of circuit complexity to analyze nonequilibrium quantum phase transitions driven by a periodic field in the transverse field Ising model. We further identify a universal behavior of the time-dependent complexity which is manifest at early times. The study is supplied by some evidences regarding the use of circuit complexity to diagnose additional types of critical behavior, in particular dynamical quantum phase transitions. This chapter is based on [22].

Chapter 3 deals with the role played by chaos in the spreading of quantum information for one-dimensional quantum circuits with periodic dynamics. We derive a bound on the rate of entanglement entropy production as a function of time for this class of models and present an example of a system that saturates this bound: a circuit composed of parallel SWAP gates acting on entangled pairs. This chapter is based on [23].

In Chapter 4, we construct a supersymmetric many-body chain out of an algebraic structure called symmetric inverse semigroups. The method consists in associating a supercharge at each lattice site mirroring the case of spin chains. We discuss how to obtain supersymmetric phases of matter for some choices of supercharges. Furthermore, we introduce disorder in a particular toy model and then show that it describes a many-body localized phase. Such conclusions are drawn from the early-time behavior of an out-of-time-ordered correlation function. This chapter is based on [24].

Chapter 5 addresses the problem of emergent three-dimensional anti-de Sitter geometries out of two-dimensional conformal field theories. By introducing a geometric structure in the Hilbert space of the conformal field theory via the concept of Fubini-Study distance between states, we sketch how one could obtain the metric of an asymptotically anti-de Sitter space.

1

From many-body systems to quantum gravity

"Se o desenvolvimento não passa da repetição da mesma fórmula, a ideia, embora para si bem verdadeira, de fato fica sempre em seu começo."

— *Fenomenologia do Espírito*, Hegel.

Our analysis starts with a closed quantum many-body system. The most basic structure we will assume due to the *quantum* nature of the problem is a hamiltonian quantum system $(\mathcal{H}_\Lambda, H_\Phi)$. The Hilbert space $\mathcal{H}_\Lambda$ is associated with a set of points or vertices Λ on a graph $\Gamma = (\Lambda, E)$ and it admits a tensor product structure; the set of edges $E \subset 2^\Lambda$ contains pairs of vertices $\{\{x, y\} \,|\, x, y \in \Lambda \text{ and } x \neq y\}$. The hamiltonian H_Φ is built from an interaction map Φ that associates a bounded operator $\Phi(X) \in \mathcal{B}(\mathcal{H}_X)$ for every subset $X \subset \Lambda$:

$$\mathcal{H}_\Lambda = \bigotimes_{x \in \Lambda} \mathcal{H}_x, \qquad H_\Phi(\Lambda) = \sum_{X \subset \Lambda} \Phi(X). \tag{1.1}$$

This pair is the mathematical setup for a myriad of physical systems. One common example is that of a system of qubits, where $\mathcal{H}_x = \mathbb{C}^2$ represents a single one.

1.1 Locality

The word *many* in the title suggests that the number of local Hilbert space factors $\mathcal{H}_x$ in (1.1) will eventually be taken to be large, posing a mathematical question regarding the existence of the infinite tensor product. In this so-called thermodynamic limit we are faced with the possibility of the emergence of new qualitative aspects due to the accumulation of quantitative effects, a dialectical character of condensed matter systems synthetized for instance in Anderson's manifesto [25] – "*more is different*". The determinations of such collective phenomena presuppose our ability to distinguish the whole from its parts. For our purpose it will suffice to proceed as follows[1]:

1. to decompose the lattice as $\Lambda = X \cup \overline{X}$ and therefore to induce a splitting on $\mathcal{H}_\Lambda = \mathcal{H}_X \otimes \mathcal{H}_{\overline{X}}$;

2. to require physical observables $\{\mathcal{O}\}$ to take the above bipartite form, $\mathcal{O} = \mathcal{O}_X \otimes \mathbb{1}_{\overline{X}}$;

3. the cardinality of X should be bounded by a real number, $|X| \leq R$, such that $\mathcal{O} \in \mathcal{B}(\mathcal{H}_X)$: this means $\mathcal{O}_X$ is a bounded operator with support $\mathcal{H}_X$.

Operators that act on the Hilbert space according to the above conditions give us the notion of a quasi-local algebra of observables, which tackle the problem of the thermodynamic limit from a mathematical point of view. To complete our characterization, we rely on a physical fact extracted from the role played by interactions on the stability of matter: their range cannot be arbitrarily long[2]. We will use this content in a simplified form by postulating a sharp cut-off on interactions. Explicitly, this can be done by first introducing a graph distance[3] on Γ, d_Γ: take two vertices $x, y \in \Lambda$ and define path of length ℓ between x and y as the set of ℓ adjacent intersecting edges E_i starting on the former and ending on the latter, that is,

$$\{E_i\}_{i=1}^{\ell} \equiv p_\ell(x,y) \text{ with } x \in E_1,\ y \in E_\ell \text{ and } E_i \cap E_{i+1} \neq \varnothing. \quad \text{Then } d_\Gamma(x,y) = \min_\ell p_\ell(x,y).$$

The above concepts are illustrated in Figure 1.1. Next, we require the diameter of $X \subset \Lambda$ to be

[1] The rigorous approach to the matter was developed in the fundamental work of von Neumann [26], however we only appropriate its lessons in a formal way, keeping in mind that the content is well established for the many-body systems under consideration in this chapter.

[2] In [27], Lieb accounts for the stability of matter from first principles and introduces a rigorous version of screening in order to guarantee the existence of the thermodynamic limit. The range of interaction is the central concept of his analysis.

[3] One of the motivations to define the many-body system on a graph is the possibility to carry out a general discussion independent of dimensionality. However, the notion of distance allows one to introduce the dimension of a graph as follows: consider a a ball of radius s – the set of all points with distance s starting from some specific point; if the number of points within such a ball scales as s^D for all graph points, we call D the graph dimension.

bounded by a real number,

$$\operatorname{diam} X \equiv \max_{x,y\in X} d_\Gamma(x,y) \leq r\,.$$

The introduction of the two parameters, R and r, in the original structure leads us to the concept of an (R,r)-local quantum system[4]. Locality is an outcome of our analysis of the thermodynamic limit as a necessity both for mathematical consistency and from physical observations and it already contains, in a hidden way, multiple features of the quantum many-body system, as we will now proceed to expose.

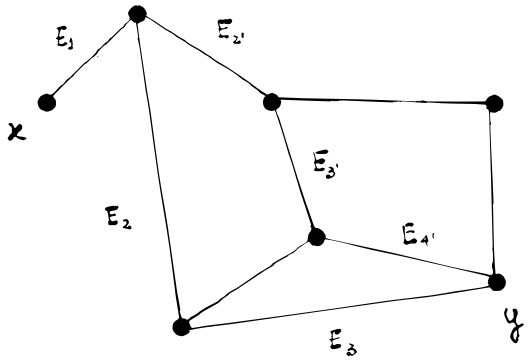

Figure 1.1: Example of a graph where the edges contain two points only. Two examples of paths from x to y of length three and four, respectively, are given by $\{E_1, E_2, E_3\}$ and $\{E_1, E_{2'}, E_{3'}, E_{4'}\}$.

1.1.1 Lieb-Robinson bounds

The kinematical facts about interactions implied in this chapter are that:

1. They are hermitian;
2. They obey the action of spatial translations τ_a, where a is a lattice spacing, in the expected way, $\Phi(X+a) = \tau_a\Phi(X)$.

Let us turn to dynamical considerations derived from interactions $\Phi(X) \in \mathcal{B}(\mathcal{H}_X)$. The dynamics is the one-parameter group of automorphisms, $\{\tau_t^\Phi\}_{t\in\mathbb{R}}$,

$$\tau_t^\Phi(\mathcal{O}) \equiv \mathcal{O}(t) = e^{\mathrm{i}tH_\Phi(\Lambda)}\mathcal{O}e^{-\mathrm{i}tH_\Phi(\Lambda)}. \tag{1.2}$$

The main character responsible for the unfolding due to locality will be the theorem of Lieb and Robinson [2]: for each finite range interaction Φ, and for all local observables $\mathcal{O}_A$ and $\mathcal{O}_B$, there exists

[4] Informally, R stands for how many bodies interact while r tells how far apart they are. For instance, the Ising model on a N-site chain, $\Lambda = \{1,\ldots,N\}$, with nearest neighbor interactions is described by

$$-H_{\text{Ising}} = \sum_{d(x,y)=1} Z_x Z_y + h\sum_{x=1}^{N} Z_x,$$

where Z_a is the Pauli-z matrix at site a and h is a constant. This is an example of a $(2,1)$-local system.

a finite group velocity v_Φ and a strictly positive function μ such that

$$\lim_{\substack{|t|\to\infty \\ |x|>vt}} e^{\mu(v)|t|}\|[\mathcal{O}_A(0,t),\mathcal{O}_B(x,0)]\| = 0, \qquad \text{for } v > v_\Phi. \tag{1.3}$$

The interpretation of this result gives rise to the first emergent property following from locality: it says that even in nonrelativistic systems the global effect of many particles together brings to existence a "light-cone", $x = v_\Phi t$, outside of which the norm of the commutator between local observables decays exponentially with time, therefore bounding the propagation of correlations. At least formally, this result can be interpreted as a fuzzy notion of causality[5] associated with a new parameter depending on the interactions and on the lattice structure only, the so-called *Lieb-Robinson speed*: $v_\Phi = \min v$ for which (1.3) holds. While the value of v_Φ depends on the model through the particularities of H_Φ, the existence of a light-cone does not and it holds for any local lattice model with bounded interactions.

Let us discuss a few determinations inherited by the many-body system due to the Lieb-Robinson bound that will play an important role in what follows[6]. Here A and B are chosen to be two non-overlapping regions where $\mathcal{O}_A$ and $\mathcal{O}_B$ act. Then:

- Exponential clustering of correlations [29, 30]: if the ground state is unique and if there is a gap $\Delta > 0$, then the correlations decay exponentially. More precisely,

$$|\langle \mathcal{O}_A\, \mathcal{O}_B\rangle - \langle \mathcal{O}_A\rangle \langle \mathcal{O}_B\rangle| \leq c \exp\left(-\frac{d_\Gamma(A,B)}{\xi}\right), \tag{1.4}$$

  where $d_\Gamma(A,B)$ is the distance between the support of $\mathcal{O}_A$ and the support of $\mathcal{O}_B$, and the constant c depends on $\|\mathcal{O}_A\|$, $\|\mathcal{O}_B\|$ and on $d_\Gamma(A,B)$. For completeness, the gap Δ is a finite number that exists in the thermodynamic limit $N \to \infty$ and it provides a lower bound for the energy separation between a finite number of lowest energy states which are infinitesimally close to all other states.

  Moreover, this result gives rise to the concept of a *correlation length* $\xi > 0$, which intuitively emerges from the time scale set by the gap Δ^{-1} multiplied by Lieb-Robinson speed. The correlation length is a function of the Lieb-Robinson speed, of the gap and of the lattice spacing a only, $\xi(v_\Phi, \Delta, a)$ – all physical quantities depending on the hamiltonian. Its particular form will not be important to us here but rather generally ξ is linearly proportional to v_Φ and inversely proportional to both Δ and a.

[5] To get the proper light-cone with $v_\Phi = c = 1$ typical of relativistic theories one would be required to take the lattice spacing to zero, so that (1.3) should become a version of $[\phi(x,t),\phi(0,0)] = 0$ for a field ϕ at spacelike distances, $x > t$.

[6] There is a number of consequences, improvements and generalizations of the Lieb-Robinson theorem that would take us too far to expose. For reference, some of them are collected in [28].

The next results were all derived in [31]:

- The amount of quantum information that can be sent from A to B outside the light-cone is exponentially small.

- Define a truncated operator supported on a subset of $\mathcal{H}_A$ of length ℓ,

$$\mathcal{O}_A^\ell(t) = \frac{1}{\dim(\chi)} \mathrm{Tr}_\chi \left(\mathcal{O}_A(t)\right) \otimes \mathbb{1}_\chi, \tag{1.5}$$

  where $\chi = \{x \in \Lambda;\, d_\Gamma(x, A) > \ell\}$. While $\mathcal{O}_A(t)$ will develop full support on the whole Hilbert space for any $t > 0$, the Lieb-Robinson bound implies that such an operator will affect only a region with support $\ell = v_\Phi t$. Indeed, it can be shown that the error in the approximation by the truncated operator is given by [32]

$$\|\mathcal{O}_A(t) - \mathcal{O}_A^\ell(t)\| \leq \frac{v_\Phi |t|}{\ell} f(\ell)|A|\|\mathcal{O}_A\|, \tag{1.6}$$

  where $f(\ell)$ decays exponentially with ℓ. The proof involves writing the truncated operator as an average over the unitary operators U acting on χ,

$$\mathcal{O}_A^\ell(t) = \int \mathrm{d}\mu(U) U \mathcal{O}_A(t) U^\dagger, \tag{1.7}$$

  where μ is the Haar measure for U, and then applying the Lieb-Robinson bound to the commutator $[U, \mathcal{O}_A(t)]$ to show that

$$\|\mathcal{O}_A(t) - \mathcal{O}_A^\ell(t)\| \leq \int \mathrm{d}\mu(U) \|[U, \mathcal{O}_A(t)]\| \leq \tilde{c} \exp\left(-\frac{\ell - v_\Phi|t|}{\xi}\right), \tag{1.8}$$

  Furthermore, this result can be used to bound $\langle \mathcal{O}_A(t)\mathcal{O}_B(t)\rangle_c \equiv \langle \mathcal{O}_A(t)\, \mathcal{O}_B(t)\rangle - \langle \mathcal{O}_A(t)\rangle \langle \mathcal{O}_B(t)\rangle$, the connected correlation function at time t, where the expectation value is taken in a state with finite correlation length:

$$|\langle \mathcal{O}_A(t)\mathcal{O}_B(t)\rangle_c| \leq \bar{c} \exp\left(-\frac{\ell - 2v_\Phi|t|}{\bar{\xi}}\right). \tag{1.9}$$

  It is then shown that there is also a maximum speed at which correlations can be build up.

- We now consider the effect of a time-dependent hamiltonian over a finite time. Let us take $B = \Lambda \backslash A$ and a class of hamiltonians of the form

$$H_\Phi(t) = H_A(t) + H_B(t) + \sum_{k=1}^{M} \alpha_k(t) \mathcal{O}_A^k \otimes \mathcal{O}_B^k, \tag{1.10}$$

  where α_k are interaction amplitudes. The discussion around (1.6) implies that the number of terms M is proportional to the perimeter of A. The amount of entanglement that can be created per unit

of time between regions A and B obeys the following inequality:

$$\frac{\mathrm{d}S(\rho_A)}{\mathrm{d}t} \leq c \sum_{k=1}^{M} |\alpha_k(t)|, \tag{1.11}$$

where c is a constant and $S(\rho) = -\operatorname{Tr}(\rho \log \rho)$ is the von Neumann entropy of the state ρ[7]. Here $\rho_A = \operatorname{Tr}_B \rho$ is the reduced state obtained by tracing out from the global density operator ρ, the degrees of freedom that do not belong to A – the so-called partial trace –, leading to the *entanglement entropy*, that is, the von Neumann entropy of the reduced state. For interactions bounded by a constant $\max_{k,t} |\alpha_k(t)| \leq \phi$, one can take one step further and integrate the previous equation to obtain

$$S(\rho_A(t)) - S(\rho_A(0)) \leq c \int_0^t \mathrm{d}t' \left(\sum_{k=1}^{M} |\alpha_k(t')| \right) \leq c\phi M t, \tag{1.12}$$

which reveals that the entanglement growth over some finite time scales as the perimeter of A, in opposition to what one would expect from thermodynamical considerations – an extensive behavior, that is, a typical "volume law".

1.1.2 Entanglement entropy and the area law

Even though the appearance of the entanglement entropy on stage may seem abrupt and without proper presentations, its part in the storytelling will be decisive for a major plot twist. For purposes of the narrative we choose to keep the mystery for the moment and to reveal the properties of $S_A \equiv S(\rho_A)$ as needed for the development of the following scenes.

The scaling of the entanglement entropy with the perimeter of the region where the reduced state is defined motivates us to take a closer look at what is going on at the boundary of A,

$$\partial A = \{x \in A \,|\, \exists\, y \in \Lambda \backslash A \quad \text{such that} \quad d_\Gamma(x, y) = 1\}. \tag{1.13}$$

The hint to explain why the boundary area shows up in (1.12) comes from the clustering of correlations in gapped systems (1.4): due to exponential decay of correlation functions, one is led to suspect that only the degrees of freedom near the boundary may entangle – those inside with the nearby outside ones. Indeed, we will see that this is exactly the case through an example for one-dimensional systems[8].

[7] We use the words "state" and "density operator" interchangeably. Obviously one can always build a density operator $\rho = |\psi\rangle\langle\psi|$ from a given state $|\psi\rangle$.

[8] There is a need for an insert to clarify the choice regarding the examples adopted in this chapter, which mostly concern one-dimensional lattice models. First, these are the best understood cases where rigorous results exist. Second, since all the works to be presented in Chapters 2-4 also deal with one-dimensional models, we will focus on such cases.

For one-dimensional gapped systems with a unique ground state, finite range interactions with support on nearest neighbors and bounded interactions, that is,

$$H_\Phi = \sum_{\substack{x,y\in\Lambda \\ |x-y|=1}} \Phi(|x-y|), \qquad \|\Phi(|x-y|)\| \leq J, \quad \text{for some } J, \tag{1.14}$$

the *area law* can be rigorously stated as a theorem[9] [43]:

$$S(\rho_A^0) \leq S_{\max} = \mathcal{O}\left(|\partial A|\right). \tag{1.15}$$

Here ρ_A^0 is the reduced ground state on the interval A. Of course the boundary of a one-dimensional region contains two points only, and as a consequence $S_{\max}$ is just a constant – which can be computed as a function of the Lieb-Robinson speed and correlation length. The proof of the above theorem strongly relies both in the Lieb-Robinson bound (and its consequences) and in the exponential clustering of correlations, to wit, on locality and in the existence of a gap.

1.1.3 The quantum butterfly effect

As we have seen in Section 1.1.1, the commutator $[\mathcal{O}_A(0,t), \mathcal{O}_B(x,0)]$ can have a nonzero norm for any $t > 0$ and separation x, although this is a bounded quantity. Due to the Baker-Hausdorff-Campbell formula, $\mathcal{O}_A(0,t)$ will contain nested commutators with H of increasingly large support. Moreover, as long as the support of the two operators are connected at $t = 0$ through a path in the graph Γ, $\mathcal{O}_A(0,t)$ and $\mathcal{O}_B(x,0)$ will have overlapping support for any $t > 0$. One can measure this growth under Heisenberg evolution, called *operator growth*, by means of the radius of the operator $R[\mathcal{O}]$, defined as the minimal distance such that the support of $\mathcal{O}$ lies in a ball of such radius (up to an exponential tail).

Consider the radius of this commutator $R\left[[\mathcal{O}_A(0,t), \mathcal{O}_B(x,0)]\right] \equiv R_{AB}(x,t)$. This clearly dependents on a velocity $v = x/t$, nonetheless it can still be transformed into a (velocity-dependent) rate

$$v_S(v) = \lim_{t\to\infty} \frac{1}{t} R_{AB}(vt,t), \tag{1.16}$$

which is sometimes referred to as the *scrambling velocity*. We will address this terminology later[10]. It

[9] For higher dimensional versions there is no general proof, although the area law holds for systems that can be represented by *matrix product states* [33, 34]. There are rigorous proofs in specific cases, for instance for some quasi-free bosonic systems [35, 36, 37], fermionic sytems [38, 39, 40, 41] and disordered systems [42].

[10] Some of the concepts that will be exposed from now on are still under development and there is no general consensus on their definitions and interpretations, meaning that no theoretical results can be derived without clear statements. The following definitions and terminology are mainly based on [44].

is shown in [44] that

$$v_S \leq v_\Phi \,. \tag{1.17}$$

While it guarantees a finite speed for the propagation of information, the Lieb-Robinson bound is an algebraic statement about dynamics and it is independent of the state of the system. Equation (1.6) elucidates that the growth of $\mathcal{O}_A(t)$ cannot be arbitrarily fast, but it makes no reference to the rate of spreading as a function of the state upon which the operator acts. To probe this rate of growth we thus need an object that is more sensitive to the dynamics and that is able to capture how the universal determinations about propagation of information manifest in a particular state of the system.

We have already analyzed the commutator $[\mathcal{O}_A(0,t), \mathcal{O}_B(x,0)]$ by means of its norm and its growth under Heisenberg evolution. We now turn to yet another perspective. The following scenes will develop under the theme of the causal influence generated by local perturbations. The main stage will continue to be a local system. However, to address the previously mentioned occurrence, we will relax the state independent analysis of Lieb and Robinson and specialize to the case where the perturbation is probed within a subspace of many-body states. The next character to play a central role will be the so-called *out-of-time-ordered correlator* (OTOC)[11],

$$\mathcal{C}(x,t) \equiv \mathrm{Tr}\left(\rho\,[\mathcal{O}_A(0,t), \mathcal{O}_B(x,0)]^\dagger [\mathcal{O}_A(0,t), \mathcal{O}_B(x,0)]\right), \tag{1.18}$$

defined for $\mathcal{O}_{A,B}$ in the state ρ.

Let us approach (1.18) from a quantitative perspective. First of all, note that this quantity is bounded by the operator norm which is obtained by taking $\rho \sim \mathbb{1}$. Now, among the disguises assumed by the OTOC, the known results for the many models where it was computed can all be summarized in the following form [47, 48]:

$$\mathcal{C}(x,t) \sim \exp\left[-c_0 \frac{(x/v_B - t)^{\alpha+1}}{t^\alpha}\right] \equiv e^{\lambda(v)t}, \qquad \frac{x}{t} \to v_B^+. \tag{1.19}$$

We will have much to say about the two quantities that characterize the OTOC, $\lambda(v) = \lambda(v,\rho)$ and $v_B = v_B(\rho)$, but for now we just highlight that they are both state-dependent. The parameter α determines the OTOC for two categories of systems: those with many local degrees of freedom – such as large-N systems – have $\alpha = 0$ and spin lattice systems, for which in general $\alpha > 0$.

The limit that gives rise to the form of (1.19) can be understood as follows: fix $x = vt$ for some $v > v_B$, where $\mathcal{C}(vt,t)$ is small and then take $v \to v_B^+$; as an effect, the correlations between A

[11] The words OTOC are usually reserved to the four-point function $\langle \mathcal{O}_A(t)\mathcal{O}_B(0)\mathcal{O}_A(t)\mathcal{O}_B(0)\rangle$, which is one of the terms that appears in the expansion of $\mathcal{C}(x,t)$. Historically, this object was first introduced by Larkin and Ovchinnikov [45] in the context of semiclassical chaos and later rediscovered in the study of the firewall paradox [46]. For clarity in the exposition, we will skip the chronological route and leave this discussion for Chapter 4.

and B will build up to point where the given shape becomes prominent. In this process, we note the emergence of another cone $x = v_B t$ in the same spirit as the one underlying the Lieb-Robinson bound. As a matter of fact, since the operator norm bounds $\mathcal{C}(x,t)$, it follows that [44]

$$v_B \leq v_\Phi. \tag{1.20}$$

Let us take a step back and look at Eq. (1.3) closely. The function $\mu(v)$ bounds the exponential decay rate outside the light-cone. Analogously, one can mirror a similar role to be played by $\lambda(v)$ in Eq. (1.19). Building on this intuition and on the work of [49, 50, 51], Khemani *et al.* [47] proposed the identification of $\lambda(v)$ with a *velocity-dependent Lyapunov exponent* for generic many-body systems. Formally, one can define

$$\lambda(v) \equiv \lim_{t\to\infty} \frac{1}{t} \log \mathcal{C}(x = vt, t), \tag{1.21}$$

which gives the rate of change of the OTOC along a ray. Equipped with this concept, the reasoning behind the Lieb-Robinson speed allows us to further identify

$$v_B \equiv \sup_v \{v;\, \lambda(v) \geq 0\}. \tag{1.22}$$

The subscript "B" in v_B stands for "butterfly". This is motivated by the quantum version of the butterfly effect, whose classical version is captured by the exponential growth of the OTOC when $\alpha = 0$. The interpretation of the resulting *butterfly speed* as a state-dependent effective velocity and its relation to quantum chaos was initially put forward in [52]. Alternatively, for $\alpha > 0$ the wavefront representing the information spread will get broader as it propagates, leading to a sub-exponential growth. The concept of a butterfly speed applies whenever there is a positive quantum Lyapunov exponent, otherwise despite of its existence, the meaning has no resemblance with chaos, since a negative $\lambda(v)$ corresponds to some exponential decay of correlations outside the butterfly cone, $x = v_B t$. Equation (1.22) introduces us to a third emergent speed that follows from locality only. Unlike v_Φ, the state-dependence of v_B allows one to probe the effects of temperature, for instance, in the dynamics of quantum information.

To complement the characterization of the quantum butterfly effect, consider a localized amount of quantum information created by the action of a local operator. As the operator grows, this information may become more and more delocalized among the many-body states depending whether the system is chaotic or not. Eventually, the quantitative accumulation of this effect can therefore render a qualitative transition, when the initial information can no longer be probed by local measurements. This process connecting local and non-local is denominated *scrambling* and the time that it takes to happen is the *scrambling time*. We will come back to this topic on Chapter 4.

1.2 Quantum phase transitions and universality

The interplay between local and global that appeared in the beginning of our analysis returns once again, albeit in a different level. It is now mediated by the concept of correlation length, as we explain next. Besides the short-range correlations coming from the exponential decay on (1.4), there is the possibility that an infinite correlation length comes into play. This happens when the gap closes, such that the correlations do not decay exponentially, giving rise to the so-called *long-range order*. Note that taking ξ to infinity means the withdrawal of the emergent length scale. Of course another way to remove the length scale is to set it to zero, meaning a divergent energy gap. The two cases, $\xi = 0$ or $\xi = \infty$, describe *fixed points* of the *renormalization group flow* and they unveil a central property in the system – the *scale invariance* that exists at such special points due to the absence of a physical scale. One the one hand, a vanishing correlation length leads to an infinite energy gap and therefore it expresses a stable phase of a many-body system. On the other hand, a diverging correlation length, and therefore a vanishing gap, categorizes the system at criticality. The latter case will be our focus in what follows.

1.2.1 Scaling behavior of the correlation length

We have introduced several ideas without the proper analysis in the previous paragraph, so let us proceed by illustrating some of the notions in a concrete example. Consider a system close to a critical fixed point where the distance from it is parametrized by a coupling constant λ. This means that the hamiltonian can be split as

$$H_\Phi = H^*_\Phi + \lambda \mathcal{P}, \tag{1.23}$$

where $\mathcal{P}$ can be thought of as a local operator coupled with strength λ to a fixed point hamiltonian H^*_Φ – one that is invariant under scale transformations. Our reasoning is valid as long as the hamiltonian and its perturbation are time-independent. From dimensional analysis, one expects that $\xi = a\eta(\lambda)$, where a is the lattice spacing and $\eta(\lambda)$ is a dimensionless function, yet to be determined. At the fixed point, ξ is no longer part of the problem and, as a consequence, it should remain invariant under the rescaling of a – which intuitively means that we are looking either closer or farther away from the fixed point. This condition can be rephrased as

$$\frac{\partial \xi}{\partial \log a} = 0 = a\eta(\lambda) + a\frac{\partial \eta}{\partial \lambda}\frac{\partial \lambda}{\partial \log a}. \tag{1.24}$$

The differential equation for $\eta(\lambda)$,

$$\eta(\lambda) + \beta(\lambda)\frac{\partial \eta}{\partial \lambda} = 0, \qquad \beta(\lambda) = a\,\frac{\partial \lambda}{\partial a} \tag{1.25}$$

is a flow equation known as a renormalization group equation[12].

The β-function, $\beta(\lambda)$, characterizes a fixed point λ_* by $\beta(\lambda_*) = 0$. It follows immediately by integration of (1.25) and from linearly approximating the β-function close to the fixed point, $\beta(\lambda) \sim \beta'(\lambda_*)(\lambda - \lambda_*)$, that

$$\xi(\lambda_1) = \xi(\lambda_2) \exp\left(\int_{\lambda_1}^{\lambda_2} \frac{\mathrm{d}\lambda}{\beta(\lambda)}\right) \sim \xi(\lambda_2) \left(\frac{\lambda_2 - \lambda_*}{\lambda_1 - \lambda_*}\right)^{1/\beta'(\lambda_*)} . \tag{1.26}$$

When $\beta'(\lambda_*) > 0$, the perturbation $\mathcal{P}$ is called a *relevant operator* and the system will be driven away from the fixed point to a *phase*[13] – understood here as a sort of equivalence class of systems parametrized by λ that can be continuously deformed into each other – with finite correlation length. We can thus set the dilation from λ_* up to a point where the correlation length is given by the lattice spacing, $\xi(\lambda_2) \simeq a$, in order to write the previous equation as

$$\xi(\lambda) \sim a \left|\frac{\lambda_2 - \lambda_*}{\lambda - \lambda_*}\right|^{\nu} . \tag{1.27}$$

The gist is clear: as the fixed point is approached, the correlation length must diverge, $\lim_{\lambda \to \lambda_*} \xi(\lambda) = \infty$, with a power-law controlled by $\nu = 1/\beta'(\lambda_*)$. This quantity ν does not depend on the lattice-spacing a or even on the hamiltonian – and therefore on the microscopic details of the model. Thereby we have discovered a *universal critical exponent* of the correlation length, which can be thought as an example of how *universality* emerges from the *renormalization group*.

Let us now expand on the concept of a *quantum phase*. The inverse of the energy gap defines a time scale which can then be used to introduce a notion of slow deformations, in the sense of the motion taking place in the space of couplings. Although in this example we have only one coupling, λ, later on we will generalize the analysis. The equivalence class we mentioned in the previous paragraph is thus constituted by all states that can be adiabatically connected starting from any representative. More precisely, the error introduced by the deformation of a state can be made arbitrarily small by doing so slowly enough. With such premise, two states cannot be adiabatically connected when the gap closes, therefore they do not belong to the same phase[14].

[12] The concept of renormalization group and differential equations of this type, also called Callan-Symanzik equations – who presented a practical formulation in the context of particle physics [53, 54] – are certainly more general than we are sketching here. A polished understanding of the subject in the scope of condensed matter physics came from Kadanoff in terms of the so-called block-spin transformations [55] and later with major contributions from Wilson [56, 57, 58, 59].

[13] In classical statistical mechanics, the theorem determining a phase can be state as: 'if the free energy density exists, then it is an analytic function of its parameters except (possibly) for a domain of codimension-1'. The classical definition of a phase as a domain of analyticity of the free energy does not carry over to the quantum world. The main point is that classically all the expectation values of the observables can be written as some derivative of the free energy, while in quantum mechanics the expectation values are taken in some state.

The correlation length is purely derived from locality and its emergent determinations, however it captures the collective behavior that yield to one notion of order in a quantum many-body system and further categorize a *quantum phase transition* – when the metamorphosis from one phase into another is driven by quantum fluctuations alternatively to thermal ones. This situation, together with the symmetry (breaking) analysis of the hamiltonian has been the paradigm for describing the emergence of order in quantum many-body systems until two decades ago. The failure of two states belonging to the same phase, described in the previous paragraph, can be given a geometric interpretation in terms of a non-analytic curvature obtained after the introduction of a metric in the Hilbert space. We will develop this approach in what follows leading to a different point of view on the phenomena under consideration here.

1.2.2 Geometry of quantum phase transitions

We now turn to the rephrasing of the quantum phase transitions determinations by means of geometrical concepts in the Hilbert space.

Consider a family of hamiltonians $\{H(\lambda)\}$, where the parameters are points in some smooth manifold, $\lambda \in \mathcal{M}$. One important example is the manifold of coupling constants generated by introducing additional perturbations in (1.23). The distance between two nearby states induces a metric on the parameter space [61],

$$\|\psi(\lambda + \mathrm{d}\lambda) - \psi(\lambda)\|^2 = \langle \partial_a \psi | \partial_b \psi \rangle \, \mathrm{d}\lambda^a \mathrm{d}\lambda^b \equiv (\gamma_{ab} + \mathrm{i}\sigma_{ab}) \mathrm{d}\lambda^a \mathrm{d}\lambda^b = \gamma_{ab} \, \mathrm{d}\lambda^a \mathrm{d}\lambda^b, \tag{1.28}$$

where we have decomposed the Hermitian product into its real symmetric part, γ, and an imaginary antisymmetric piece, σ. As a matter of fact, γ is not an actual metric on $\mathcal{M}$, despite of being symmetric and transforming correctly under diffeomorphisms of the type $\lambda \to \lambda'(\lambda)$. The reason is that γ is not "gauge invariant". Specifically, by considering any representative on the ray of $|\psi(\lambda)\rangle$ one expects to get the same distance. Nevertheless, the choice of $|\psi'(\lambda)\rangle = e^{\mathrm{i}\alpha(\lambda)}|\psi(\lambda)\rangle$, leads to

$$\gamma'_{ab} = \gamma_{ab} - A_a \partial_b \alpha - A_b \partial_a \alpha + \partial_a \alpha \partial_b \alpha, \tag{1.29}$$

where

$$A_b(\lambda) = \mathrm{i} \langle \psi(\lambda) | \partial_b \psi(\lambda) \rangle \tag{1.30}$$

is called the Berry connection. The connection transforms itself as

$$A'_b = \mathrm{i} \langle \psi' | \partial_b \psi' \rangle = A_b - \partial_b \alpha. \tag{1.31}$$

[14] This heuristic explanation can be put in more rigorous terms by means of the Adiabatic theorem and its geometrical consequences. We refer the reader to Sections 2.1.2 and 2.1.3 of [60] for the details.

With this observation, it is possible to define a gauge invariant metric as

$$g_{ab} = \gamma_{ab} - A_a A_b. \tag{1.32}$$

This metric measures distances between rays, not states. One can also write g and σ in terms of the so-called Fubini-Study metric,

$$Q_{ab} \equiv \langle \partial_a \psi | \partial_b \psi \rangle - \langle \partial_a \psi | \psi \rangle \langle \psi | \partial_b \psi \rangle, \tag{1.33}$$

such that

$$g_{ab} = \mathrm{Re}\, Q_{ab}, \qquad \sigma_{ab} = \mathrm{Im}\, Q_{ab}. \tag{1.34}$$

In other words, Q is a Kähler metric on the projective Hilbert space, which is equipped with a Riemannian structure provided by g and a symplectic structure provided by σ. The curvature of $\mathcal{M}$ is usually called the Berry curvature and it is given by

$$F_{ab} = \partial_{[a} A_{b]} = -2\sigma_{ab}, \tag{1.35}$$

which allows us to write

$$Q_{ab} = g_{ab} - \frac{\mathrm{i}}{2} F_{ab}. \tag{1.36}$$

Consider the Fubini-Study distance, $D_{\mathrm{FS}}(\psi_1, \psi_2)$, between two arbitrary pure states. One can recover its differential form by taking $\psi_1 = \psi(\lambda)$ and $\psi_2 = \psi(\lambda + \mathrm{d}\lambda)$, such that $\mathrm{d}s^2_{\mathrm{FS}} = Q_{ab} \mathrm{d}\lambda^a \mathrm{d}\lambda^b$. A related quantity that will gain an important role in Chapters 2 and 5 is the so-called *quantum fidelity*, $F(\psi_1, \psi_2)$, which can be defined as

$$D_{\mathrm{FS}}(\psi_1, \psi_2) = \sqrt{2 - 2F(\psi_1, \psi_2)}\,. \tag{1.37}$$

For pure states, the quantum fidelity is just the absolute value of the overlap between them, $F(\psi_1, \psi_2) = |\langle \psi_1 | \psi_2 \rangle|$. By choosing two infinitesimally close states, one can perform the same reasoning we have developed for D_{FS} to show that

$$F\left(\psi(\lambda), \psi(\lambda + \delta\lambda)\right) = 1 - \frac{(\delta\lambda)^2}{2} \chi_F + \mathcal{O}(\delta\lambda^3), \tag{1.38}$$

where the so-called *fidelity susceptibility* reads

$$\chi_F = \sum_{a,b} g_{ab}(\lambda) \frac{\partial \lambda_a}{\partial \lambda} \frac{\partial \lambda_b}{\partial \lambda}. \tag{1.39}$$

Given the Riemannian structure on the manifold of quantum states, there is just one missing step in order to clarify the description of quantum phase transitions within this language. Let us

focus on ground states, $|\psi_0(\lambda)\rangle$ of a gapped system. Its infinitesimal displacement is triggered by a perturbation $\delta H \equiv \partial_a H \, \delta\lambda^a$. Thinking of g_{ab} as a matrix, one can then use second order perturbation theory to get a bound on its elements [62],

$$|g_{ab}| \leq \frac{1}{\Delta^2} \left(\langle \psi_0 | \delta H^2 | \psi_0 \rangle - \langle \psi_0 | \delta H | \psi_0 \rangle^2 \right), \tag{1.40}$$

that is, g_{ab} is upper-bounded by the fluctuations of H.

Since the hamiltonian is a sum of local operators, one can also expand its perturbation as $\delta H = \sum_x \delta\Phi_x$. Thus, it is possible to write the fluctuations as a sum over the connected correlation functions, $C_{xy} \equiv \langle \delta\Phi_x \, \delta\Phi_y \rangle_c$. If one further assumes rotational invariance, then C_{xy} becomes a function of the distance only, $C(|x-y|)$. Finally, in the presence of a gap and a unique ground state, the clustering theorem (1.4) comes into play to guarantee that the sum over correlations will always converge,

$$|g_{ab}| \leq \frac{1}{\Delta^2} \sum_{x,y} C(|x-y|) \leq \frac{N \, c_0}{\Delta^2}, \tag{1.41}$$

for some constant c_0. Thus, the metric density g_{ab}/N does not diverge in the thermodynamic limit when there is a gap, which confirms our assertion in the previous section that a quantum phase transition cannot occur unless there is a dramatic change of the state. In the absence of a gap, the divergence of the metric density or, equivalently, of the fidelity susceptibility, is a practical tool when searching for the presence of phase transitions, although a robust statement should rely on geometrical invariants. Indeed, the corresponding critical behavior of g_{ab} can usually be phrased in a coordinate-free manner – for instance, the divergence of the metric components can reflect on a discontinuity in its Ricci scalar – as reviewed in [63].

In Chapter 2, we will elevate the geometrical analysis of the Hilbert space to the space of unitary operators acting on its states. Endowed with the concept of *circuit complexity*, we will propose another form of understanding quantum phase transitions. Although we do not have yet an organized theory for this description in general systems, we will provide evidence through some examples that such extension covers a larger class of models, where one can even relax the previous hypothesis of time-independent hamiltonians. The complexity-based characterization of critical behavior will then allow us to dive into nonequilibrium phenomena and dynamical phase transitions, and to get a glimpse for a unified description of them.

1.2.3 Renormalization group and universality

We should pause for a moment and reflect about the meaning of universality from the perspective of the narrative under conduction. The insensitivity of (1.27) to the microscopic attributes of the system leads us to the conclusion that the fixed point seems to be reverting the logic of "more is different"

– taken on here since the beginning of the analysis – to its negation "more is the same". A careful look, however, reveals that the objects to which "more" refer to are, as a matter of fact, different. The apparent puzzle of such inversion can be readily solved by recognizing that the arising of a symmetry (the scale invariance), not present from the starting point, manifests itself on the pass into oblivion of the different interactions binding the local degrees of freedom, therefore leading to the same critical behavior. Thus, perhaps the correct assertive to explain the issue should be "different is the same".

The above consideration is just a moment of the exposition indicating that some determinations of the system have become more prominent. To wit, the abstraction of the physical consequences from locality – incorporated here by the correlation length – enables us to replace the system at the fixed point by an effective description overdetermined by scale invariance. This portrait captures the critical behavior of many different hamiltonians, with distinct interactions, forming the so-called *universality class* – a classification of the models according to their dimensionality, overall symmetries and the range of the interactions. In the regime where $\xi \gg a$, the lattice structure can be replaced by a continuum, and the family of theories belonging to such a universality class admits a universal formulation according to a so-called *conformal field theory* (CFT).

Let us indicate a more general description of the renormalization group (RG) analysis beyond the example of the scaling behavior for the correlation length that was given previously. A system in the vicinity of a fixed point can be expressed as

$$\mathcal{H}_\Phi(\lambda, a) = \mathcal{H}^*_\Phi + \sum_{\alpha=1}^{M} \lambda_\alpha \mathcal{P}_\alpha. \tag{1.42}$$

The reason why we made explicit mention to the lattice spacing will become clear in the following. Once again, $\mathcal{H}^*_\Phi$ is a scale-invariant hamiltonian, $\mathcal{P}_\alpha$ are perturbations and the set $\lambda \equiv \{\lambda_\alpha\}$ defines a manifold of coupling constants $\mathcal{M}$, as in the previous section. We will assume λ to be dimensionless, which can always be chosen by rescaling dimensionful couplings by an appropriate power of the lattice spacing.

In such terms, the generalization of the RG flow that we had for the correlation length in Section 1.2.1 takes the form of a dynamical system $(\mathcal{M}, \mathcal{R})$, where the evolution rule $\mathcal{R}^\tau : \mathcal{M} \to \mathcal{M}$ is a continuous one-parameter family of flows (labelled by τ). That said, the fixed point clearly obeys $\mathcal{R}^\tau \lambda_* = \lambda_*$. Under scale transformations, a point x is mapped into bx, where b is the rescaling parameter. Alternatively, sometimes it will be convenient to parametrize it in terms of the RG dimensionless "time" via $\tau = \log b$, which implies $x \to e^\tau x$. The theory described by $\mathcal{H}(\mathcal{R}^\tau \lambda, e^\tau a)$ is equivalent to $\mathcal{H}(\lambda, a)$ in the sense that they both belong the same renormalization group trajectory generated by the action of $\mathcal{R}$ on a point λ, where all points on the orbit represent the same physical

content yet at different levels of magnification[15]. To sum up, $\mathcal{R}$ implements a recursive magnifying of the neighborhood of a point by performing a rescaling in the manifold of couplings and restricting the initial model to the magnified regions.

One can expand the analysis and classify the fixed points according to their stability in the sense of dynamical systems: attractive, repulsive or even mixed. As usual in this field, the exact nature of λ_* can be determined by understanding the dynamics applied to its infinitesimal neighborhood, $\lambda_* + \delta\lambda$, whose deformation is described by the Jacobian matrix,

$$\mathcal{J}_{\alpha\beta} \equiv \frac{\partial \mathcal{R}_\alpha(\lambda)}{\partial \lambda_\beta}. \tag{1.43}$$

According to the magnitude of the eigenvalues of $\mathcal{J}$, whether they are larger/smaller than, or equal to one, nearby RG trajectories will approach/separate exponentially (with respect to the RG time) along (un)stable directions, or keep their distance less than exponential at marginal directions. At fixed points, $\mathcal{J}^\tau(\lambda_*) = e^{\tau\mathcal{A}(\lambda_*)}$. The so-called stability matrix $\mathcal{A}$ governs the dynamics in the tangent bundle $\mathcal{TM} \ni (\lambda, \delta\lambda)$ obtained by assembling a tangent space $\mathcal{T}_\lambda\mathcal{M}$ to every $\lambda \in \mathcal{M}$ and it describes the rate of deformation of the linearized neighborhood of the fixed point. In equations, this reads

$$\frac{\mathrm{d}\lambda}{\mathrm{d}\tau} = \beta(\lambda) \quad \text{and} \quad \frac{\mathrm{d}(\delta\lambda)}{\mathrm{d}\tau} = \mathcal{A}\,\delta\lambda, \quad \text{where} \quad \mathcal{A} = \frac{\mathrm{d}\beta}{\mathrm{d}\lambda}. \tag{1.44}$$

We meet the β-function once again, the difference being on the parametrization of the flow, which is now in terms of the RG time. The above formulation converging to a differential equation for the RG flow presupposes arbitrarily small rescalings, $b = 1 + \delta\tau$, such that $\mathcal{J}^{\delta\tau} \sim \mathbb{1} + \mathcal{A}\,\delta\tau$. For future reference, it is also usual to write the eigenvalues of the Jacobian either as $e^{\tau\mu + \mathrm{i}\theta}$, where the phase $\theta = \omega\tau$ defines an angular velocity ω or, alternatively, to parameterize its real part by the scaling factor, $e^{\tau\mu} = b^\mu$.

More precisely, the stability classification is given in terms of the eigenvalues of $\mathcal{A}$ evaluated at λ_*. We will assume the eigenvalues to be non-degenerate. Thus:

- If $\mu_*^{(i)} < 0 \;\; \forall\, i$, then the fixed point is *stable*. For $\omega^{(i)} = 0$, λ_* it is approached in node; for $\omega^{(i)} \neq 0$, it is approached in spiral.

- If $\mu_*^{(i)} > 0 \;\; \forall\, i$, then the fixed point is *unstable*. For $\omega^{(i)} = 0$, λ_* it is exited out node; for $\omega^{(i)} \neq 0$, it is exited out spiral.

[15] In order to exemplify the above situation, we refer back to the behavior of the correlation length. It can be proved that under the action of the renormalization group at the fixed point,

$$\mathcal{R}^\tau \lambda_* = \lambda_* \quad \Longrightarrow \quad \xi(\lambda_*) = b^{-1}\xi(\lambda_*),$$

showing that, indeed, $\xi = 0$ (a trivial fixed point) or $\xi = \infty$ (a critical point).

- If $\mu_*^{(i)} < 0$ and $\mu_*^{(j)} > 0$ for some $i \neq j$, then the fixed point is *hyperbolic*.
- If $\mu_*^{(i)} = 0$, then the fixed point is *marginal*.

Recall the reasoning that led to (1.26). There we considered an unstable fixed point and then we found out that $\beta'(\lambda_*)$ determines the critical exponent of the correlation length after linearization around λ_*. Here we carried over a parallel discussion in terms of the stability matrix and (1.44) puts us in position to close the argument. The connection between the two quantities is the already delineated one: the eigenvalues of the stability matrix are nothing but the derivatives of β-function at fixed points. Additionally, the deformations $\mathcal{P}_\alpha$ corresponding to the classification of the fixed points are designated: *irrelevant* if λ_* is stable, *relevant* if λ_* is unstable, and *marginal* if λ_* is marginal.

1.2.4 Critical behavior of entanglement

We end this section with the accompanying discussion of the critical determinations of the many-body quantum system from the entanglement perspective. For definiteness, we will keep the line of reasoning in Section 1.1.2 and apprehend the content of universality for the one-dimensional case in light of a gapless condition.

For the sake of the exposition, consider a chain at the critical point and an interval A of length $|A| = L$. The results obtained for the ground state entanglement entropy in the context of many different models can be brought to the form[16] [64] :

$$S_A = \frac{c + \bar{c}}{6} \log \frac{L}{a} + \mathcal{O}(1). \tag{1.45}$$

We will have a lot of important facts to say about this formula. First, note that the appearance of the lattice spacing a avoids a divergence for small L. Also, the dependence on the ratio L/a is consistent with the scale invariance proper of the fixed point. The constants c and $\bar{c}$ will gain a distinguished role in the next section. Their values depend on the number of local degrees of freedom as well as on the quantum statistics obeyed by them. Apart from the actual meaning of c and $\bar{c}$, for now it is evident that the entanglement entropy provides an alternative measure for them.

Notice, in addition, the parallel with the previous discussion about the critical exponents: in the lifting from the particularities of a local hamiltonian to its belonging to a universality class, all information about the individual degrees of freedom that are entangled gets lost in the process, and it manifests into a unique attribute of the whole[17].

[16] We have cited [64] for a review. Nevertheless, the critical behavior of entanglement close to a quantum phase transition from the perspective of lattice models was first presented in [65, 66].

[17] The referred constants are the central charges of a conformal field theory describing the fixed point and they give a universal characterization of the degrees of freedom of the theory. Additionally, the entanglement entropy in a $(1+1)$-dimensional

Finally, if one starts to move away from the fixed point keeping the correlation length very large compared to the lattice spacing, but finite, both tendencies present in Equations (1.15) and (1.45) merge together into a single expression [68],

$$S_A \sim |\partial A| \frac{c+\bar{c}}{6} \log \frac{\xi}{a}, \tag{1.46}$$

with the correlation length taking place of L.

1.3 Conformal field theories

A scaling transformation of the lengths corresponds to a change of the coupling constants that leaves the physical content of a theory unchanged. These transformations are a subgroup of the more general global conformal transformations. For systems that are additionally homogeneous and isotropic, scale invariance is almost always enhanced to full conformal invariance[18], which in addition to rotation and translation symmetries include the so-called special conformal transformations.

Let $\{\phi_\alpha\}$ be a set of operators that provide a description of a d-dimensional scale invariant theory in the continuum limit, $\xi \gg a$. We will further consider the case where such operators transform irreducibly under scale transformations: $x \to bx$ leads to $\phi_\alpha(bx) = b^{-\Delta_\alpha}\phi_\alpha(x)$, and then $\{\phi_\alpha\}$ are called *primary operators*. The quantity Δ_α is the *scaling dimension* of the operator ϕ_α. By taking derivatives of a primary operator ϕ_a, one gets its *descendant operators* with scaling dimensions equal to Δ_a plus the number of derivatives. The coupling constants change as $b^{\mu_a}\lambda_a$. In order to keep the theory invariant one finds[19] a relation between the eigenvalues of the stability matrix and the scaling dimensions, $\mu_a = d - \Delta_a$.

Global conformal invariance constrains the form of the two-and three-point correlators. Let $\phi_a(x)$, $\phi_b(y)$, and $\phi_c(z)$ be three operators with scaling dimensions Δ_a, Δ_b and Δ_c respectively. It can then be shown [70] that, at the fixed point, they assume the following form:

$$\langle \phi_a(x)\phi_b(y)\rangle_* = \frac{\delta_{\Delta_a,\Delta_b}}{|x-y|^{2\Delta_a}} \tag{1.47}$$

and

$$\langle \phi_a(x)\phi_b(y)\phi_c(z)\rangle_* = \frac{C_{abc}}{|x-y|^{\Delta_{ab}}|y-z|^{\Delta_{bc}}|z-x|^{\Delta_{ca}}}, \tag{1.48}$$

conformal field theory is known to give Equation (1.45) since the 90s [67]. This point of view is complementary to the one in the previous footnote and it will be further explored as we advance.

[18] A good review about the matter is [69].

[19] This result follows from dimensional analysis of the action, which is the more convenient quantity to represent the theory in the continuum limit rather than the hamiltonian description we are adopting so far.

where we have defined

$$\begin{aligned}\Delta_{ab} &= \Delta_a + \Delta_b - \Delta_c\,,\\ \Delta_{bc} &= \Delta_b + \Delta_c - \Delta_a\,,\\ \Delta_{ca} &= \Delta_c + \Delta_a - \Delta_b\,,\end{aligned} \tag{1.49}$$

and the universal amplitudes $\{C_{abc}\}$ are coefficients also denominated as the *structure constants of the operator product expansion (OPE)*. The reason for this name follows from the possibility of replacing the product of two operators, whenever they are taken inside an expectation value, by the following series:

$$\lim_{x\to y}\phi(x)\phi(y) \equiv \lim_{x\to y}\sum_c \frac{C_{abc}}{|x-y|^{\Delta_a+\Delta_b-\Delta_c}}\phi_c\left(\frac{x+y}{2}\right). \tag{1.50}$$

While this formula approximately holds in general quantum field theories for operators at very close distances, it is exact in conformal ones even at large distances, as long as there is no other operator insertion in between them. It is usual to summarize this expression by introducing an operation $\star$ to represent the fusion between the two operators,

$$\phi_a \star \phi_b = \sum_c C_{abc}\,\phi_c. \tag{1.51}$$

Higher-order correlation functions are not completely fixed by symmetry arguments. They have non-trivial conformal invariants built up from ratios of distances between the fields which obstruct their determination. Nevertheless, at least in principle, OPEs can be used to compute any other correlation function.

1.3.1 Conformal data and critical exponents

The knowledge about the conformal field theory that takes place in the description of the many-body quantum system in a fixed point of the RG flow is concluded once the scaling dimensions of the primary operators, $\{\Delta_a\}$, and the structure constants $\{C_{abc}\}$ are determined – the so-called *conformal data*.

Using the properties listed in the previous section, it is possible to develop a perturbative analysis of the RG around a fixed point. The reasoning was started by Zamolodchikov in [71] for specific two-dimensional CFTs and nowadays it usually goes under the name of conformal perturbation theory. With this approach one can perform a one-loop computation of the β-function, which is given by [72]

$$\beta_a = (d-\Delta_a)\lambda_a - \sum_{b,c} C_{abc}\lambda_b\lambda_c + \mathcal{O}(\lambda^3). \tag{1.52}$$

This expression shows that the spectrum of scaling dimensions, besides its dimensionality, determines

the linear behavior of the β-function, while the so-called one-loop correction amounts to quadratic terms in the coupling constants determined by the structure constants of the OPE. Alternatively, if the β-function is known, one could in principle extract the conformal data directly from the above equation. Lastly, as we have seen in Section 1.2.3, $\beta'_a(\lambda_*)$ is responsible for the universal critical behavior. Hence, Equation (1.52) shows that there are also quantum corrections to the scaling dimensions due to non-vanishing OPE coefficients. These corrections are important features of the CFT and they are captured by quantities named anomalous dimensions, however we will not get into the details of how to calculate them.

The brief considerations of this section conclude the first half of the main plot. Starting from a general quantum many-body system, we exposed several of its determinations by understanding the relation between local and global. Our analysis was guided towards the unveiling of the universal behavior that emerges from the abstraction of the particularities of distinct systems. Before moving on to the final part, we will tie up some loose ends in the context of $2d$ CFTs following the examples elaborated within this chapter.

1.3.2 The central charge

We will address the announced interpretation of the constant c (and consequently $\bar{c}$) appearing on (1.45), the so-called *central charge*[20]. First, consider a reshaping – not necessarily conformal – that distorts the lattice, $x \to x + \epsilon(x)$. If one imagines an RG transformation that maps a fixed point hamiltonian to the distorted one, the additional deformation is given by

$$\delta H_\Phi \propto \int \mathrm{d}^2 x T_{ab}(x)\, \partial^a \epsilon^b(x)\,, \tag{1.53}$$

where T_{ab} is the *stress tensor*. This is a symmetric object, traceless, $T^a{}_a = 0$, and a conserved current, $\partial^a T_{ab} = 0$.

Let us specialize to the two-dimensional case once again. Consider the CFT with coordinates defined on the complex plane. By mapping – using a conformal transformation – the theory to a cylinder $\mathbb{R} \times S^1$ of circumference L, one can show that the change in the vacuum energy per unit length is dictated by

$$\langle T \rangle_{\mathbb{R}\times S^1} \propto \frac{c}{L^2}\,, \tag{1.54}$$

where T is the holomorphic component of T_{ab}.

[20] The results of this section are textbook material that we include mostly for completeness. We refer the reader to e.g. [70] for details.

The central charge also appears in the two-dimensional trace anomaly: define the theory on a curved (ambient) manifold with metric g – meaning that there is no dynamics associated to g – and Ricci scalar R. Then,

$$\langle T^a_{\ a}(x)\rangle_g \propto c\, R\,. \tag{1.55}$$

This also called conformal anomaly indicates a "soft" breaking of conformal symmetry due to the introduction of an intrinsic length scale.

Next, consider the vacuum state of the theory on $\mathbb{C}$, and a single interval A of length L taken at some instant of time. The entanglement entropy can be evalutated using the replica trick technique and it takes the same form of (1.45) [67],

$$S_A = \frac{c+\bar{c}}{6}\log\left(\frac{L}{\epsilon}\right) + \mathcal{O}(1), \tag{1.56}$$

as anticipated on Footnote 17. Here ϵ is an ultra-violet (UV) cutoff, which could be the lattice spacing a (although not necessarily), required to regulate the divergences due to short-range correlations present in any state of a local quantum field theory. The rescaling of the cutoff amounts to shifting the $\mathcal{O}(1)$ constant term, which is non-universal. The existence of $\bar{c}$ comes from the fact that in $d = 2$ the (local) conformal transformations act independently as (anti-)holomorphic maps, resulting in a factorization of the full Hilbert space into sectors that carry possibly different central charges. We will address this point with more details on Chapter 5.

Finally, we briefly mention that $c = 1$ for bosons, $c = 1/2$ for fermions and, more generally, $c = N$ for a system with N different types of noninteracting bosons. Such results suggest that the central charge and, as consequence, the entanglement entropy can provide a sort of measure of the number of degrees of freedom. This assertion happens to hold in two-dimensions[21]. For higher dimensions its extension does not always make sense and thus it requires extra care.

1.4 The AdS/CFT correspondence

We start the remaining part of this chapter with a note of warning. Our journey has brought us to an awkward point. Up to now, we were presenting a story where, at least in spirit, all the main determinations emerge from the basic structure that is required to apprehend a physical system with a well-behaved thermodynamic limit and screened interactions. We have neither the tools nor the space required to develop the full formalism of the so-called AdS/CFT correspondence from the

[21] The connection between the central charge and the degrees of freedom in this case is established by the c-theorem [71], which presents a function defined on the manifold of coupling constants that monotonically decreases along RG flows. At the fixed points, this function coincides with the central charge of the CFT. The intuition is that information about the degrees of freedom is lost as the flow proceeds from a CFT in the UV to another one in the IR.

current premises. The follow-up approach will thus proceed in a less paved way then the previous sections, not only due to the alluded problem, but also because the complete understanding of the topic under the emergence paradigm we have being adopting is a subject of current research.

1.4.1 Renormalization group and the Anti-de Sitter spacetime

The CFTs equipped with RG can be faced under a radically distinct perspective: the scaling transformations allow one to picture a continuous family of effective QFTs at different length (therefore energy[22]) scales, each providing a different canvas of the theory according to the degree of magnification. One can therefore merge those screens together into an additional dimension furnished by the RG energy scale r, which can be interpreted as a geometrization of the scaling transformations. Thus, this procedure enables one to picture a foliation for a higher dimensional $(d+1)$-manifold, each copy at a given r being a d-dimensional flat space, where the quantum field theory is defined.

To understand what is the geometry behind the curtains, note that the CFT is relativistic and, in particular, invariant under the Poincaré group. In this first approach to the matter, we simply claim that those symmetries are to become isometries of the unknown metric of the higher dimensional space, such that one can promptly write[23]

$$\mathrm{d}s^2 = f(r)\eta_{ab}\mathrm{d}x^a\mathrm{d}x^b + g(r)\mathrm{d}r^2. \tag{1.57}$$

We should now invoke invariance under scaling symmetry of the CFT to get the conformal group, $SO(d,2)$, and also demand it to be an isometry, which then fixes the previous functions,

$$f(r) = \frac{r^2}{\ell^2} \quad \text{and} \quad g(r) = \frac{\ell^2}{r^2}\,, \tag{1.58}$$

where ℓ is a free parameter with dimensions of length. These functions together with (1.57) give rise to the metric of the Anti-de Sitter (AdS) spacetime in $d+1$ dimensions, which is the unique invariant metric satisfying our requirements. Accordingly, from now on we will denote the AdS radius of curvature by $\ell = \ell_{\mathrm{AdS}}$. The UV limit, $r \to \infty$, takes us to the boundary of AdS, where $g(r) \to 0$ and one reaches the CFT defined in Minkowski space with metric η_{ab}. Alternatively, it is possible to transform the extra radial direction into an RG length dimension by setting $z = \ell^2_{\mathrm{AdS}}/r$, which results in the so-called Poincaré patch,

$$\mathrm{d}s^2_{\mathrm{AdS}} = \frac{\ell^2_{\mathrm{AdS}}}{z^2}\left(\eta_{ab}\mathrm{d}x^a\mathrm{d}x^b + \mathrm{d}z^2\right). \tag{1.59}$$

[22] The energy in the CFT can be defined as follows: consider the theory on a cylinder $\mathbb{R}\times S^{d-1}$, then its energy spectrum is given by the spectrum of the dilation operator on $\mathbb{R}^{d-1}$ (the operator that generates scaling transformations).

[23] See Section 1.4.4 for a second approach with further determinations.

Poetically, and inaccurately, one can declaim that there is an apparent trade-off between two length scales: it is as if somehow the CFT still remembers about the emergent length set by the Lieb-Robinson speed. Its information does not simply disappear – it reemerges as the radial direction of a different theory in a different spacetime. Of course this is just a metaphorical expression and it is not sustained under theoretical pillars.

We should now conciliate some RG setups under this geometric frame. In Section 1.3.2, for instance, we considered a deformation of a CFT creating a non-trivial RG flow. The question of how the higher dimensional spacetime will react under such perturbation can be answered by assigning a dynamical role for the metric. Then, the emergent geometry acquires a life of its own and it can evolve according to the rules that are proper of its kind – general relativity (GR). Concretely, we can implement these ideas by recognizing that the AdS metric is a solution of the equations of motion governed by the Einstein-Hilbert action with negative cosmological constant,

$$S = \frac{1}{16\pi G^{(d+1)}} \int \mathrm{d}^{d+1}x \sqrt{-g}\,(R - 2\Lambda_{\mathrm{AdS}} + \cdots)\,, \tag{1.60}$$

where $g = \det g_{ab}$, $G^{(d+1)}$ is the gravitational coupling constant in $d+1$ dimensions and, in terms of AdS radius, the cosmological constant reads

$$\Lambda_{\mathrm{AdS}} = -\frac{d(d-1)}{2\ell_{\mathrm{AdS}}^2}\,. \tag{1.61}$$

The ellipsis in the action accounts for whatever produces the fluctuations responsible for the CFT deformations, which includes higher-derivative corrections[24] and matter fields.

So far, the story of this section tells us that the concept of RG is mirrored into GR with the entrance of two new actors: the ℓ_{AdS} radius and Newton's constant, $G^{(d+1)}$, which can also be expressed in terms of the Planck length, $G^{(d+1)} \propto \ell_{\mathrm{P}}^{d-1}$. For a consistent description within GR, no large quantum gravity effects can take place. This restriction can be stated by requiring the radius of curvature of AdS to be way above the Planck scale,

$$\frac{\ell_{\mathrm{AdS}}}{\ell_{\mathrm{P}}} \gg 1\,. \tag{1.62}$$

At this point, our reasoning of reproducing the CFT deformations from GR is not a necessity of the analysis, as well as the choice to avoid quantum gravity effects expressed in the above limit[25]. Given that, one could further imagine the following related situations:

- First, and the more obvious one, to face the possibility of large curvature effects taking place, which urges the passage from general relativity to string theory for a consistent framework.

[24] Those are covariant derivatives of the curvature which schematically can be written as powers of ∇^2 acting on R.

[25] Indeed, this is possible for very special CFTs only, as we will see in the next section.

- Second, to demand nothing. Actually, no more than what it is already contained in the analysis so far. Then one could try to extract the dynamical determinations obeyed by the *dual gravitational theory*, its geometry and the additional fields. This approach requires pushing the conceptual framework of CFTs to its limits and further specialize to particular classes of them. Nonetheless, it could in principle provide a definition of quantum gravity from an emergent paradigm.

Both approaches are under scrutiny in the current literature. In the first scenario, there would be an additional length scale, the string length ℓ_s, which appears in the higher derivative corrections to the Einstein-Hilbert action and it would then define another dimensionless parameter, ℓ_{AdS}/ℓ_s, governing the strength of gravitational interactions – and therefore this parameter should be large when quantum gravity effects are small. This is the better understood case which has started under very different premises with the work of Maldacena [12], the symbol of the so-called *AdS/CFT correspondence*. In this context, there exists explicit constructions of particular CFTs and their corresponding AdS duals, strongly supported by a myriad of tests with various degrees of precision.

We will explore the second situation in what follows starting from a question: Which CFTs admit an effective description matching the above sketch and (1.62)?

1.4.2 Large-N conformal field theories and the holographic duality

Among CFTs, there is a special class that fits in the part we have designed in the previous section and, therefore, they will play the leading figure from now on. This is a family that carries a parameter N[26] and displays the following properties [73]:

1. There exists a finite number of single-trace primaries $\{\phi_a\}$ such that, by normalizing their two-point function to be a constant independent of N, then the three-point function decays with some power of N, $\langle\phi_a\phi_b\phi_c\rangle \sim \mathcal{O}(N^{-1})$.
2. There exists one single-trace spin-2 primary operator with $\Delta = d$: the *energy-momentum tensor*, T_{ab}.
3. There is an associated multi-trace primary $\phi_{a_1,\ldots,a_M}$, $M = \mathcal{O}(N^0)$, with scaling dimension $\Delta_{a_1} + \cdots + \Delta_{a_M}$, to every family of single trace operators $\{\phi_{a_1},\ldots,\phi_{a_M}\}$.
4. The correlation functions obey the so-called factorization in the large N limit: $\langle\phi_a\phi_b\rangle \sim \langle\phi_a\rangle\langle\phi_b\rangle + \mathcal{O}(N^{-2})$ and similarly for higher-order correlators.

[26] In practice, such CFTs are usually gauge theories where N is the rank of the gauge group and then, the so-called *single-trace* operators that will appear next are gauge invariant operators of the form

$$\phi_a(x) = \frac{1}{N}\,\text{Tr}\left(\prod_{b=1}^{a}\Phi_b(x)\right).$$

Here Φ_b are the fundamental fields which would, for instance, be part of the Lagrangian description of the model. Correspondingly, *multi-trace* operators have more than one trace in their definition.

5. Only single/multi-trace primaries and their descendants have $\Delta = \mathcal{O}(N^0)$.

The answer to the question ending the previous section appears to be: any d-dimensional large-N CFT satisfying points 1-5 has a semiclassical dual description near the vacuum. Although there is no formal proof of this statement, there is plenty of evidence that those conditions seem to be sufficient to guarantee the existence of an effective bulk gravitational theory in $(d+1)$-dimensional asymptotically AdS spacetime [74]. Such gravitational theory is then described by an effective action $S_{\text{eff}}[\varphi_a, \Lambda]$, where $\{\varphi_a\}$ are the bulk fields – there should be a finite number of them – and Λ is a cutoff satisfying

$$1 \ll \Lambda \ell_{\text{AdS}} \ll \frac{\ell_{\text{AdS}}}{\ell_{\text{P}}}. \tag{1.63}$$

The statement about the duality should be complemented by a map between observables on the two sides, the so-called *dictionary*:

$$\int [\mathrm{d}\varphi_a]\, e^{\mathrm{i}S_{\text{eff}}[\varphi_a,\Lambda]} \phi_{a_1} \cdots \phi_{a_M} \simeq \langle \phi_{a_1} \cdots \phi_{a_M} \rangle_{\text{CFT}}\,, \tag{1.64}$$

where, once again, $M = \mathcal{O}(N^0)$.[27] As seen from (1.63), the combination $(\Lambda \ell_{\text{AdS}})^{-1}$ provides a small parameter which can be used to determined the validity of Equation (1.64) – it should hold perturbatively to all orders in $(\Lambda \ell_{\text{AdS}})^{-1}$.

The missing connection between the operators in the CFT and the bulk fields is provided by an entry dictionary, namely, the ϕ_a on the left hand side of (1.64) are obtained through

$$\phi_a(t,x) = \lim_{r\to\infty} r^{\Delta_a} \varphi_a(r,t,x), \tag{1.65}$$

with Δ_a being the scaling dimension of ϕ_a. To sum up, the AdS fields φ_a correspond to the single-trace primaries ϕ_a. As a concrete example, for scalars and massive spin two fields, one can derive the following relation between the scaling dimension and the mass m_φ,

$$\Delta_\phi = \frac{d}{2} + \sqrt{\frac{d^2}{4} + m_\varphi^2 \ell_{\text{AdS}}^2}\,. \tag{1.66}$$

Given Equation (1.64), one can also imagine determining the OPE coefficients, and therefore the conformal data, in terms of parameters of the gravity side. Indeed, the OPE coefficients can be extracted, at least in principle, from their holographic representation in terms of the so-called Witten diagrams [75], providing universal information irrespective of dynamical particularities.

We still have not touched upon the necessity for N to be large. A calculation of the three-point function of the stress-energy tensor compared to the same one with its dual field – the graviton –

[27] To call it a duality one needs an isomorphism between the Hilbert spaces, which is implicitly assumed, but Equation (1.64) is good enough for our purposes.

reveals the following relation between N and the AdS radius in units of Planck length,

$$\left(\frac{\ell_{\mathrm{P}}}{\ell_{\mathrm{AdS}}}\right)^{d-1} = \mathcal{O}\left(\frac{1}{N^2}\right) \tag{1.67}$$

implying that we must have $N \gg 1$ for consistency with (1.63)[28]. With this last thought, we declare the claim about the *holographic duality* to be concluded, or at least a crude level of it, where the emphasis was given to its kinematical aspects.

1.4.3 Universality of chaos

In Section 1.1.3, we have discussed the out-of-time-ordered correlation function, where we briefly mentioned its form for large-N systems (1.19). In examples of such systems that are already known to exhibit a holographic dual described by general relativity in the semiclassical limit, the evaluation of the OTOC in a thermal state $\rho \propto e^{-\beta H}$ of temperature β^{-1} gives [76, 77, 78, 79]

$$\mathcal{C}(0,t) = \frac{1}{N^2} e^{\lambda_* t} + \mathcal{O}\left(\frac{1}{N^4}\right), \qquad \lambda_* = \frac{2\pi}{\beta}. \tag{1.68}$$

The exponential growth is a sign of the quantum butterfly effect mentioned in 1.1.3, where the quantity λ_* resembles a quantum Lyapunov exponent and, indeed, it is denominated as such henceforth.

Inspired by these results, Maldacena, Shenker and Stanford showed the imposition of a universal bound [80] for quantum systems – the so-called chaos bound,

$$\lambda_{\mathrm{L}} \leq \frac{2\pi}{\beta}, \tag{1.69}$$

such that holographic systems described semiclassically by general relativity saturate the inequality. Here λ_{L} is the analog of λ_* in (1.68) for general chaotic systems, where it may depend on the operators that enter in the definition of $\mathcal{C}(x,t)$.

Kitaev [17] has conjectured that a maximal Lyapunov exponent provides a necessary – and possibly sufficient – condition for the existence of a holographic dual to a large-N CFT,[29] therefore leading to another criterion besides the listed properties 1-5.

Recalling our discussion of Section 1.2, we can sight the arrival point of the chapter: it is an artist's impression of a bridge between our initial many-body quantum system and a theory of (quantum) gravity. The holographic generation of spacetime and the accompanying framework to account for

[28] For two-dimensional CFTs, the parameter N is related to the central c in such a way that the large N limit corresponds to $c \gg 1$.

[29] The conjecture is guided by the analysis of the so-called Sachdev-Ye-Kitaev model, which provides both motivation and a testing ground for the ideas of this subsection. We will spend more words on that in Chapter 4.

non-gravitational concepts, such as the CFT data, brings together all the emergent features that were previously tacit in the (R, r)-local quantum system from the beginning of our journey. In spite of our focus towards the search for universal patterns in collective phenomena, derived from abstracting dynamical particularities, such process is further determined and subjected to different categories that will also gain an important role in the next chapters – entanglement, chaos and complexity, for instance. With this in mind, we turn to the a last effort to improve the traits of the analysis by including the entanglement point of view that we have being pointing out throughout the chapter.

1.4.4 Holographic entanglement entropy

Historically, the connection between gravity in Anti-de Sitter space and conformal field theories has followed a very different path from the one of our exposition. The hints for such correspondence started within studies in black hole physics – the Bekenstein-Hawking formula as a hallmark – demonstrating the amount of entropy of a black hole in order to guarantee its compatibility with the laws of thermodynamics,

$$S_{\text{BH}} = \frac{A}{4\,\ell_{\text{P}}^2}. \tag{1.70}$$

A is the area of the black hole event horizon.

Subsequently, an area law was also found for the leading behavior of the entanglement entropy of free field theories [81, 82]. The interpretation of such result was used to argue for an explanation of the area showing up on S_{BH} and, eventually, this was latter generalized to the holographic principle [10, 11, 83]: that the information stored in volume of space is encoded in its boundary surface measured in units of Planck area.

The genesis of quantum entanglement in holography dates back to the work of Ryu-Takaynagi [13, 14], with the connection between entanglement entropy (of a reduced density matrix defined in a timeslice) in a quantum field theory and the area (of a particular minimal surface) in gravity. The proposal was later generalized by Hubeny-Rangamani-Takayanagi to include time-dependent states [84] and a proof within the AdS/CFT correspondence was given to both formulations respectively on [85] and [86]. More specifically, given an asymptotically AdS manifold, the so-called Hubeny-Rangamani-Ryu-Takayanagi (HRRT) formula assigns the quantity

$$S(A) = \frac{\text{Area}(\gamma_A)}{4\ell_{\text{P}}^{d-1}} \tag{1.71}$$

to a spatial region A of a holographic CFT. This region lies in a Cauchy slice Σ of the AdS boundary, such that $\Sigma = A \cup \bar{A}$. In addition, γ_A is the minimal area codimension-two spacelike superface in the bulk restriced to be homologous to A – in particular, A and γ_A have the same boundary. These ideas ultimately culminated in the seminal essays of Van Raamsdonk [15, 16], where entanglement

was identified as a central category for the building of spacetime geometry.

Bypassing the sinuous path connecting these cornerstone concepts up to the present developments, the subject of an emergent spacetime encounters one realization in the work of Faulkner et al [87], where the necessity of nonlinear gravitation equations is demonstrated to follow from a broad class of conformal field theories[30]. More specifically, the authors show that states defined by the following wave functional,

$$\langle \varphi_0(x)|\Psi_\lambda(\varepsilon)\rangle = \int_{\Phi(\tau=0,x)=\varphi_0(x)} [\mathrm{d}\Phi(\tau)]_{\tau<0} \exp\left(-S_{\mathrm{CFT}}[\Phi(\tau)] - \int_{-\infty}^{0} \mathrm{d}\tau\, \lambda_a^{(\varepsilon)}(x,\tau)\phi_a(x,\tau)\right), \quad (1.72)$$

give rise to an associated geometry which satisfies Einstein equations perturbatively up to second order, $g^{(0)}_{\mathrm{AdS}} + \varepsilon\delta g^{(1)} + \varepsilon^2\delta g^{(2)} + \ldots$, that correctly computes entanglement entropies up to order ε^2 for all ball-shaped regions via the HRRT formula (1.71). The Euclidean path integral in the above equation defines the vacuum state of the CFT with the addition of sources λ_a for local primary operators ϕ_a. These states can be interpreted as coherent states of light quantum fields in AdS dual to the operators ϕ_a [88]. Evidence that (1.72) can describe any near-AdS spacetime was presented in [89].

At this point, we have the seed for understanding the holographic generation of spacetime and gravity as consequence of the qualitative change arising from complex patterns of entanglement due to eminence of quantum effects.

[30] A remarkable feature in this work is that it contains no assumptions about the AdS/CFT correspondence, therefore the results can be viewed as a consistency check of the duality as well.

2

Complexity and non-equilibrium phase transitions

"Todo dia ela faz tudo sempre igual
Me sacode às seis horas da manhã
Me sorri um sorriso pontual
E me beija com a boca de hortelã."

— *Cotidiano*, Chico Buarque

This chapter was first presented as [22] under the title:

"*Complexity and Floquet dynamics: non-equilibrium Ising phase transitions*".
– Phys. Rev. B 102 (2020), no. 17 174304, [arXiv:2009.00069],

and it is a collaboration with Giancarlo Camilo.

The concept of universality is a necessity in the process of abstraction from an experimental condensed matter system to its theoretical description at equilibrium, both at classical and quantum levels. As we have outlined in Section 1.2, universality can be understood as an emergent property of the renormalization group. There, we emphasized the validity of the analysis for time-independent hamiltonians.

Out of equilibrium, even classically there is no unique answer to the question of what probability measure describes the (non-equilibrium) states of a system. The absence of a general result, as in the equilibrium case, is mainly because we are not only concerned about the asymptotic values of physical quantities, but also in the way that such values are approached. This reflects on a lack of understanding of how universality emerges when the dynamics cannot be forgotten, which poses a problem on a general description of phase transitions.

While the complete theory of nonequilibrium processes does not exist, there are particular types of dynamics where one may have some analytical control over the quantitative analysis. One such case that will be the focus of this chapter is the periodic driving of a system. This mechanism can induce qualitative changes of the dynamics causing an integrable system to become nonintegrable – for intance, this can happen in autonomous systems with one degree of freedom only, which are integrable at classical level. Additionally, and more importantly to the current work, periodic driving can lead to phase transitions that are not present in its undriven counterpart.

In Section 1.2.2, we have sketched the description of a quantum phase transition using the conceptual framework of Riemannian geometry applied to the Hilbert space of a quantum system. Here we will take one step forward by lifting the analysis to the space of unitary operators acting on the Hilbert space, where the concept of circuit complexity will turn out to be the protagonist. The immediate results consist in a tool for determining non-equilibrium phase transitions for special systems. The long term goal would be the validation of such method for determining critical behavior in more general systems, encompassing topological and even dynamical phase transitions, as we sketch in Section 2.6.

Concretely, we will use Nielsen's geometric approach [90, 91] to analyze the time-dependent circuit complexity of the periodically driven transverse field Ising model. We will show that the complexity can distinguish between the nonequilibrium phase transitions displayed by the system in the high frequency limit. In addition, it captures a universal linear behavior at early times. Moreover, we provide evidence that the time averaged complexity presents non-analytic behavior at the critical points. Lastly, we will show some preliminary analysis of the use of circuit complexity in the determination of dynamical quantum phase transitions.

2.1 Introduction

Understanding the organizing principles underlying the non-equilibrium dynamics of quantum many-body systems is of key importance for the development of new quantum materials. The concept of universality, which provides a unified description of equilibrium critical phenomena, is not well understood for systems far from equilibrium. In the case of adiabatic dynamics the so-called Kibble-Zurek mechanism and its quantum extension can provide some insights into the breakdown of adiabaticity close to a quantum phase transition (QPT) point and the associated scaling behavior of the excitation density of defects [92, 93, 94, 95, 96], which opened a venue for the analysis of universal features in non-equilibrium QPT. The preclusion of adiabatically connecting states belonging to different quantum phases can be given a geometric interpretation as a diverging curvature with the introduction of a metric on the Hilbert space [62]. This geometric paradigm is part of an ongoing effort in the last two decades to employ concepts and tools from quantum information science to improve our understanding of quantum many-body physics. This approach has led to remarkable progresses, such as the discovery of topologically ordered states and of the critical behavior of entanglement close to a QPT [65, 66] (see [6] for a review).

As part of this effort, [97, 98, 99] proposed to characterize QPTs, including topological ones, using a geometric notion of circuit complexity introduced by Nielsen [90, 91]. Inspired by its computer science analogue, this object quantifies how difficult it is to construct a particular unitary operator that maps between a pair of given reference and target states, i.e., the minimum number of basic operations needed to implement this task. With an appropriate definition of depth functional associated with each circuit, the space of allowed unitaries acquires a Riemannian structure and the problem of finding the optimal circuit reduces to finding minimal geodesics in this geometry. Nielsen's complexity has recently also attracted a lot of interest from the high energy physics community due to conjectured connections with black hole properties within the scope of the holographic duality [100, 101, 102, 103, 104].

A major difficulty to unravel universal non-equilibrium properties independent of specific models comes from the variety of ways in which a system can be put away from equilibrium. Perhaps the simplest and one of the most studied among these non-equilibrium protocols is that of a quantum quench, where a parameter of the hamiltonian is suddenly changed and the system is let evolve under the new hamiltonian [105, 106]. This also includes the study of the quench dynamics of circuit complexity [107, 108, 109, 97, 98, 110]. Here we propose to go a step further in the endeavour of using circuit complexity as a novel tool to understand the dynamics of quantum many-body systems and explore a different non-equilibrium protocol corresponding to the periodic driving of many-body systems. These so-called Floquet systems can be experimentally realized with ultracold quantum gases in optical lattices (see [111, 112] for a review of theoretical and experimental results) and give

rise to several exotic phenomena such as dynamical localization, Floquet topological insulators, and driving-induced phase transitions [111, 112, 113, 114, 115].

We shall focus on the Ising model under periodic driving of the transverse field [116, 117, 118, 119]. The model can be solved analytically in the fast driving limit, where it is effectively described by a time-independent hamiltonian and it displays quantum phase transitions of non-equilibrium nature controlled by the transverse field amplitudes. It also exhibits the phenomenon of dynamic localization [120], where the time evolution gets frozen to the initial state as a consequence of a many-body version of the coherent destruction of tunneling (CDT) [121] that occurs in each momentum sector of the Hilbert space. CDT has been observed experimentally and it is particularly important for quantum dynamics control [122, 123, 124].

In this setup, we compute the circuit complexity of the instantaneous time-evolved state and argue that it can be used to characterize these non-equilibrium phase transitions, showing that its time-average exhibits non-analytic behavior at the critical points. We also unveil a universal linear behavior at early times and show that the CDT phenomenon is naturally diagnosed by points of vanishing complexity. Our work takes to a next level the connection between circuit complexity and quantum phase transitions, opening the route for periodically driven systems and dynamical phase transitions.

2.2 The driven transverse field Ising model

We consider a periodically driven transverse field Ising model (TFIM) described by the hamiltonian

$$H(t) = -J \sum_{i=1}^{L} \sigma_i^z \sigma_{i+1}^z - g(t) \sum_{i=1}^{L} \sigma_i^x, \tag{2.1}$$

where σ_i^α are Pauli matrices at the i-th lattice site, $J > 0$ is the exchange coupling, and $g(t) = g_0 + g_1 \cos \Omega t$ is the transverse field, made of a constant contribution g_0 and a monochromatic driving with frequency Ω. Here we assume a closed lattice with periodic boundary conditions $\sigma_{L+1}^\alpha \equiv \sigma_1^\alpha$ and restrict to even L. The $\mathbb{Z}_2$ symmetry of the model is implemented by the parity operator $\mathcal{P} = \prod_{i=1}^{L} \sigma_i^x$, resulting in a decomposition of the Hilbert space into a direct sum of parity odd ($\mathcal{P} = -1$) or even ($\mathcal{P} = +1$) subspaces [125], each of dimension 2^{L-1} – the so-called Ramond (R) and Neveu-Schwarz (NS) sectors, respectively. We shall focus on the NS sector only.

In terms of Jordan-Wigner fermions c_j, after the discrete Fourier transform,

$$c_j = \frac{e^{-i\pi/4}}{\sqrt{L}} \sum_{k \in \mathrm{BZ}} c_k e^{ikj}, \tag{2.2}$$

the hamiltonian can be written as $H(t) = \sum_{k>0} H_k(t)$ with

$$H_k(t) = [2g(t) - \omega_k](c_k^\dagger c_k + c_{-k}^\dagger c_{-k}) + \Delta_k(c_k^\dagger c_{-k}^\dagger + c_{-k} c_k) - \omega_k, \tag{2.3}$$

where $\omega_k = 2J\cos k, \Delta_k = 2J\sin k$, and we have neglected the trivial contribution $-2Lg(t)$. The momenta are constrained to the first Brillouin zone, $\mathrm{BZ} = \{\pm\frac{\pi}{L}, \pm\frac{3\pi}{L}, \ldots, \pm\frac{(L-1)\pi}{L}\}$ by the antiperiodic boundary condition satisfied by the c_j in the NS sector.

Since the hamiltonian conserves momentum and parity, the state of a system initialized in a ground state of the undriven model will acquire at any time t the following form [94, 116, 126],

$$|\psi(t)\rangle = \bigotimes_{k>0} \left[u_k(t)\,|1_{-k}1_k\rangle + v_k(t)\,|0_{-k}0_k\rangle\right], \tag{2.4}$$

that is, for each k-th mode the dynamics is restricted to the two-level Nambu subspace spanned by $\{|0_{-k}0_k\rangle, |1_{-k}1_k\rangle\}$. One can unify the coefficients into the spinor $\Psi_k(t) \equiv (u_k(t)\ v_k(t))^\intercal$, which obeys Schrödinger equation generated by the Bogoliubov-de Gennes (BdG) hamiltonian (2.3), such that the dynamics of each momentum mode takes the form of a driven two-level system. In terms of $\mathfrak{u}(2)$ generators, one has

$$H_k(t) = \big(2g(t) - \omega_k\big)\,\sigma_k^z + \Delta_k\,\sigma_k^x - \omega_k\,\mathbb{1}_k\,. \tag{2.5}$$

We now make an insert on some basic facts from Floquet theory that will be used in what follows.

2.2.1 Elements of Floquet dynamics

When the hamiltonian is a periodic function of time,

$$H(t) = H(t+T)\,, \qquad T \equiv \frac{2\pi}{\Omega}\,, \tag{2.6}$$

where T is the period and Ω is the driving frequency, we have to deal with the time-dependent Schrödinger equation,

$$\mathrm{i}\partial_t \Psi(t) = H(t)\Psi(t)\,. \tag{2.7}$$

This is a first order differential equation with periodic coefficients, such that the Floquet theorem [127, 128] applies and, accordingly, the solution to (2.7) reads

$$\Psi(t) = \sum_a c_a\, e^{\mathrm{i}\,t\,\varepsilon_a}\,\Phi_a(t), \tag{2.8}$$

where ε_a denote the quasi-energies of the state $\Psi(t)$ and the so-called Floquet states inherit the periodicity of the hamiltonian, $\Phi_a(t) = \Phi_a(t + 2\pi\Omega^{-1})$. This periodicity reflects on a family of shifted quasienergies that could be associated to the same state $\Psi(t)$ – and therefore they are not actual energies – which are defined modulo Ω: $\varepsilon_{a,n} \equiv \varepsilon_a + n\Omega$. For each equivalence class, $\{(\Phi_{i,n}(t), \varepsilon_{i,n})\}_{n\in\mathbb{Z}}$, one can choose an integer n in order to translate the corresponding quasienergy to lie in the interval $[-\Omega/2, \Omega/2)$.

The eigenvalue equation for the quasienergies is obtained by inserting a Floquet state, $e^{\mathrm{i}\,t\,\varepsilon_a}\Phi_a(t)$,

into (2.7), which leads to

$$\mathcal{H}(t)\Phi_a(t) = \varepsilon_a \Phi_a(t)\,, \tag{2.9}$$

where

$$\mathcal{H}(t) = H(t) - \mathrm{i}\,\partial_t \tag{2.10}$$

is the so-called Floquet hamiltonian.

Given the above collection of results, we can resume the discussion that led to (2.5). According to the Floquet theorem, the solution of Schrödinger equation can be written as

$$\Psi_k(t) = \sum_{\lambda=\pm} A_\lambda e^{\mathrm{i}\,\varepsilon_k^{(\lambda)} t} \Phi_k^{(\lambda)}(t)\,, \tag{2.11}$$

where the Floquet modes $\Phi_k^{(\pm)}(t) = \Phi_k^{(\pm)}(t + 2\pi\Omega^{-1})$ are periodic with the same period of the external driving and satisfy the time-independent Schrödinger equation for the Floquet hamiltonian $\mathcal{H}_k \equiv H_k(t) - \mathrm{i}\,\partial_t$. The Floquet quasienergies $\varepsilon_k^{(\lambda)}$ are only defined modulo Ω since $e^{\mathrm{i}\,m\Omega t}\,\Phi_k^{(\pm)}(t)$ for any $m \in \mathbb{Z}$ obviously defines another Floquet mode with quasienergy shifted by $m\Omega$, meaning in particular that the driven system admits no notion of ground state. For simplicity, in the following section we discuss exact solutions in the limit of high Ω following [129, 119]. Generalizations to low Ω are possible using the full exact solution [130] or the $1/\Omega$ expansion of [131].

2.2.2 Warm-up: Floquet dynamics of a two-level system in the high frequency limit

This section is based on [129]. We will show how to reduce a two-level system with a time-dependent harmonic perturbation to a time-independent problem when the external frequency is large. The upshot of this exercise will be used as a guide for the next section.

Let us consider a two-level system described by the following time-dependent hamiltonian

$$H(t) = -\frac{\Delta}{2}\sigma^x - \frac{g(t)}{2}\sigma^z = -\frac{1}{2}\begin{pmatrix} g(t) & \Delta \\ \Delta & -g(t) \end{pmatrix}, \tag{2.12}$$

where σ^i are Pauli matrices, Δ is a constant coupling, and $g(t) = g_0 + g_1 \cos\Omega t$ is a periodic driving.

Our strategy consists in invoking a unitary transformation $U(t)$ to a new frame that rotates in phase with $g(t)$. This can be achieved by going to the interaction picture and writing $H(t) = H_0(t) + H_1$, with $H_1 \equiv -\frac{\Delta}{2}\sigma^x$ treated as a perturbation with respect to $H_0(t) \equiv -\frac{1}{2}(g_0 + g_1\cos\Omega t)\sigma^z$. The corresponding transformation is given by

$$\mathcal{R}(t) = e^{-\mathrm{i}\int_0^t \mathrm{d}t'\, H_0(t')} = e^{\frac{\mathrm{i}}{2}\alpha(t)\sigma^z}, \tag{2.13}$$

where

$$\alpha(t) = \int_0^t \mathrm{d}t' \, \left(g_0 + g_1 \cos \Omega t'\right) = g_0 t + \frac{g_1}{\Omega} \sin \Omega t. \tag{2.14}$$

The hamiltonian in the interaction picture is $H_I(t) = \mathcal{R}^\dagger(t) H(t) \mathcal{R}(t) = H_0(t) + \widetilde{H}_1(t)$, which has the same free contribution and a rotating part,

$$\widetilde{H}_1(t) = -\frac{\Delta}{2} \begin{pmatrix} 0 & e^{-\mathrm{i}\,\alpha(t)} \\ e^{\mathrm{i}\,\alpha(t)} & 0 \end{pmatrix} = -\frac{\Delta}{2} \cos \alpha(t)\, \sigma^x - \frac{\Delta}{2} \sin \alpha(t)\, \sigma^y \,. \tag{2.15}$$

States $|\psi(t)\rangle$ are therefore mapped to $|\widetilde{\psi}(t)\rangle = \mathcal{R}^\dagger(t)|\psi(t)\rangle$, whose Schrödinger evolution is fully dictated by $\widetilde{H}_1(t)$.

The key-point in the following is the use of the Jacobi-Anger identity,

$$e^{\mathrm{i}\, z \sin \Omega t} = \sum_{\ell=-\infty}^{\infty} \mathcal{J}_\ell(z) \exp(\mathrm{i}\, \ell \Omega t) = \sum_{\ell=-\infty}^{\infty} (-1)^\ell \mathcal{J}_\ell(z) \exp(-\mathrm{i}\, \ell \Omega t), \tag{2.16}$$

where $\mathcal{J}_\ell(z)$ are Bessel functions of the first kind, to rewrite (2.15) in the Fourier-like form

$$\widetilde{H}_1(t) = -\frac{\Delta}{2} \sum_{\ell=-\infty}^{\infty} \mathcal{J}_\ell \left(\frac{g_1}{\Omega}\right) \begin{pmatrix} 0 & e^{-\mathrm{i}(g_0 - \ell\Omega)t} \\ e^{\mathrm{i}(g_0 - \ell\Omega)t} & 0 \end{pmatrix} . \tag{2.17}$$

We now perform the high-frequency approximation by assuming that all terms in the summation oscillate wildly and can be neglected with respect to a single resonant term defined by the condition

$$g_0^{(\ell)} = \ell\, \Omega, \qquad \ell \in \mathbb{Z}. \tag{2.18}$$

We shall refer to $g_0^{(\ell)}$ as the ℓ-th resonance.

Therefore, the effective hamiltonian describing the dynamics of the system in the ℓ-th resonance becomes time-independent and it assumes the simple form

$$H_{1,I}^{(\ell)} = -\frac{\Delta}{2} \mathcal{J}_\ell \left(\frac{g_1}{\Omega}\right) \sigma^x \,. \tag{2.19}$$

Thus, an initial eigenstate of σ_z, $|\psi_I(0)\rangle = |0\rangle$, for instance, that evolves in time under (2.19) is well-known to oscillate between $|1\rangle$ and $|0\rangle$ with frequency $\omega^{(\ell)} = \left|\Delta\, \mathcal{J}_\ell\, (g_1/\Omega)\right|$.

The lesson of our warm-up can be summarized as follows: in the high-frequency approximation for the system at the ℓ-th resonance, the analysis reduces to a very simple static problem in the rotating frame, given by (2.19). As soon as one finds the time-evolution of a state $|\psi_I(t)\rangle$, the outcome of interest, $|\psi(t)\rangle$, can be found by rotating back to the original – Schrödinger – frame with the action of $\mathcal{R}^\dagger(t) = e^{-\frac{\mathrm{i}}{2}\alpha(t)\sigma^z}$.

2.2.3 High-frequency driving approximation

We are now in position to evoke the experience of Section 2.2.2 to proceed the analysis of the hamiltonian (2.5).

It will be convenient to split the constant part of the transverse field as $g_0 = \delta g_0 + \tilde{g}_0$, where $\tilde{g}_0$ is a resonant value (to be determined) and $\delta g_0 \equiv g_0 - \tilde{g}_0$ is a detuning measuring the distance to this resonance.

The dynamics can then be solved by going to a rotating frame tweaked to the driving field $g(t)$ through a unitary transformation $\mathcal{R}_k(t)$. First we split $H_k(t) = H_k^0(t) + H_k^1$ with $H_k^0(t) \equiv 2(\tilde{g}_0 + g_1 \cos\Omega t)\,\sigma_k^z$ and $H_k^1 \equiv \Delta_k\,\sigma_k^x + (2\delta g_0 - \omega_k)\,\sigma_k^z - \omega_k\,\mathbb{1}_k$ and go to the interaction picture with H_k^1 as the interaction hamiltonian. The desired transformation is the time evolution operator associated with $H_k^0(t)$, namely

$$\mathcal{R}_k(t) = e^{-\frac{\mathrm{i}}{2}\alpha(t)\sigma_k^z}, \quad \alpha(t) = 4\tilde{g}_0 t + \frac{4g_1}{\Omega}\sin\Omega t\,. \tag{2.20}$$

The rotated hamiltonian $\tilde{H}_k(t) \equiv \mathcal{R}_k^\dagger(t) H_k(t) \mathcal{R}_k(t) = H_k^0(t) + \tilde{H}_k^1(t)$ has the same free contribution and a rotating part given by

$$\tilde{H}_k^1(t) = \begin{pmatrix} 2\delta g_0 - 2\omega_k & \Delta_k e^{\mathrm{i}\,\alpha(t)} \\ \Delta_k e^{-\mathrm{i}\,\alpha(t)} & -2\delta g_0 \end{pmatrix}. \tag{2.21}$$

States $|\psi(t)\rangle_k$ whose dynamics is governed by Equation (2.5) are mapped to rotated states $|\tilde{\psi}(t)\rangle_k = \mathcal{R}_k^\dagger(t)\,|\psi(t)\rangle_k$ with Schrödinger time evolution dictated by (2.21). The full rotated hamiltonian $\tilde{H}^1(t) \equiv \sum_{k>0} \tilde{H}_k^1(t)$ in terms of the original spins contains all possible nearest-neighbor free fermion terms σ_i^x, $\sigma_i^z\sigma_{i+1}^z$, $\sigma_i^y\sigma_{i+1}^y$, $\sigma_i^z\sigma_{i+1}^y$, $\sigma_i^y\sigma_{i+1}^z$ [119].

In order to determine the resonance condition, we first make use of the Jacobi-Anger expansion $e^{\mathrm{i}\,z\sin\Omega t} = \sum_{n\in\mathbb{Z}} \mathcal{J}_n(z)\exp(\mathrm{i}\,n\Omega t)$, where $\mathcal{J}_n(z)$ are Bessel functions of the first kind, to rewrite (2.21) in the form $\tilde{H}_k^1(t) = \sum_{n\in\mathbb{Z}} \tilde{h}^{(n)} e^{\mathrm{i}(4\tilde{g}_0 - n\Omega)t}$ for some $\tilde{h}^{(n)}$. Then, the high-frequency approximation (sometimes referred as rotating wave approximation) is performed assuming that all the terms in the summation oscillate wildly and can be neglected with respect to a single resonant term given by

$$\tilde{g}_0^{(\ell)} = \ell\frac{\Omega}{4}, \quad \ell \in \mathbb{Z}\,. \tag{2.22}$$

The corresponding detuning parameter will be denoted by $\delta g_0^{(\ell)} = g_0 - \tilde{g}_0^{(\ell)}$. As a result, the effective hamiltonian describing the dynamics of the system at the ℓ-th resonance becomes time-independent.

In terms of the original spins, the full rotating frame hamiltonian $\tilde{H}^{1(\ell)} = \sum_{k>0} \tilde{H}_k^{1(\ell)}$ takes the form

$$\tilde{H}^{1(\ell)} = -\sum_{j=1}^{L}\left[\delta g_0^{(\ell)}\sigma_j^x + J_+^{(\ell)}\sigma_j^z\sigma_{j+1}^z + J_-^{(\ell)}\sigma_j^y\sigma_{j+1}^y\right] \tag{2.23}$$

with $J_\pm^{(\ell)} \equiv \frac{J}{2}(1 \pm \gamma^{(\ell)})$ and

$$\gamma^{(\ell)} \equiv (-1)^{\ell} \mathcal{J}_{\ell}\left(\frac{4g_1}{\Omega}\right). \tag{2.24}$$

This is unitarily equivalent to the familiar transverse XY chain with anisotropy parameter $\gamma^{(\ell)}$ [125, 132]. The non-trivial dependence of $\gamma^{(\ell)}$ on ℓ, Ω, g_1 already anticipates the influence of the driving on the critical behavior of the system, to be confirmed in the next section. Near the resonance there is pure coupling between the two-level system basis states at $\min_k |\omega_k|$, with oscillation frequency given by $\omega_{\text{eff}} = J|\gamma^{(\ell)}|$, indicating that this large-Ω approximation remains valid as long as $\delta g_0^{(\ell)}, \omega_{\text{eff}} \ll \Omega$.

2.2.4 Nonequilibrium QPTs in the rotating frame

The XY model (2.23) describing the high-Ω dynamics in the rotating frame is exactly solvable via Jordan-Wigner and discrete Fourier transforms following closely the discussion for the TFIM in Section 2.2. The Bogoliubov angle $\vartheta_{k,\ell}$ defined by

$$\tan(2\vartheta_{k,\ell}) = \frac{\Delta_k \gamma^{(\ell)}}{2\delta g_0^{(\ell)} - \omega_k} \tag{2.25}$$

diagonalizes the corresponding BdG hamiltonian to the free fermion form $\tilde{H}^{1(\ell)} = \sum_{k>0} \epsilon_{k,\ell}\left(b_k^{\dagger} b_k - \frac{1}{2}\right)$ with

$$\epsilon_{k,\ell} = \sqrt{\left(2\delta g_0^{(\ell)} - \omega_k\right)^2 + \left(\Delta_k \gamma^{(\ell)}\right)^2}. \tag{2.26}$$

The positive and negative energy eigenstates, with eigenvalues $\epsilon_{k,\ell}^{\pm} = -\omega_k \pm \epsilon_{k,\ell}$, are $\phi_{k,+}^{(\ell)} = (\cos\vartheta_{k,\ell} - \sin\vartheta_{k,\ell})^{\intercal}$ and $\phi_{k,-}^{(\ell)} = (\sin\vartheta_{k,\ell} \;\; \cos\vartheta_{k,\ell})^{\intercal}$.

The model is known to present two critical lines: an Ising-like QPT between a ferromagnetic and a paramagnetic phase at $|\delta g_0^{(\ell)}| = J$; and an anisotropic QPT at $\gamma^{(\ell)} = 0$ (provided that $|\delta g_0^{(\ell)}| < J$) between two distinct phases FMY ($\gamma^{(\ell)} < 0$) and FMZ ($\gamma^{(\ell)} > 0$) with ferromagnetic order along the y and z directions, respectively. For a given ℓ, the former defines a pair of lines $\delta g_0^{(\ell)} = \pm J$ while the latter corresponds to an infinite family of critical lines, one for each zero of $\mathcal{J}_{\ell}(z)$. The phase diagram as a function of the transverse field strengths g_0, g_1 for fixed (and large) Ω is illustrated in Figure 2.1. The FMY-FMZ transition lines are almost evenly spaced (except for the first few) since the sequence $\{z_{i+1} - z_i\}_{i\in\mathbb{Z}^+}$ of differences between two subsequent Bessel zeros converges very quickly to the constant value π, as seen intuitively from the asymptotic behavior $\mathcal{J}_{\ell}(z) \approx \sqrt{\frac{2}{\pi z}}\cos\left[z - (2\ell+1)\frac{\pi}{4}\right]$ at $z \gg \ell$. Note that in the special case $\delta g_0^{(\ell)} = 0$, i.e., when g_0 is tuned exactly to the resonant value $g_0^{(\ell)}$, the transverse field in (2.23) disappears and we are left only with the anisotropic transitions.

The horizontal lines in Figure 2.1 occur at $\gamma^{(\ell)} = 0$, where $\omega_{\text{eff}} = 0$ forces the quantum tunneling between σ_k^z eigenstates to completely freeze. This phenomenon, known as coherent destruction of tunneling (CDT), occurs at every sector k once the driving amplitude is fine-tuned to one of the Bessel zeros, leading to a coherent suppression of the dynamics even at infinite L. We will show how

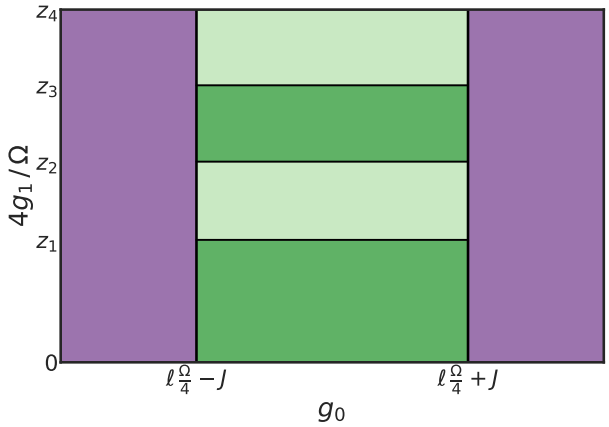

Figure 2.1: Non-equilibrium phase diagram as a function of the transverse field strengths g_0, g_1 in the high-Ω regime. The phases are PM (purple), FMZ (green) and FMY (light green). Vertical and horizontal lines identify the Ising-like and anisotropic phase transitions, respectively. The latter are located at z_i, the i-th root of $\mathcal{J}_\ell(z)$ ($\ell = 2$ shown in the plot); the width $z_{i+1} - z_i$ quickly approaches π as i grows.

this dynamic localization effect manifests in the circuit complexity in the next section.

2.2.5 Floquet modes and quasienergies

The Floquet modes that define a basis for the dynamics in the Schrödinger picture follow by applying $\mathcal{R}_k$ to the eigenstates of the XY hamiltonian,

$$\Phi^{(\ell)}_{k,\pm}(t) \equiv e^{-\mathrm{i}\left(\frac{\ell\Omega}{2}t + \frac{2g_1}{\Omega}\sin\Omega t\right)} \mathcal{R}^{(\ell)}_k(t)\, \phi^{(\ell)}_{k,\pm} \tag{2.27}$$

(the $U(1)$ phase is added for convenience) and correspond to quasienergies

$$\varepsilon^{\pm}_{k,\ell} \equiv -\omega_k \pm \epsilon_{k,\ell} + \frac{\ell\Omega}{2}\,. \tag{2.28}$$

Here we recall that there is an infinite family of Floquet modes, labelled by an integer m that is omitted here, corresponding to the rescaling $\Phi^{(\ell)}_{k,\pm}(t) \to e^{\mathrm{i}m\Omega t}\, \Phi^{(\ell)}_{k,\pm}(t)$ and shift $\varepsilon^{\pm}_{k,\ell} \to \varepsilon^{\pm}_{k,\ell} + m\Omega$. We choose the $m = 0$ representative without loss of generality.

Finally, the general solution (2.11) with initial condition $\Psi^{(\ell)}_k(0) \equiv \left(u^{(\ell)}_k(0)\ v^{(\ell)}_k(0)\right)^{\intercal}$ is completely determined due to the orthogonality of the Floquet modes by the coefficients $A^{\pm}_{k,\ell} \equiv \Psi^{(\ell)}_k(0)\, \phi^{(\ell)}_{k,\pm}$. We will focus on $\Psi^{(\ell)}_k(0) = \left(0\ 1\right)^{\intercal}$, i.e., a system initialized in the paramagnetic state of the undriven model with all the spins aligned along the x direction, $\bigotimes_{k>0} |0_k 0_{-k}\rangle$, corresponding to $A^{+}_{k,\ell} = -\sin\vartheta_{k,\ell}$ and $A^{-}_{k,\ell} = \cos\vartheta_{k,\ell}$. In terms of the spinor components introduced in (2.4), the explicit solution $\Psi^{(\ell)}_k(t)$ reads (up to a global phase $e^{-\mathrm{i}\varepsilon^{-}_{k,\ell}t}$)

$$\begin{pmatrix} u^{(\ell)}_k(t) \\ v^{(\ell)}_k(t) \end{pmatrix} = \begin{pmatrix} e^{-\mathrm{i}\,\alpha^{(\ell)}(t)}\left(1 - e^{-2\mathrm{i}\,\epsilon_{k,\ell}t}\right)\sin\vartheta_{k,\ell}\cos\vartheta_{k,\ell} \\ \cos^2\vartheta_{k,\ell} + e^{-2\mathrm{i}\,\epsilon_{k,\ell}t}\,\sin^2\vartheta_{k,\ell} \end{pmatrix}. \tag{2.29}$$

2.3 Complexity across nonequilibrium QPTs

In this Section we discuss the circuit complexity of the instantaneous states (2.4) using the geometric approach introduced in [90, 91]. Namely, we look for the optimal circuit $U = U(t)$ connecting the reference and target states, $|T\rangle = U|R\rangle$, with $|R\rangle = \bigotimes_{k>0} |0_k 0_{-k}\rangle$ and $|T\rangle = |\Psi(t)\rangle$. Note that we choose $|R\rangle$ to be the same as the initial condition $|\Psi(0)\rangle$ so that the complexity starts from a vanishing value at $t = 0$. Factorization of states in fixed-momentum sectors implies that $U = \bigotimes_{k>0} U_k$. In terms of Nambu spinors, each admissible U_k is a Bogoliubov transformation taking the reference spinor $\Psi_k^R = (0\ 1)^\intercal$ to $\Psi_k^{(\ell)}(t) = (u_k^{(\ell)}(t)\ v_k^{(\ell)}(t))^\intercal$ derived in (2.29). Since these are $SU(2)$ transformations, it is natural to seek for factorized circuits $\mathcal{U}(s) = \bigotimes_{k>0} \mathcal{U}_k(s)$ with each factor having the hamiltonian form

$$\mathcal{U}_k(s) = \mathcal{P} e^{\int_0^s H_k(s')\mathrm{d}s'}, \quad H_k(s') \equiv \sum_I Y_k^I(s') \mathcal{O}_I, \tag{2.30}$$

where $s \in [0,1]$ is a continuous parameter, the functions $Y_k^I(s) = -\frac{1}{2} \operatorname{Tr}\left[\partial_s \mathcal{U}_k(s)\, \mathcal{U}_k(s)^{-1} \mathcal{O}_I\right]$ identify a particular circuit, $\mathcal{O}_I \in \{\mathrm{i}\sigma^x, \mathrm{i}\sigma^y, \mathrm{i}\sigma^z\}$ are the $\mathfrak{su}(2)$ generators (our fundamental gates), and $\mathcal{P}$ a path-ordering operator ensuring that the circuit is built from smaller to larger values of s. The boundary conditions $\mathcal{U}_k(s=0) = \mathbb{1}$ and $\mathcal{U}_k(s=1) = U_k$ guarantee that any such circuit implements the desired task of connecting the two given states. The optimal circuit is found by minimizing an associated depth functional, $\mathcal{D}[\mathcal{U}_k] = \int_0^s \mathrm{d}s' F\big(\{Y_k(s')\}\big)$, and the corresponding complexity corresponds to the depth of this optimal circuit,

$$\mathcal{C}[\mathcal{U}_k] = \min_{\{Y_k^I(s)\}} \mathcal{D}[\mathcal{U}_k] = \mathcal{D}[\mathcal{U}_k^{\mathrm{opt}}]\,. \tag{2.31}$$

We choose as cost function F the Euclidean norm $F\big(\{Y_k\}\big) = \big(\sum_I |Y_k^I|^2\big)^{1/2}$, which is the simplest one satisfying all the required properties from complexity measures [90] (see [102] for alternatives).

To solve the minimization problem it will be convenient to use the polar representation of the components of (2.29), namely $v_k^{(\ell)}(t) \equiv \cos\Theta_{k,\ell}(t)\, e^{\mathrm{i}\,\varphi^v_{k,\ell}(t)}$ and $u_k^{(\ell)}(t) \equiv \sin\Theta_{k,\ell}(t)\, e^{\mathrm{i}\,\varphi^u_{k,\ell}(t)}$ with $0 \leq \Theta_{k,\ell}(t) \leq \pi/2$, and further discarding a global phase to choose the element in the ray of $\Psi_k^{(\ell)}(t)$ to be

$$\Psi_k^{(\ell)}(t) = \begin{pmatrix} e^{\mathrm{i}\,\beta_{k,\ell}(t)} \sin\Theta_{k,\ell}(t) \\ \cos\Theta_{k,\ell}(t) \end{pmatrix} \tag{2.32}$$

with $\beta_{k,\ell}(t) \equiv \varphi^u_{k,\ell}(t) - \varphi^v_{k,\ell}(t)$. The Bogoliubov transformation to be implemented thus assumes the form

$$U_k = \begin{pmatrix} \cos\Theta_{k,\ell}(t) & e^{\mathrm{i}\,\beta_{k,\ell}(t)} \sin\Theta_{k,\ell}(t) \\ -e^{-\mathrm{i}\,\beta_{k,\ell}(t)} \sin\Theta_{k,\ell}(t) & \cos\Theta_{k,\ell}(t) \end{pmatrix}. \tag{2.33}$$

This suggests a parametrization of the circuit $\mathcal{U}_k(s) \in SU(2)$ for each momentum sector k in terms of Hopf coordinates (ϕ_1, ϕ_2, ω),

$$\mathcal{U}_k(s) = \begin{pmatrix} e^{i\phi_1(s)}\cos\omega(s) & e^{i\phi_2(s)}\sin\omega(s) \\ -e^{-i\phi_2(s)}\sin\omega(s) & e^{-i\phi_1(s)}\cos\omega(s) \end{pmatrix} . \tag{2.34}$$

With this at hand, it is straightforward to show that the optimal circuit minimizes the functional

$$\mathcal{D}[\mathcal{U}_k] = \int_0^1 ds' \sqrt{\omega'^2 + \cos^2\omega\,\phi_1'^2 + \sin^2\omega\,\phi_2'^2}\,. \tag{2.35}$$

The minimum corresponds to constant phase functions $\phi_1(s) = \phi_1^0, \phi_2(s) = \phi_2^0$ and the linear profile $\omega(s) = \omega_0 + s\,\omega_1$, which immediately implies $\mathcal{D}[\mathcal{U}_k^{\rm opt}] = |\omega_1|$. The boundary condition at $s = 0$ then fixes $\phi_1^0 = 0$ and $\omega_0 = 0$, while the one at $s = 1$ fixes $\omega_1 = \Theta_{k,\ell}(t)$ and $\phi_2^0 = \beta_{k,\ell}(t)$. Putting all together and summing over all momentum sectors we obtain the circuit complexity $\mathcal{C}(t) = \sum_{k>0} |\Theta_{k,\ell}(t)|$ or, explicitly,

$$\mathcal{C}(t) = \sum_{k>0} \left| \arcsin\left(\frac{\Delta_k \gamma^{(\ell)}}{\epsilon_{k,\ell}} \sin(\epsilon_{k,\ell} t) \right) \right| . \tag{2.36}$$

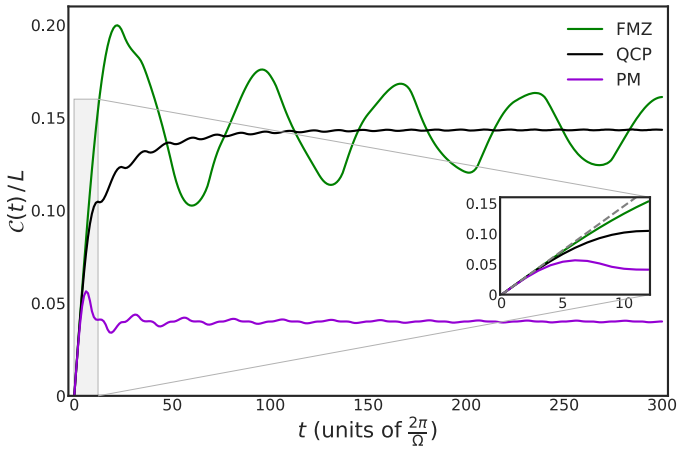

Figure 2.2: Time evolution of the complexity (2.36) near the Ising non-equilibrium transition. The parameters are $L = 1000, \ell = 2, J = 0.01\Omega, g_1 = \Omega$ and varying $\delta g_0^{(\ell)} = (0, J, 2J)$, corresponding respectively to the ferromagnetic phase (FMZ), the quantum critical point (QCP), and the paramagnetic phase (PM). The dashed line in the inset shows the universal linear growth (2.37) at early times.

The full time evolution of $\mathcal{C}(t)$ is depicted in Figure 2.2 for the Ising-like non-equilibrium QPT controlled by g_0. The early time behavior is readily obtained by a series expansion of (2.36), with the summation over momenta performed analytically for the leading term to yield

$$\mathcal{C}(t \to 0) = \frac{2J\,|\gamma^{(\ell)}|}{\sin\frac{\pi}{L}}\, t + \mathcal{O}(t^3)\,. \tag{2.37}$$

Note that in the thermodynamic limit $L \to \infty$ one has a volume law, $\mathcal{C} \sim L$. Interestingly, the linear growth at early times is independent of the constant field g_0. The inset in Figure 2.2 shows this universal early time behavior, which can be estimated to hold up to a time scale $t_*(g_0) \sim \min_k |2\delta g_0^{(\ell)} - \omega_k|^{-1} \approx \big|2|g_0 - g_0^{(\ell)}| + 2J\big|^{-1}$.

The complexity clearly distinguishes between the two phases and the critical point – in particular, it never equilibrates for g_0 in the FMZ phase. In the PM phase, it reaches the steady value $\mathcal{C}_\infty^{\rm PM}$ more

rapidly for increasingly g_0, as one can infer from $t_*(g_0)$ estimated above and confirm numerically. Note that $\mathcal{C}_\infty^{\rm PM}$ is bounded from above by the value at the critical point $\mathcal{C}_\infty^{\rm QCP}$ and, in particular, it decreases as g_0 grows. Physically, this is an expression of the disordered character of the PM phase: complex (i.e., non-local) operations are required to create order in a state prepared on it, while simple (local) operations, like a phase shift, would maintain the disorder of such state. When g_0 is large, the effect of the driving field is suppressed and does not favor the possibility of creating operators complex enough to order the system, keeping it close to the initial paramagnetic ground state.

The critical behavior becomes more evident in terms of the time-averaged complexity

$$\overline{\mathcal{C}} = \lim_{T\to\infty} \frac{1}{T} \int_0^T \mathrm{d}t\, \mathcal{C}(t)\,. \tag{2.38}$$

This quantity develops a non-analytic behavior at the QCP, as shown in Figure 2.3. Such discontinuity becomes manifest as divergences in the derivatives at the critical points. This critical behavior is reminiscent from the behavior of the complexity in the undriven Ising model, which is discussed in Section 2.4.

Independently of g_0 it is evident that the complexity vanishes at the special anisotropic QPT points $\gamma^{(\ell)} = 0$ designed by tuning g_1 and Ω to the Bessel zeros. This is a manifestation of the previously mentioned dynamic localization or CDT phenomenon happening at these points that freezes the quantum dynamics to the initial paramagnetic state. We also note that (2.36) is symmetric under $\gamma^{(\ell)} \to -\gamma^{(\ell)}$, showing that the complexity is unable to distinguish between the FMY and FMZ phases separated by the CDT point. Near these points, we can check that $\overline{\mathcal{C}} \propto |\gamma^{(\ell)}| \propto |g_1 - g_1^c|$ to first order, which explains the type of non-analyticity observed in Figure 2.3(c). Such behavior is essentially due to the complexity of the Floquet mode Φ^-, since in this limit the Bogoliubov angle (2.25) approaches zero and, therefore, the amplitude for positive mode in (2.11), $A^+_{k,\ell} = -\sin\vartheta_{k,\ell}$, vanishes.

In fact, the similarity between $\overline{\mathcal{C}}$ and the complexity of Floquet modes is to be expected on more general grounds. At late times, after transients die out, the system synchronizes with the driving field and the dynamics is known to be governed by the Floquet modes [118]. Indeed, one can take a step further and make a concrete comparison by explicitly evaluating the complexity for each of the Floquet modes.

We first note that those are easily put in the convenient form (2.32),

$$\begin{aligned}
\Phi_k^{+(\ell)}(t) &\simeq \begin{pmatrix} e^{-\mathrm{i}\,\alpha^{(\ell)}(t)-\mathrm{i}\,\pi}\sin(\vartheta_{k,\ell}-\frac{\pi}{2}) \\ \cos(\vartheta_{k,\ell}-\frac{\pi}{2}) \end{pmatrix} \\
\Phi_k^{-(\ell)}(t) &\simeq \begin{pmatrix} e^{-\mathrm{i}\,\alpha^{(\ell)}(t)}\sin\vartheta_{k,\ell} \\ \cos\vartheta_{k,\ell} \end{pmatrix},
\end{aligned} \tag{2.39}$$

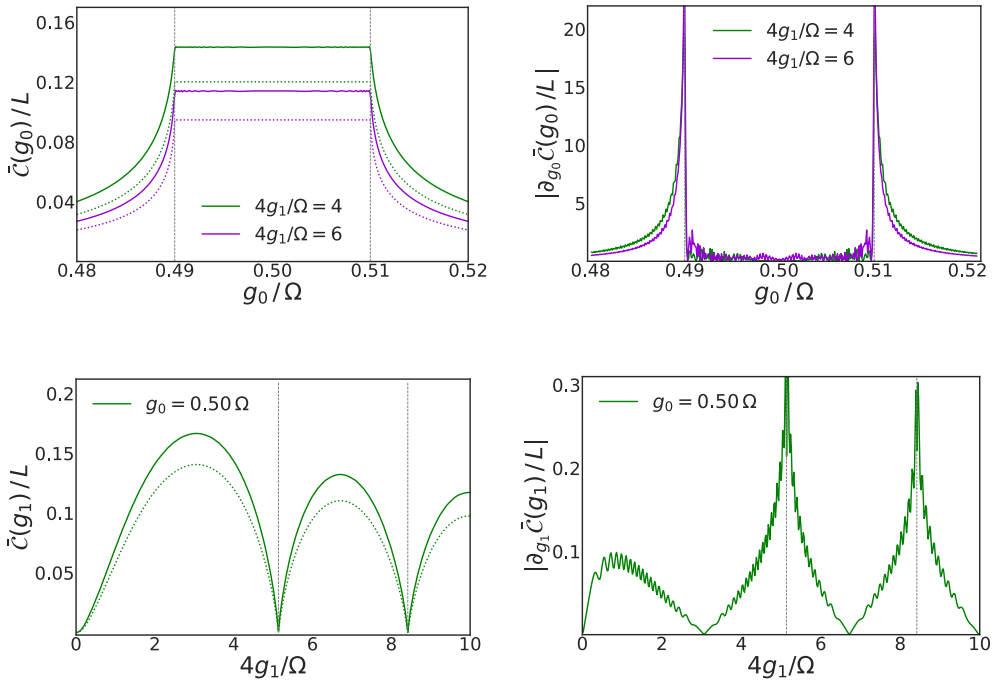

Figure 2.3: Time-averaged complexity $\overline{\mathcal{C}}$ over $T = 1000$ periods and its derivatives for $\ell = 2, \Omega = \pi, J = 0.01\Omega, L = 1000$. (a) $\overline{\mathcal{C}}$ close to the Ising QPT for two values of g_1; the dotted lines show the corresponding Floquet mode complexity $\mathcal{C}^-$; (b) singular behavior of the first derivative of $\overline{\mathcal{C}}$ at the QPT points; (c) and (d) repeat the analysis of (a) and (b) for the first two anisotropic QPT points.

from which the complexity follows trivially by paralleling the previous calculation and will be constant in time, namely $\mathcal{C}^+ = \sum_{k>0} \left|\vartheta_{k,\ell} - \frac{\pi}{2}\right|$ and $\mathcal{C}^- = \sum_{k>0} \left|\vartheta_{k,\ell}\right|$. When $t \to \infty$ we expect that the $e^{-2i\epsilon_{k,\ell}t}$ oscillations in (2.29) results in small contributions to the time-averaged complexity due to destructive interference (the same cannot be said about the $e^{-i\alpha^{(\ell)}(t)}$ prefactor, which contains the resonant term that survives to wild oscillations), so that the main contributions to $\overline{\mathcal{C}}$ come from the Floquet state $\Phi_k^{-(\ell)}(t)$. In other words, $\mathcal{C}(t \to \infty) \sim \mathcal{C}^-$ and, as consequence, the time average $\overline{\mathcal{C}}$ should replicate the behavior of $\mathcal{C}^-$, as indeed seen in Figure 2.3(a) and (c).

2.4 Insert: Complexity in the Ising model

In order to further illustrate how the circuit complexity can be used to diagnose an equilibrium QPT as well, let us evaluate it for the standard Ising model with a constant transverse field. We take both reference and target states belonging to the ground state manifold, that is, they can be written as $(\cos\eta_k^{(\mathrm{R,T})} + \mathrm{i}\sin\eta_k^{(\mathrm{R,T})})^{\otimes k>0}|0\rangle$ such that the complexity assumes the simple form $\mathcal{C} = \sum_k |\Delta\eta_k|$,

where $\Delta\eta_k$ is the relative Bogoliubov angle between $|R\rangle$ and $|T\rangle$. Here it is straightforward to work even in the infinite chain limit, where

$$\mathcal{C} = \frac{1}{2\pi}\int_0^\pi \mathrm{d}k\,|\Delta\eta_k|\,. \tag{2.40}$$

Using the usual spectrum and Bogoliubov angle of the Ising model, one can easily compute this object which is illustrated in Figure 2.4 where, for simplicity, we have chosen $\eta_k^{(\mathrm{R})} = 0$. The first derivative is discontinuous at the quantum critical point, $g_0 = J$, while the second-derivative diverges with a unit critical exponent, that is $\sim |g_0 - J|^{-1}$, as shown in Figure 2.4 (b).

Figure 2.4: (a) Complexity of the ground state of the undriven Ising model with $J = 1$; (b) $|g_0 - J|^{-1}$ behavior of the second derivative near the critical point.

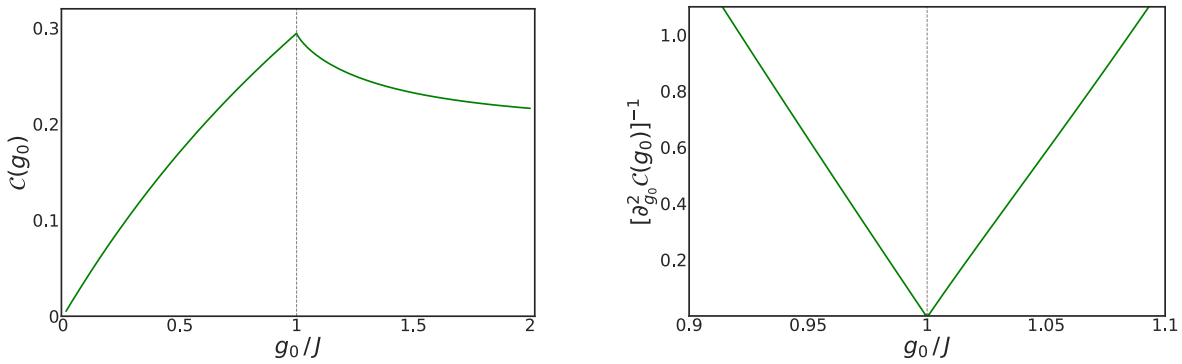

2.5 Final remarks

We have studied the Floquet dynamics of Nielsen's circuit complexity for the Ising model driven by a time periodic transverse field. At high enough driving frequency, the model is analytically tractable and admits an exact determination of the non-equilibrium phase transitions induced by the external field. Here we showed that the complexity is able to diagnose these non-equilibrium QPTs, extending previous ideas in the literature for quantum quench protocols and hence strengthening the case for complexity as a tool to understand the non-equilibrium physics of many-body systems. In particular, we showed that for a paramagnetic reference state, the complexity of the instantaneous time-evolved state can only equilibrate at large times provided the critical point is not crossed, otherwise it oscillates indefinitely in time. We also proved that the early time transient behavior of the complexity is linear and independent of the constant driving field g_0 up to a time scale inversely proportional to g_0. The long-time average of the complexity presents non-analytical behavior at the critical points, which can be traced back to the fact that the asymptotic dynamics is governed by the Floquet modes.

The sensitivity of the circuit complexity to non-equilibrium critical phenomena encourages us to investigate its role in the description of dynamical phase transitions (DQPTs) [133], which are characterized by a non-analytical behavior in the time domain and whose scaling and universality properties are not fully understood. These phenomena can be engineered using quantum quenches or in periodically driven systems similar to the one studied here [134]. The time evolution of complexity (analogue of Figure 2.2) should develop a singular behavior at the critical time and may help in the classification of non-trivial topological Floquet phases. We devote Section 2.6 to the preliminary analysis of such ideas.

Another interesting future direction to pursue would be to see how the present analysis generalizes to the case of interacting models, where more elaborate gates than simple $SU(2)$ rotations used here are required to produce physically interesting states. Here the set of integrable spin chains immediately comes to mind [135]. A more ambitious goal would be the study of a many-body localization/thermal transition, which can be modeled with a Floquet system with no conserved charges [136].

2.6 Afterword: Dynamical quantum phase transitions

The results presented in this section are currently under development and they will appear somewhere else [137].

Alternatively to the QPTs we have encountered in the previous sections, DQPTs are not caused by external perturbations from some field. Instead, such transitions emerge due to an intricate internal dynamics that eventually gives rise to a qualitatively new behavior. Analogous to what we have described during the discussion of QPTs in Section 1.2.2, DQPTs are usually diagnosed by a quantity closed to the quantum fidelity, the so-called *Loschmidt amplitude*,

$$\mathcal{G}(t) = \langle \Psi_i | \Psi_i(t) \rangle = \langle \Psi_i | e^{-\mathrm{i}Ht} | \Psi_i \rangle \,, \tag{2.41}$$

where $|\Psi_i\rangle$ is some initial state. To wit, a DQPT occur whenever $\mathcal{G}(t)$ displays a non-analyticity.

The critical behavior of the Loschmidt amplitude can be exposed by considering its analytic continuation to the complex plane via $z = t + \mathrm{i}\tau$. For a lattice system with finite number of spins, N, one can express $\mathcal{G}(z)$ in the energy eigenbasis $\{|E_a\rangle\}$ as

$$\mathcal{G}(z) = \sum_{a=1}^{N} |\langle E_a | \Psi_i \rangle|^2 e^{-\mathrm{i}E_a z} \,, \tag{2.42}$$

where each term in the sum is analytic and, therefore, this is an entire function. As such, we can use

the Weierstrass factorization theorem to write

$$\mathcal{G}(z) = e^{f(z)} \prod_a (z_a - z)\,, \tag{2.43}$$

where the isolated poles z_a are known as Fisher zeros and $f(z)$ is an analytic function. By taking the thermodynamic limit $N \to \infty$, there exits the possibility of z_a to condense into a branch cut, which is a sign of a phase transition.

2.6.1 DQPT in the driven transverse Ising model

Let us take a closer look at the k-th mode complexity (2.36), which we repeat here for convenience,

$$\mathcal{C}_k(t) = \left| \arcsin \left(\frac{\Delta_k \gamma^{(\ell)}}{\epsilon_{k,\ell}} \sin(\epsilon_{k,\ell} t) \right) \right| . \tag{2.44}$$

Whenever $\Delta_k \gamma^{(\ell)} = \epsilon_{k,\ell}$, this will develop a $\sim |t|$ type of non-analyticity. The particular mode which satisfies this condition is found to be

$$\cos k^* = \frac{\delta g_0^{(\ell)}}{J} . \tag{2.45}$$

Then, the critical mode complexity reads

$$\mathcal{C}_{k^*}(t) = \left| \arcsin \left[\sin \left(\frac{\pi t}{t^*} \right) \right] \right| , \tag{2.46}$$

where

$$t^* = \frac{\pi}{\epsilon^*_{k,\ell}} = \frac{\pi}{2|\gamma^{(\ell)}| \sqrt{J^2 - \left(\delta g_0^{(\ell)}\right)^2}} . \tag{2.47}$$

In conclusion, the non-analyticities in the time evolution will show up at

$$t_n = \left(n + \frac{1}{2} \right) t^* , \tag{2.48}$$

when the arcsine changes to another branch. For instance, if we restrict to $t \in [0, t^*]$, equation (2.46) can be written in the more suggestive form $\mathcal{C}_{k^*}(t) = \left| \pi/2 - |\pi t/t^* - \pi/2| \right|$ that clearly shows the presence of a kink at $t = t^*/2$. Therefore, unless $t^* = \infty$, which happen at the critical points, $|\delta g_0^{(\ell)}| = J$ and $\gamma^{(\ell)} = 0$, the critical time is finite and it defines a Floquet DQPT.

2.6.2 DQPT for quenches in the transverse Ising model

We now consider a different nonequilibrium protocol – a quantum quench. For simplicity, let us consider the transverse field Ising model by taking $g_1 = 0$ in (2.1) and a quench from $g_0 = g_\mathrm{i}$ to $g_0 = g_\mathrm{f}$ that crosses the critical point.

The instantaneous post-quench state can be written as [138, 139]

$$|\Psi(t)\rangle = \prod_k \left[\cos(\Delta\theta_k) - \mathrm{i}\, e^{2\mathrm{i}\epsilon_k t} \sin(\Delta\theta_k) A_k^\dagger A_{-k}^\dagger\right] |0\rangle\,, \tag{2.49}$$

where the dispersion relation is simply

$$\epsilon_k = \sqrt{(g_0 + \cos k)^2 + \sin^2 k}, \tag{2.50}$$

and $\Delta\theta_k = \theta_k(g_\mathrm{f}) - \theta_k(g_\mathrm{i})$ is the relative Bogoliubov angle, defined as

$$\tan 2\theta_k(g_0) = \frac{\sin k}{g_0 - \cos k}\,. \tag{2.51}$$

Both the energy levels ϵ_k and the creation operators $A_k^\dagger$ are associated with the post-quench hamiltonian.

The complexity again takes the factorized form, $\mathcal{C}(t) = \sum_k \mathcal{C}_k(t)$, with [97]

$$\mathcal{C}_k(t) = \left|\arccos\sqrt{1 - \sin^2(2\Delta\theta_k)\sin^2(\epsilon_k t)}\right| = \left|\arcsin\left(\sin(2\Delta\theta_k)\sin(\epsilon_k t)\right)\right|\,.$$

One more time, non-analyticities will occur for $|\sin(2\theta_k)| = 1$, i. e. for the particular mode k^* such that $|\Delta\theta_{k^*}| = \pi/4$. In parallel with (2.45), the critical mode is given by

$$\cos k^* = \frac{1 + g_\mathrm{i} g_\mathrm{f}}{g_\mathrm{i} + g_\mathrm{f}}\,. \tag{2.52}$$

The critical times are now given by

$$t^* = \frac{\pi}{\epsilon_{k^*}} = \pi\sqrt{\frac{g_\mathrm{i} + g_\mathrm{f}}{(g_\mathrm{f} - g_\mathrm{i})(g_\mathrm{f}^2 - 1)}}\,, \tag{2.53}$$

which precisely match the values identified in [140] characterizing DQPTs in the Ising model.

Therefore, the circuit complexity is able to identify the same DQPT points defined in the standard way by means of the Loschmidt amplitude. The non-analytic behavior manifests in the particular contribution from the k^*-mode only.

2.6.3 DQPTs for topological chains

The same reasoning of the previous sections can be repeated straightforwardly to models where the hamiltonian can be mapped to free fermions. With this in mind, we will briefly state the results for a quantum quench in a $1d$ Kitaev chain in order to show that our method can also be used in the context of topological phase transitions.

The model is defined by the hamiltonian

$$H = -\frac{J}{2}\sum_{j=1}^{N}\left[\left(a_j^\dagger a_{j+1} + \text{c. c.}\right) - \mu\left(a_j^\dagger a_j - \frac{1}{2}\right) + \frac{\Delta}{2}\left(a_j^\dagger a_{j+1}^\dagger + \text{c. c.}\right)\right], \tag{2.54}$$

where J is the hopping amplitude, μ is the chemical potential and Δ is the superconducting pairing strength. We will perform the quench in the chemical potential and, for simplicity, assume a fixed Δ.

The dispersion relation is

$$\epsilon_k = \sqrt{(\mu + \cos k)^2 + \Delta^2 \sin^2 k} \tag{2.55}$$

and the Bogoliubov angle is defined through

$$\tan 2\theta_k = \frac{\Delta \sin k}{\mu + \cos k}\,. \tag{2.56}$$

In this scenario, the variation of the Bogoliubov angle can be shown to be

$$\Delta\theta_k = \frac{1}{2}\arctan\left(\frac{\Delta \sin k\,(\mu_\text{f} - \mu_\text{i})}{(\mu_\text{f} + \cos k)(\mu_\text{i} + \cos k) + \Delta^2 \sin^2 k}\right) \tag{2.57}$$

There are two solutions of the condition for critical modes, $\Delta\theta_k = \pm\pi/4$, namely

$$\cos k_\pm^* = \frac{\mu_\text{i} + \mu_\text{f} \pm \sqrt{4\Delta^2 + (\mu_\text{i} - \mu_\text{f})^2 + 4\Delta^2(\mu_\text{i}\mu_\text{f} - 1)}}{2(\Delta^2 - 1)}\,. \tag{2.58}$$

As previously, $t^* = \pi/\epsilon_{k^*}$. These are the same values found following the reasoning in [141], for instance.

The preliminary study of this section opens a lot of perspectives. More or less directly, we have touched upon the characterization of quantum phase transitions in several scenarios built under different premises: equilibrium, nonequilibrium, topological and dynamical transitions. Our analysis indicates that the use of the circuit complexity as a *general* tool to categorize QPTs of various kinds deserves further scrutiny.

3

Entanglement dynamics in periodic quantum circuits

"Beware of all enterprises that require new clothes,
and not rather a new wearer of clothes."

— *Walden*, Thoreau.

This chapter was first presented as [23] under the title:

"Maximally entangling states and dynamics in one dimensional nearest neighbor Floquet systems"
– arXiv: arXiv:1901.02944 ,

and it is a collaboration with David Berenstein.

There is a bound on the entropy production as a function of time for two complementary regions, A and B, that are entangled, as we have seen in Section 1.1.1, in particular on the discussion around Equations (1.11-1.12). The bound applies to any local hamiltonian of the form (1.10) and, in particular, the rate at which entanglement is generated scales at most as the boundary area of A. One can reverse the reasoning behind this situation and ask for the determinations obeyed by the entanglement entropy that could lead to a maximal rate of growth, which is the subject of this chapter.

The setup consists, as in the previous chapter, of systems evolving according to a periodic dynamics. Here we focus on a class of of one-dimensional quantum circuits, where conditions for generating entanglement between two regions at the optimal rate are described. The optimal value follows from subadditivity and Araki-Lieb inequalities [142]. As an example of a system saturating such bound, we will study a quantum circuit composed of parallel SWAP gates that act periodically on entangled pairs.

In the unfolding of the analysis, we argue that any other system that entangles at this maximal rate must act as a generalized SWAP gate dynamics on the relevant states of the Hilbert space. Furthermore, some characterizations of states according to entropy generation are discussed, where we will reason that states with multipartite entanglement generically fail to entangle efficiently as time evolves. Our results suggests that chaos, which tend to produce such entanglement patterns, is expected to work against the process of spreading information efficiently. Finally, we give a simple intuition for why the entangling tsunami velocity must be slower than the Lieb-Robinson velocity.

3.1 Introduction

The dynamical evolution of isolated quantum systems is unitary. This means that all the information encoded in their initial state can in principle be recovered by a clever experimenter. Such remark, however, does not apply to a subsystem of a larger system. Subsystems evolve and seem to thermalize, thereby effectively losing information to the rest of the system as time passes by. Experimental progress recently achieved in the fine control of the environmental setup, in order to isolate quantum systems, has enabled implementing unitary time evolution to a good approximation for long time-scales. The possibility of addressing long term open questions, such as the understanding of the dynamics leading to thermalization in experimental setups, has stimulated a wave of theoretical developments on its side. For recent reviews on both theoretical and experimental advances and perspectives about this vast subject, see [143, 144, 145, 146] and also references contained therein.

A central role in the description of nonequilibrium phenomena is played by entanglement dynamics. This is particularly interesting in quantum field theories either on a lattice or in the continuum limit. The simplest nonequilibrium protocol in quantum field theory is a global quantum quench in $1+1$ dimensions. In this scenario, quasiparticle excitations propagate in an effective light-cone defined from the Lieb-Robinson bound [2], which also renders an upper bound on the generation of entanglement – it can grow at most linearly with time [147, 148, 31]. In particular, the work of [147] describes an intuitive model for entanglement entropy production that captures these results: the excitations are sourced from nearby points by the quench and after that they follow a ballistic journey with opposite quasimomenta. Freely propagating quasiparticles that are entangled display the linear behavior on entanglement entropy growth.

The aforementioned works deal with spin chains or two dimensional conformal field theories and they are valid for specific protocols. On the other hand, for holographic field theory setups that admit a classical gravity description, one can make considerable progress in computing the entropy dynamics via the holographic entanglement entropy proposals [13, 84]. In general quantum field theories and protocols, however, the generation of entanglement does not have such a comprehensible overall view. Still, the lack of a complete picture compels us to study simplified models that resemble quantum field theories. These models can be used to understand at least the phenomenology of entanglement dynamics, for instance by providing a classification of quantum states according to entropy production.

We will study a simple model of a lattice quantum field theory, given by certain constructions of quantum circuits with Floquet time evolution. By Floquet dynamics we mean that the system has a discrete unitary evolution which is periodic in time. We highlight one example among this set, implemented through SWAP gates, that reproduces the picture of Cardy and Calabrese [147]. This will provide some insights into different protocols for inhomogeneous quenches. This is a

natural problem and of particular relevance, since initial states which are not translational invariant, as in local quenches, have concrete realizations in some experimental setups. For example, cold atoms subjected to a harmonic confinement or quantum wires subjected to a voltage difference [149]. More importantly, the setup considered here can be in principle efficiently simulated in a quantum computer.

3.2 The model and maximally entangling states

Let us start with a one-dimensional chain of N sites, each with a Hilbert space H_i of dimension $\dim(H_i) = M$ and implement the dynamics through the action of quantum gates U at discrete times of length $\Delta t = 1/2$ (two layers are one unit of time). Such systems naturally realize a finite speed of propagation as would be required by the Lieb-Robinson bound. We shall consider two layers of unitaries connecting two sites, which operate on alternating nearest neighbors, and that are repeated after a period $T = 1$ producing a checkerboard pattern, as shown in Figure 3.1.

The input state is pure and for simplicity it is prepared with entangled pairs between alternating adjacent sites, which is also displayed in Figure 3.1 together with the partition we will consider in what follows.

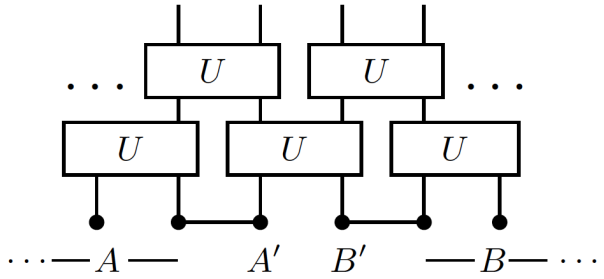

Figure 3.1: Illustration of the quantum circuit under consideration. Dots represent lattice sites and segments joining two of them account for the fact that degrees of freedom on these sites are entangled.

Such a system could be typically thought of as a quantum simulation of a quantum field theory in a system of qubits (or some other local Hilbert space), where U is a discretization of the dynamical evolution obtained by some Suzuki-Trotter steps.

We will be in general interested in protocols where two parts of the system, which we label as AA' and BB', begin in a pure state. Subsequently, they exchange information and become entangled as time evolves. The sites at which these two subsystems communicate are A', B', while we take A, B to be the rest of the system. Notationally, we have implicitly defined joined regions by adding labels, so that for example $AA' = A \cup A'$.

Subadditivity of the entanglement entropy together with the Araki-Lieb (or triangle) inequality read

$$|S_A(t) - S_{A'}(t)| \leq S_{AA'}(t) \leq S_A(t) + S_{A'}(t), \tag{3.1}$$

for all times t, where we can assume $S_A(t) > S_{A'}(t)$ without loss of generality and remove the absolute value. In the rest of the discussion, we will always consider t to be an integer. By construction, the unitaries acting at half-integer times do not mix regions A and A', such that $S_A(t) = S_A(t+1/2)$. Using this fact and (3.1), a bound on the entropy production at region AA' during a period follows immediately,

$$\begin{aligned} \Delta S_{AA'}(t+1/2) &\equiv S_{AA'}(t+1/2) - S_{AA'}(t) \\ &\leq S_{A'}(t) + S_{A'}(t+1/2). \end{aligned} \tag{3.2}$$

The entanglement entropy bound is controlled by (a trivial constant times) the average entropy at site A'. Of course $\Delta S_{AA'}(t) = 0$, since the unitaries act within regions AA' and BB' separately. By symmetry, the same reasoning as above and the one that follows below applies once AA' is replaced by BB'.

This bound is independent of the set of gates one has chosen to construct the circuit with, and it is saturated whenever $S_{AA'}(t+1/2)$ and $S_{AA'}(t)$ obey, respectively, subadditivity and Araki-Lieb inequalities with an equal sign. In the former case, the mutual information between A and A', $I_{A,A'}(t+1/2)$, is obviously zero meaning that A' is completely entangled with BB', while in the later event $I_{A',BB'}(t) = 0$ – which holds since the input state is pure. It follows that $S_{AA'}(t) = S_{BB'}(t)$ and $S_{A'BB'}(t) = S_A(t)$ – showing that A' shares correlations only with A. In particular, strong subadditivity $I_{A',BB'}(t) \geq I_{A',B'}(t)$ implies that

$$S_{A'B'}(t) = S_{A'}(t) + S_{B'}(t). \tag{3.3}$$

As a consequence, mutual information saturates a monogamy inequality $I_{A',BB'}(t) \geq I_{A',B}(t) + I_{A',B'}(t)$ in a trivial way. Necessary and sufficient conditions for the saturating Araki-Lieb inequality are classified in [150], for instance, by means of other measures of entanglement – entanglement of formation and squashed entanglement.

Saturating both inequalities in (3.1) for many consecutive steps, and not just at one instant of time, is a nontrivial property of a system that depends both on the dynamics and on the initial state. When it holds, this leads to maximal entropy production at each step. Such feature motivate us to name a state as *maximally entangling* if it saturates both inequalities simultaneously for both partitions, AA' and BB', in the sense that it achieves the highest rate of entanglement entropy production that is allowed. A state can be maximally entangling at one instant of time or within an interval $[t_1, t_2]$.

The idea is to understand what types of gates admit a large collection of maximally entangling states and how generic they are. We will call the full dynamical system *maximally entangling* if it admits a large class of generic states that are maximally entangling for long times. Here we provide an example of such a system through the choice of SWAP gates, whose action on any two states is given by $\mathrm{SWAP}(|a\rangle \otimes |b\rangle) = |b\rangle \otimes |a\rangle$ when acting on two sites.

3.3 SWAP circuit

Thus, we now focus on the SWAP gate, where

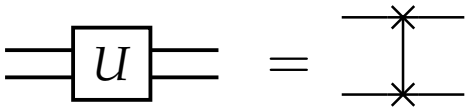

The corresponding circuit is a model for a discrete non-interacting quantum field theory, where swapping two sites corresponds to a free streaming of particles to the left and right. This is an integrable model that can realize the intuition developed by Cardy and Calabrese in [147], where a quantum quench acts as a source of quasiparticle excitations that propagate freely with entangled left and right movers. Moreover, one can easily deal with input states that display an inhomogeneous entanglement pattern in this circuit model, which generalizes the free streaming picture to include a broader class of states.

In what follows, we will always take N to be large and ignore finite size effects. Roughly speaking, we are taking A, B to be infinite in a first order approximation.

Denoting the entanglement entropy at site i at time $t = 0$ by s_i and assuming only nearest neighbor entanglement between pairs in the initial state (site $2k$ entangled only with site $2k+1$, but not necessarily maximally), it is straightforward to write down corresponding formulas for all regions. For instance, setting A' to be at site j, one has

$$S_{A'}(t) = s_{j-2t}, \qquad S_{A'}(t+1/2) = s_{j+2+2t}, \tag{3.4}$$

where t is an integer. In the above, we have also used the fact that for this class of states $s_{j+2+2t} = s_{j+1+2t}$.

Also,

$$S_A(t) = s_j + \sum_{k=1}^{t} (s_{j-2k} + s_{j+2k}) \tag{3.5}$$

and

$$S_{AA'}(t+1/2) = \sum_{k=0}^{t} (s_{j-2k} + s_{j+2+2k}). \tag{3.6}$$

These equations clearly lead to the saturation of (3.1) for the relevant times discussed previously. Likewise, similar conclusions can be drawn for the BB' side. In particular, since the SWAP model mimics the Cardy-Calabrese quench dynamics, this suggests that the Cardy-Calabrese setup should also saturate similar quantum information inequalities for entanglement generation. The quench should be maximally entangling in a certain sense for continuous time, rather than discrete time as above. This is a nontrivial result about entanglement production in a quantum field theory that can be inferred from the simple discrete approximation we are considering.

One can easily check further properties of the SWAP circuit. For instance, the entanglement between A' and the rest of the system is swapped with the entanglement of B' and the rest of the system at each step, in the sense that $S_{A'}(t+1/2) = S_{B'}(t)$ and, similarly, $S_{B'}(t+1/2) = S_{A'}(t)$. Moreover, for this class of initial states with bipartite entanglement, the tripartite information remains zero for all times,

$$I_3(A, B, B') \equiv I_{A,BB'} - I_{A,B} - I_{A,B'} = 0, \tag{3.7}$$

meaning that the mutual information is always monogamous and extensive. This is of course expected since there is no generation of multipartite entanglement: information is only carried through the chain by the left and right movers which are correlated and remains localized, though in different locations.

One can generalize the system to start in a pure state in AA' and BB' keeping the single site entropies fixed, $s_i = s_{A,B}$, differing only if they are in A or B. One then expects based on Page's observation [151] that generically on each half AA' and BB', the left movers should be (maximally) entangled only with the right mover Hilbert space. This should be true even if s_i is slowly varying on AA' and BB'. Such generic states would evolve in a way that saturates the inequalities as well.

On the other hand, states with multipartite entanglement, like GHZ states will fail to saturate (3.1) for many consecutive instants of time. It is easier to analyze this case for a system of qubits starting in a state of the form $a|0\rangle^{\otimes 2k} + b|1\rangle^{\otimes 2k}$, for definiteness. Then, even if there is initially an entanglement growth when the first particle crosses the interface between two subregions, the next set of particles will not contribute to increase the entropy further on, therefore such class of states will fail to saturate the bound. This happens because left movers are partially entangled with left movers in each region, AA' and BB', and not only with right movers as in the case with bipartite entanglement, as illustrated in Figure 3.2. Thus, states with multipartite entanglement will end up generating net entanglement between AA' and BB' at a slower rate. In other words, multipartite states are not maximally entangling.

This can be made very precise. Assume that there is some entanglement between left movers and left movers on side BB' with some characteristic length ξ. Let us denote the postion at B' as i_1. What this means for us is that if we have ξ consecutive left-movers in B, then due to subaditivity of the

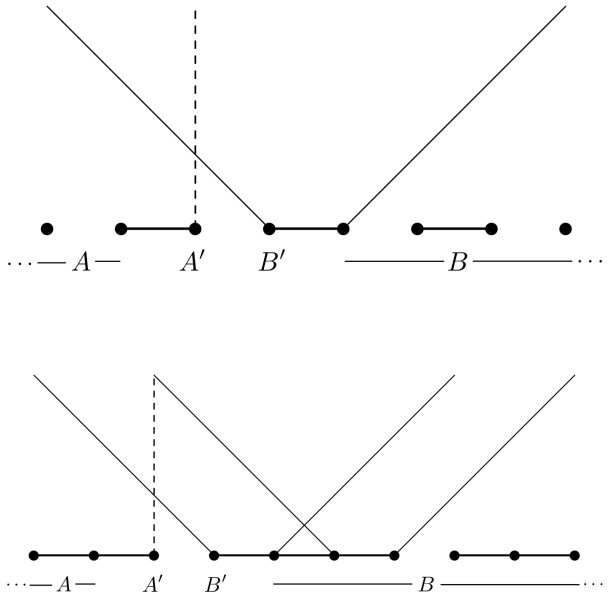

Figure 3.2: Streamlines followed by quasiparticles with bipartite entanglement (top) versus the multipartite case (bottom). In the former scenario, once a left-moving particle gets into AA', it will give its maximum contribution to the entanglement entropy of this region. Alternatively, for a GHZ-like block of size $2k$, while there is an increase of $S_{AA'}$ once the leftmost particle enters AA', there is a delay proportional to k before additional entanglement between the two regions is generated due to the next block.

entropy we have that $S_{i_1 \ldots i_\xi} \leq S_{i_1} + \cdots + S_{i_\xi}$, but we insist on a strict inequality at distance ξ. As a consequence there is some mutual information between the left movers characterized by the distance scale ξ. One can then show that once the ξ-th qubit has traveled through the interface between AA' and BB', then equation (3.5) will not hold any longer, because $S_{AA'}(t+\xi) \leq S_{i_1 \ldots i_\xi} + S_{\text{rest}} < s_j + \sum_{k=1}^{t}(s_{j-2k} + s_{j+2k})$.

The SWAP model provides insight into the role played by interactions in the process of generating entanglement. It shows that an integrable field theory already accomplishes the task of producing entanglement entropy at the optimal rate. By including chaos, if it has any effect on entangling regions at all, it must be the case that it slows down the rate of entanglement growth: since entanglement production is saturated in the integrable case, it cannot increase further. Chaotic dynamics is notable for producing multipartite entanglement. Therefore, we conclude that chaos should mostly work against the process of spreading information efficiently. We emphasize, however, that our reasoning does not rule out chaotic models to be maximally entangling. These models can still be maximally entangling as suggested for instance by the results obtained in [152]. In fact, such example matches our expectation of realizing maximal rates for very specific dynamics – self-dual points in the parameter space were considered in [152] – at a very particular choice of initial states. At the same time, such system admits a quasiparticle description, like the integrable models, where our discussion will apply more generally (see the considerations concerning generalized SWAP gates below).

It is worthwhile to notice that generic states that are maximally entangling in the SWAP model will fail to be so for different sets of gates. Cellular automata models with CNOT and $\mathrm{SL}(2,\mathbb{Z})$ gates were considered respectively in [153] and [154], for instance, in the study of integrable and chaotic

properties of many-body systems. The system of gates generically produce multipartite entanglement, such that our input state will not be maximally entangling according to those dynamics. Even more dramatically, if we use the CNOT dynamics, and we start with all states set to $|0\rangle$ on the AA' side, irrespective of what state we put on BB', no entanglement between A, B will be ever generated, even if the local entropy at B' is maximal. This is because the system will evolve to states that are of the same form: a product of $|0\rangle$ in AA' times another state in BB'. For comparison, in general such states on BB' would be maximally entangling by our criteria in the SWAP gate model.

Let us get back to the general set of gates and consider the case when there is no local entropy production beyond some time t_*. This is one of the properties of the SWAP gate model. That is, we require that

$$S_{A'}(t_*) + S_{B'}(t_*) = S_{A'}(t_* + 1/2) + S_{B'}(t_* + 1/2). \tag{3.8}$$

Such situation could arise, for instance, when the system reaches local equilibrium. Note that, by construction, mutual information between A and $A'B'$ is conserved when we act only on $A'B'$, that is, $I_{A,A'B'}(t) = I_{A,A'B'}(t + 1/2)$, and we can easily compute it for a maximally entangling system. Using $S_{AA'}(t) = S_A(t) - S_{A'}(t)$ together with (3.3) we get

$$\begin{aligned} I_{A,A'B'}(t) &= S_A(t) + S_{A'B'}(t) - S_{AA'B'}(t) \\ &= S_A(t) + S_{A'}(t) + S_{B'}(t) - S_B(t) \\ &= S_{AA'}(t) + 2S_{A'}(t) - S_{BB'}(t) = 2S_{A'}(t). \end{aligned} \tag{3.9}$$

Here the local equilibrium (3.8) does not play a role in this case. We will use it for half-integer times as well as $S_{AA'}(t + 1/2) = S_A(t + 1/2) + S_{A'}(t + 1/2)$. Then, the corresponding steps to the ones above lead to

$$I_{A,A'B'}(t + 1/2) = 2S_{B'}(t + 1/2). \tag{3.10}$$

Hence, due to equality between (3.9) and (3.10), and symmetry between AA' and BB', we have

$$S_{A'}(t) = S_{B'}(t + 1/2), \quad S_{B'}(t) = S_{A'}(t + 1/2), \tag{3.11}$$

meaning that, locally, entanglement in $A'B'$ is just swapped between the two sides at each time step when equilibrium holds. This suggests that, in these situations, U is essentially a SWAP gate in the relevant states. The conditions (3.8) must be achieved through a generalized SWAP gate, where we promote SWAP $\to \widetilde{\text{SWAP}} = \text{SWAP}\cdot(U_1 \otimes U_2)$, for some one-site gates U_1, U_2, since in this case U_1, U_2 will not change the local entropy at each site. Then, SWAP $\cdot \widetilde{\text{SWAP}}$ acts as a product of unitaries on bipartite spaces. This statement is not true for the CNOT gate, for instance.

In the context of the SWAP model, entropy conservation happens to be true even though energy is not conserved. However the system is integrable and has a lot of conserved quantities. In fact, (3.8) holds for all periods. The physics responsible for this equilibration condition is a conservation law, which is usually energy conservation. If we consider the SWAP circuit with qubits, the conservation law can be taken to be the number of spins up, leading to a conserved spin density. Lack of entropy production can thus be thought of in terms of a conserved entropy current. Alternatively, this allows one to fix the maximal entropy density per unit of conserved charge as a proxy for temperature.

3.4 Continuum limit

Now, returning to the field theory limit in $1+1$ dimensions, we expect a continuum version of (3.2) to take place, that is,

$$\frac{\mathrm{d}S_A}{\mathrm{d}t} \leq \alpha\, \sigma(t), \tag{3.12}$$

where $\sigma(t)$ is an entropy density and α has units of velocity (or velocity times area in general dimensions). One should expect that this velocity is related to the velocity of propagation of interactions, defined from the Lieb-Robinson bound, which we will call v_{LR}. When the equality holds, α is the so-called entanglement tsunami velocity [155], v_{E}. This requires the assumption that the system thermalizes at late times, such that $\sigma(t)$ converges to some thermal entropy density. Since v_{LR} is defined independent of an equilibrium hypothesis, we expect that $v_{\mathrm{E}} \leq v_{\mathrm{LR}}$, a result that can be proved for translation invariant states using causality arguments [156] or by considering the relative entropy with respect to a thermal state [157].

Recall that in the discrete case $\sigma(t)$ is proportional to the average entropy at a site. To get a finite entropy density in the limit where the lattice spacing goes to zero, we should consider situations where the local entropy per site is small. More precisely, since usually the entanglement entropy of a quantum field theory on an interval is divergent, we need $\sigma(t)$ to be a regularized entropy. For long enough times, we expect a system to achieve some notion of local equilibration, which sets a thermal scale given by the inverse temperature. Note that, while demanding low entropy per site naively suggests a slow entropy growth according to (3.12), it turns out that product states (where the state is pure at each site) can be instantaneously maximally entangling, no matter how small is the entropy production, as long as it is not zero. The idea is that since we start with zero entropy at each site, when we act with a non-trivial unitary on the boundary of the regions we are studying, one automatically saturates the bounds (3.2) because there is no mutual information between A, A' and the state in A is pure. Similarly for B', B. What this means is that the Lieb-Robinson velocity does not play a direct role in the instantaneous single gate model. To have such a bound, one needs enough time evolution so that the dynamical features of long distance physics can be applied locally.

This requires some notion of local equilibration. This argument shows that such an assumption, or a similar one, cannot be avoided in general.

As a special case, in a conformal field theory, the quantity $\sigma(t)$ can be related to the central charge c in a (locally) thermal state by $\sigma \propto cT$, where T is the temperature. The natural value for α is the Lieb-Robinson velocity: the speed of light in the conformal field theory. This strongly suggests that the Cardy-Calabrese quench is maximally entangling, since it saturates (3.12) with the conformal field theory values. While in $d = 2$ we have $v_E = v_{LR} = 1$, this illustrates again that, in general, the entanglement tsunami velocity should then be smaller than or equal to the speed of propagation of fluctuations. The expectation from our analysis is that chaos is generically reducing the speed of entanglement between regions by increasing the multipartite entanglement among the microscopic degrees of freedom. This is in agreement with the results of [156].

4

Scrambling in supersymmetric many-body systems

"A verdade não rima."

— *Onze Fitas*, Fátima Guedes

This chapter was first presented as [24] under the title:

"*Supersymmetric many-body systems from partial symmetries – integrability, localization and scrambling*".
– JHEP 05 (2017) 136, [arXiv:1702.02091],

and it is a collaboration with Pramod Padmanabhan, Soo-Jong Rey and Diego Trancanelli.

The search for necessary and sufficient conditions that guarantees the existence of a holographic duality has drawn our attention in Section 1.4. In particular, the role played by quantum chaos in this scenario was pointed out in Section 1.4.3 while the attempts to interpret spacetime as an emergent phenomena were described in Section 1.4.4. In the latter context, one utter aspiration would be the determination of the region behind the black hole horizon, where toy models for holography have stolen the spotlight in those studies during the last years.

One particular model of the kind has awaken many efforts towards this goal – the so-called Sachdev-Ye-Kitaev (SYK) model [17]. The model describes N Majorana fermions satisfying $\{\chi_i, \chi_j\} = \delta_{ij}$ with action

$$S = \int \mathrm{d}\tau \left(\frac{1}{2} \sum_{i=1}^{N} \chi_i \frac{\mathrm{d}}{\mathrm{d}\tau} \chi_i + \frac{\mathrm{i}^{q/2}}{q!} \sum_{i_1,\ldots,i_q=1}^{N} J_{i_1 \ldots i_q} \chi_{i_1} \cdots \chi_{i_q} \right), \tag{4.1}$$

where the coupling $J_{i_1 \ldots i_q}$ is totally antisymmetric and taken from a Gaussian ensemble with variance

$$\frac{1}{(q-1)!} \sum_{i_2 \ldots i_q=1}^{N} \langle J_{i_1 i_2 \ldots i_q} J_{i_1 i_2 \ldots i_q} \rangle = J^2. \tag{4.2}$$

This quantum system is fully solvable, even at strong coupling. In addition, it has an emergent conformal symmetry and it is maximally chaotic (recall the discussion of Section 1.4.3). This last property is also shared by black holes and, in fact, the model saturates the same bound on Lyapunov exponents as black holes do [80, 18]. The importance of the SYK model should not be underestimated, despite of being a toy model. Strongly chaotic systems are often very hard to study and the results obtained so far suggest the SYK model might be a disguised black hole – see [158], for instance – whose analytic control can help us to extract lessons for quantum gravity.

The discovery of the SYK model has driven the search for both generalizations and other examples of many-body systems displaying similar features. The achievements include models with complex fermions [159, 160], higher-dimensional lattices [161], global symmetry [162], supersymmetry [163] and tensor models without disorder [164].

In this chapter, as a part of the above movement, we construct a supersymmetric many-body quantum systems on a chain by means of an algebraic structure called partial symmetries, which are described by symmetric inverse semigroups. This construction consists in associating appropriate supercharges to chain sites, in analogy to what is done in spin chains. For simple enough choices of supercharges, we show that the resulting states have a finite non-zero Witten index, which is invariant under perturbations, therefore defining supersymmetric phases of matter protected by the index.

The hamiltonians we obtain are integrable and display a spectrum containing both product and entangled states. By introducing disorder and studying the out-of-time-ordered correlators (OTOC), we find that these systems are in the many-body localized phase and do not thermalize. Finally, we reformulate a theorem relating the growth of the second Rényi entropy to the OTOC on a thermal state in terms of partial symmetries.

4.1 Introduction

In quantum mechanics, a symmetry is implemented by requiring a system to be invariant under a certain set of transformations. These transformations must form a group, whose action on the associated Hilbert space is realized by unitary or anti-unitary operators, as stated by Wigner's theorem [165]. If the symmetry is obeyed only by part of the system, one can still implement it by the use of sets of transformations, but these have to be taken to form an *inverse semigroup* rather than a group. This generalization leads to the notion of *partial symmetries*.

An inverse semigroup $(\mathcal{S}, *)$ is a pair formed by a set $\mathcal{S}$ and an associative binary operation $*$, such that every element has a unique inverse. So, for a given $x \in \mathcal{S}$, there exists a unique $y \in \mathcal{S}$ such that

$$y * x * y = y \qquad \text{and} \qquad x * y * x = x. \tag{4.3}$$

There is no single identity on an inverse semigroup, but only idempotents or projectors which can be thought of as partial identities. The elements of $\mathcal{S}$ are called partial symmetries. Since they do not act on the entire Hilbert space, but only on parts of it, there is no unitary representation of these operators. Such structures do arise in quantum mechanics but have often been discarded without getting much consideration. It turns out, however, that inverse semigroups are relevant for physics as they provide the precise description for invariances that underlie certain physical systems [166]. To convince the readers, we illustrate this point in two instances of physical interest.

The first instance concerns a complete classification of tilings of $\mathbb{R}^n$. It is known that, for every such tiling, there exists an inverse semigroup associated with it [167]. Whereas periodic crystal structures - familiar to n-dimensional crystallography - are well described by group theory, aperiodic structures like quasicrystals [168, 169, 170] – see Fig. 4.1 – are associated to aperiodic tilings described by inverse semigroups [171, 172, 173, 174]. The classic examples of quasicrystals are the Fibonacci tiling in one dimension and the Penrose tiling in two dimensions. Further studies on aperiodicity include the motion of particles in quasicrystal potentials like the Fibonacci hamiltonian [175], works on gap-labelling theorems for such systems and, more generally, for substitution sequence hamiltonians [176, 177].

The second instance concerns operators in Hilbert space. In a finite-dimensional vector space $\mathcal{V}$, a complex matrix A is always decomposable to polar factorization, $A = UR$ or $A = LU$, where L, R are non-negative Hermitian matrices and U is a unitary matrix. In an infinite-dimensional Hilbert space $\mathcal{H}$, a bounded linear operator A is decomposable to polar factorization, $A = PR$ or LP, where L, R are non-negative self-adjoint operators and P is an element of an inverse semigroup. Here, P should be in general an element of an inverse semigroup, not of a unitary group, as exemplified by the creation and annihilation operators $a, a^\dagger$ (with $[a, a^\dagger] = \mathbb{I}$) that involve upper and lower shifts of the number

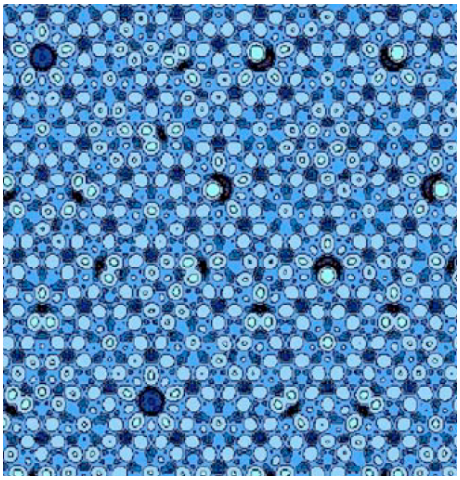

Figure 4.1: An example of quasicrystal, which is a crystal with ordered but aperiodic structure, lacking in particular translational invariance.
Picture adapted from [171].

basis $\{|n\rangle\}$ of $\mathcal{H}$[1]. Physically speaking, conjugate to the Hermitian number operator $N = a^\dagger a$, there is no phase operator Φ that satisfies both Hermiticity $\Phi^\dagger = \Phi$ and the commutation relation $[N, \Phi] = i$.

We shall work with a particular type of inverse semigroup, known as the *symmetric inverse semigroup* (SIS), which can be thought of as the analog of the permutation group in this context. Just like any group can be embedded into a symmetric group, according to the Wagner-Preston representation theorem [178, 179], any inverse semigroup can be embedded into a SIS such that it is isomorphic to some sub SIS [166]. This means that we can think of the SISs as building blocks of an arbitrary inverse semigroup. Thus, by working with SISs, there is no loss of generality. This result is the counterpart of Cayley's representation theorem in group theory stating that any group is isomorphic to the group of permutations or some subgroup of it.

When exploring a physical system, it is always a good idea to endow it with extra symmetries that might constrain the dynamics and bring the evaluation of observables under computation control. A symmetry that is proven notoriously capable of doing so is supersymmetry. This is a relation between bosons and fermions, which was first introduced in the context of relativistic quantum field theory as an extension of the Poincaré group, see for example [180, 181, 182, 183, 184] and [185] for a review. We shall focus on $(0+1)$-dimensional supersymmetric systems, viz. supersymmetric quantum mechanics [186, 187]. This system has proven to be a very useful arena, where problems with wide range of potentials could be solved exactly [188].

A supersymmetric system is equipped with a multiplet of fermionic charges, called supercharges, $\mathfrak{Q}$, that generate the supersymmetry transformations. By construction, the vacuum expectation value of top auxiliary components of supermultiplets is the order parameter of spontaneous supersym-

[1] For finite-dimensional Hilbert spaces, the counterpart of these shift operators is provided by the set of nilpotent operators. In this chapter, we will dwell on some particular examples of them.

metry breaking. After eliminating these auxiliary components, the system's hamiltonian is given by $H = \{\mathfrak{Q}^\dagger, \mathfrak{Q}\}$, implying that the vacuum expectation value of the hamiltonian is positive semidefinite. If the supersymmetry is unbroken, $\mathfrak{Q}|0\rangle$ is zero and $\langle 0|H|0\rangle = 0$. If supersymmetry is spontaneously broken, $\mathfrak{Q}|0\rangle$ is non-zero and $\langle 0|H|0\rangle > 0$. Thus, the ground state energy provides an easily calculable order parameter of spontaneous supersymmetry breaking.

Another related order parameter is the Witten index [189], $\Delta = N^{(0)}_{\text{boson}} - N^{(0)}_{\text{fermion}}$, the number of bosonic zero-energy ground states minus the number of fermionic zero-enegy ground states. If this quantity is non-zero, then there ought to be unequal numbers of bosonic and fermionic zero-energy ground states. If the quantity is zero, then there are either equal pairs of bosonic and fermionic zero-energy ground states or the ground states have positive energy. In the former case, the system preserves supersymmetry. In the latter case, the system breaks supersymmetry. So, provided the system's energy spectrum is discrete, the Witten index is a quantized quantity that cannot be continuously changed by supersymmetry preserving deformations.

Topological phases of matter are described by topological invariants, examples of which include the quantum double models of Kitaev described by the genus of a surface [190], or the symmetry protected states of matter described by the cohomology of corresponding symmetry groups [191]. These invariants are often computable as the partition functions of systems or as the trace of corresponding transfer matrices [192]. Along these lines, we propose to use the Witten index, which can be thought of as a twisted partition function of systems or as a supertrace[2] of the corresponding transfer matrix formed out of supersymmetric hamiltonian, to also be a useful indicator for interesting phases of many-body systems, protected by the global supersymmetry[3].

Following these lines of reasonings, we are naturally led to construct supersymmetric systems with partial symmetries, or supersymmetric SISs. We will do just that in the following, focusing in particular on supersymmetric many-body systems on a lattice, where the internal degrees of freedom are built from SIS algebra elements. In this way, we implement a supersymmetric algebra on the Hilbert space spanned by these elements, which can be thought of as realizing supersymmetric algebras out of partial symmetries. Many-body supersymmetry preserving zero-energy ground states can be constructed as eigenstates of many-body hamiltonians by considering supersymmetry in the non-relativistic setting, as in statistical physics, see [198, 199] and citations therein. Supersymmetric many-body systems have been considered in the past [200], where their lattice formulation was done by realizing the global supercharges on the total Hilbert space of the system [201, 202, 203, 204, 205, 206].

[2] We use the twisted sum or the supertrace as the Hilbert space is graded.

[3] The Witten index also has a deep connection with the topology of the bundle spaces upon which the hamiltonian acts. This is the content of the Atiyah-Pataudi-Singer index theorem [193, 194, 195, 196]. Generalizations of this index have also been considered [197].

Exact solutions for these models were obtained in [207]. Entanglement entropy in such systems have also been considered [208].

An important aspect of the models we construct with partial symmetries is that they are generically quantum integrable: all of these models have as many local integrals of motion as the number of sites, as we shall see. This is the case when we construct our supersymmetric system with a unique grading of the Hilbert space spanned by the elements of the SIS algebra[4]. Given this, we ask the question about scrambling properties in such supersymmetric systems, which forms the subject of the remaining part of the main text.

Recently, the topic of scrambling has proven to be of great interest in many fields, from the physics of black holes to quantum information. Concretely, scrambling can be used to identify the onset for quantum chaos [77] and the propagation of entanglement [209]. From a gravitational/holographic perspective, black holes are conjectured to be the fastest scramblers in Nature [210] and, in the same spirit, it has been conjectured that chaos cannot grow faster than in Einstein gravity [79, 80]. These works provide several hints connecting fast scrambling and thermalized phases, which are embedded into a large program concerned with the full understanding of thermalization in complex quantum systems.

On the opposite extreme, and the focus of this work, are systems where time evolution results in a localized phase and no thermalization occurs at all. Roughly speaking, thermalization is the process by which a system evolves to a point in which it can be well described by few thermodynamical quantities. This seems to conflict with the quantum mechanical intuition that evolution is unitary and the system is not expected to lose information about the initial state. The resolution to this puzzle is the *eigenstate thermalization hypothesis (ETH)* [211], which says that a quantum system thermalizes if it does so irrespective of the initial state it was prepared in, thereby also giving a proper definition of quantum thermalization. This brings up the possibility of the existence of systems that have states where such a process of equilibration does not occur and, consequently, the ETH is not satisfied. A classic example of such a system includes integrable models whose local integrals of motion prevent the transport of conserved quantities hindering the reach of equilibrium. The presence of disorder is another source of localization and loss of thermalization. In situations in which the phenomenon is described by one-particle effects, this is called *Anderson localization (AL)* [212], while in cases in which it is described by the many-particle effects, it is known as *many-body localization (MBL)*. A recent review on thermalization and localization is provided by [213].

The supersymmetric models we present here fall into the MBL class. The presence of "local" integrals of motion in these systems prevent the transport of the conserved quantities and thus we

[4] However, we can work in a scenario where the system is constructed out of two different gradings of the Hilbert space and in such a case we obtain non-integrable systems. This is discussed in [24].

expect to find MBL states in these systems. Since any such supersymmetric system constructed out of a unique grading of the SIS algebra is expected to have this property, we hereby developed a method of constructing supersymmetric MBL states using the SIS algebras. The system we study is a long-ranged interacting one and we emphasize that this is done just for simplicity[5].

We shall deduce the MBL property of these systems by studying the *out-of-time-order correlators* (OTOC) [77, 209, 80][6]. OTOCs have been recently used for analyzing localized systems, in particular in distinguishing MBL and AL phases in [214, 215, 216, 217, 218]. This leads to connections between the OTOC's, scrambling, and localization. We briefly summarize the procedure used for this purpose.

To probe scrambling using OTOCs, one has to consider two local, arbitrary operators at different times, say $V(0) \equiv V$ and $W(t) = e^{iHt}W(0)e^{-iHt}$, and the squared commutator between these probe operators in some state of interest, which can be taken to be a thermal state with temperature β^{-1}

$$C(t) \equiv \langle [W(t), V]^\dagger [W(t), V] \rangle_\beta, \tag{4.4}$$

or, alternatively, the out-of-time order correlator

$$F(t) \equiv \langle W(t)^\dagger V^\dagger W(t) V \rangle_\beta, \tag{4.5}$$

that is contained in Equation (4.4). The behavior of these quantities as a function of time has crucial information about the system. For example, thermalized, MBL and AL phases can be diagnosed, respectively, by an exponential decay, a power-law decay and a constant behavior of the OTOC. We will refer to the systems presenting less than exponential OTOC as *slow scramblers*. It should be noted that OTOC have been considered long ago in the context of semi-classical methods in superconductivity [45].

With this setup we organize the chapter as follows. In Section 4.2, we review the basics of partial symmetries and SIS and construct single-particle supersymmetric systems out of SISs. In Section 4.3, we construct supersymmetric models in $(0+1)$ dimensions based on SIS with supercharges leading both to free and to interacting hamiltonians. In Section 4.4, we apply this setup to investigate scrambling in interacting many-body systems. We will present a toy model with quenched disorder that exhibits a supersymmetric MBL phase and argue that systems generated using supersymmetric realizations of SIS should be slow scramblers. An outlook for future work and a discussion of the scope of these supersymmetric SIS models is given in Section 4.5.

[5] In [24], short-ranged interacting supersymmetric systems are built out of a unique grading of the SIS algebra, which continue to have local integrals of motion and are thus expected to possess MBL states.

[6] Here we adopt the more usual definition of OTOC, unlike in Section 1.1.3. For clarity, compare Equations (1.18) to (4.4) and recall Footnote 11.

4.2 Partial symmetries and supersymmetric quantum mechanics

In this section, we begin with the simplest quantum system with partial symmetries: a one-particle or one-site quantum mechanical system defined on a finite-dimensional Hilbert space.

Let $S^n = \{1, 2 \cdots, n\}$. Consider the set of all partial bijections on S^n together with the usual composition rule, which is binary and associative. This pair forms a SIS, denoted by $\mathcal{S}^n = (S^n, *)$. We can also form a class of SIS by choosing subsets of order $p \leq n$, S^p, and considering the set of partial bijections on this subset. We will refer to the resulting SIS as $\mathcal{S}_p^n$. Taking the elements of $\mathcal{S}_p^n$ as basis, we will construct a Hilbert space, whose inner product is defined by the natural pairing of the basis. In what follows, we will work with such SISs and Hilbert spaces.

4.2.1 Diagrammatics for SISs

We shall first introduce a convenient diagrammatic way of representing the elements that renders the binary operations transparent and defines an algebra over $\mathcal{S}_p^n$.

To illustrate this in a transparent manner, let us start with the simplest example, $\mathcal{S}_1^2$, whose diagrammatics are shown in Figure 4.2. The partial symmetry elements of $\mathcal{S}_1^2$ are denoted by $x_{i,j}$, with $i, j \in \{1, 2\}$, and obey the following composition rule

$$x_{i,j} * x_{k,l} = \delta_{jk} x_{i,l}. \tag{4.6}$$

The indices i and j can be thought of, respectively, as the domain and range of the partial symmetry operation. The product between these elements is null when the range of the first element is different from the domain of the second element it is being composed with. Note that this product is non-commutative.

The next step up in complexity is illustrated by $\mathcal{S}_1^3$, which is made up of nine elements, $x_{i,j}$ with $i, j \in \{1, 2, 3\}$. These partial symmetries of $\mathcal{S}_1^3$ are depicted in Figure 4.3. Further moving up, we can construct a SIS with arbitrary n and p, $\mathcal{S}_p^n$. For the sake of definiteness, we will focus on $\mathcal{S}_1^3$, but the formulation is straightforwardly generalizable to any (p, n).

We next associate Hilbert spaces to every SISs. The Hilbert spaces we consider are spanned by the partial symmetries of the chosen SIS, meaning that we are working with the algebra of this SIS. Therefore, the SIS acquires a vector space structure and an inner product is naturally defined by

$$\langle x_{i,j} | x_{k,l} \rangle = \delta_{ik} \delta_{jl} \quad \text{where} \quad |x_{i,j}\rangle \in \mathcal{H}, \quad \langle x_{i,j}| \in \mathcal{H}^c. \tag{4.7}$$

For instance, an arbitrary element of the Hilbert space spanned by the elements of $\mathcal{S}_1^2$ is given by

$$|a, b, c, d\rangle = a\, |x_{1,1}\rangle + b\, |x_{1,2}\rangle + c\, |x_{2,1}\rangle + d\, |x_{2,2}\rangle\,, \qquad a, b, c, d \in \mathbb{C}. \tag{4.8}$$

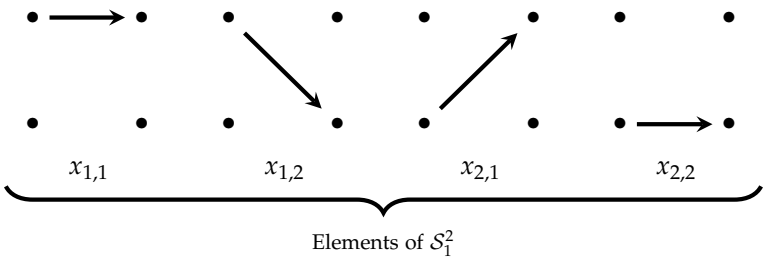

Figure 4.2: Diagrammatic representation of $\mathcal{S}_1^2$. The composition rules are obtained by tracing arrows connecting two elements. If one cannot trace a continuous arrow, the product is zero.

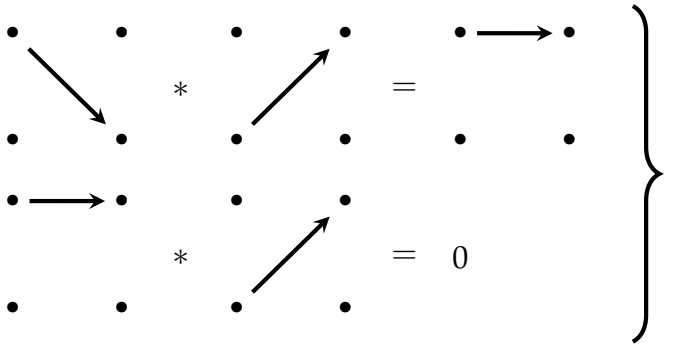

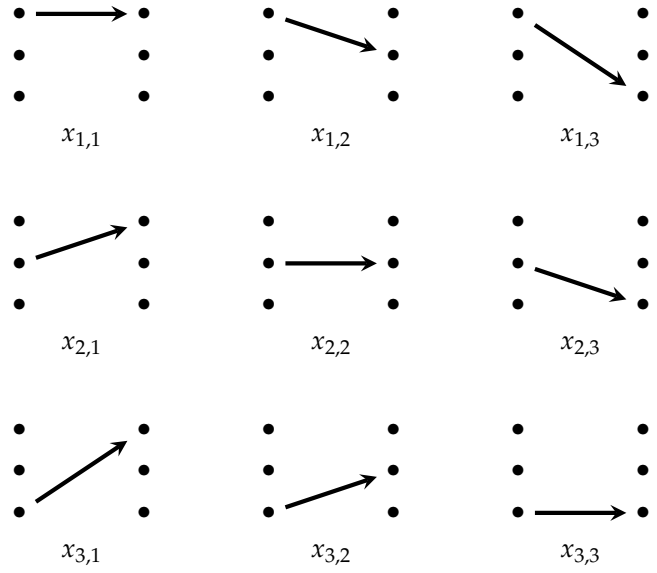

Figure 4.3: Elements of $\mathcal{S}_1^3$.

This is equivalent to working in the regular representation of the chosen SIS.

4.2.2 Supersymmetric systems from SISs

We now turn to the construction of a single-site, one-particle supersymmetric system. The first step is to realize the supersymmetry algebra from the SISs. Start with $\mathcal{S}_1^2$ and define

$$\mathfrak{q} = x_{1,2} \qquad \text{and} \quad \mathfrak{q}^\dagger = x_{2,1}, \qquad \mathfrak{q}^2 = \mathfrak{q}^{\dagger 2} = 0. \tag{4.9}$$

As $\mathfrak{q}$ and $\mathfrak{q}^\dagger$ are nilpotent, they can be thought of as supercharges. Out of these supercharges, we construct the hamiltonian H in the usual manner

$$H = \{\mathfrak{q}, \mathfrak{q}^\dagger\} = (\mathfrak{q} + \mathfrak{q}^\dagger)^2 = M + P \qquad \text{where} \qquad M = x_{1,1}, \quad P = x_{2,2}. \tag{4.10}$$

In the regular representation, this is just the identity operator and hence $\mathcal{S}_1^2$ leads to a trivial spectrum. The Hilbert space has a $\mathbb{Z}_2$-graded structure, $\mathcal{H}_b = \{x_{1,1}, x_{1,2}\}$ and $\mathcal{H}_f = \{x_{2,1}, x_{2,2}\}$, as shown in Figure 4.4. These two halves may be dubbed as the "bosonic" and the "fermionic" halves of the space corresponding to the fermion number operator, $F = x_{2,2}$. In this case this turns out to be the projector P as well. Consequently, the M and P operators are the "bosonic" and "fermionic" parts of the hamiltonian.

Note that this system admits no zero-energy ground state, for if $|z\rangle$ were such a state, it must satisfy that $\mathfrak{q}\,|z\rangle = \mathfrak{q}^\dagger\,|z\rangle = 0$ and there is no such state in $\mathcal{H}$. The Witten index for this system is zero.

We can construct a system with non-empty zero-energy ground states, the first nontrivial example provided by the partial symmetries of $\mathcal{S}_1^3$ with $\dim[\mathcal{H}(\mathcal{S}_1^3)] = 9$. We choose the one-site supercharges as

$$\mathfrak{q} = \frac{1}{\sqrt{2}}\,(x_{1,2} + x_{1,3})\,, \qquad \mathfrak{q}^\dagger = \frac{1}{\sqrt{2}}\,(x_{2,1} + x_{3,1})\,, \tag{4.11}$$

and we straightforwardly confirm that they are nilpotent. The hamiltonian is now given by

$$H = \{\mathfrak{q}, \mathfrak{q}^\dagger\} = M + P \tag{4.12}$$

where

$$M = x_{1,1}\,, \qquad P = \frac{1}{2}\,(x_{2,2} + x_{2,3} + x_{3,2} + x_{3,3})\,. \tag{4.13}$$

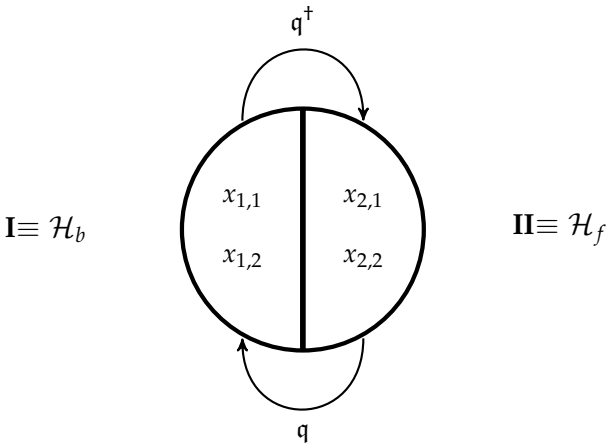

Figure 4.4: The grading of the Hilbert space spanned by the partial symmetries of $\mathcal{S}_1^2$. $\mathcal{H}_b$ and $\mathcal{H}_f$ are the "bosonic" and "fermionic" parts of this grading. The grading operator is given by $1 - 2F = 1 - 2(x_{2,2})$ which gives eigenvalue +1 on $\mathcal{H}_b$ and -1 on $\mathcal{H}_f$.

The Hilbert space $\mathcal{H}(\mathcal{S}_1^3)$ is $\mathbb{Z}_2$ graded, as shown in Figure 4.5. Note that this grading is just

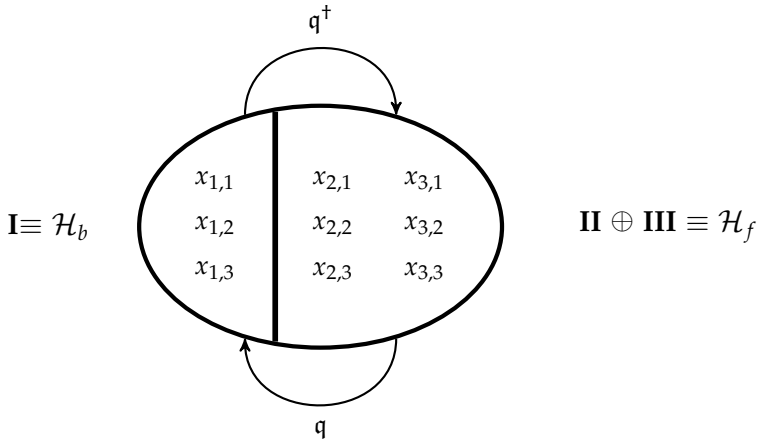

Figure 4.5: The $\mathbb{Z}_2$ grading of the Hilbert space spanned by the partial symmetries of $\mathcal{S}_1^3$. $\mathcal{H}_b$ and $\mathcal{H}_f$ are the "bosonic" and "fermionic" parts of this grading. The grading operator $1-2F$, [see Equation (4.17)], gives +1 on $\mathcal{H}_b$ and -1 on $\mathcal{H}_f$.

an arbitrary choice. We could have made the gradings which split the space as II, I+III or III, I+II, corresponding to cyclic permutations of $1,2,3$ in the choice of the supercharges[7]. It consists of two subspaces, the "bosonic" and "fermionic" subspaces, $\mathcal{H}_b$ and $\mathcal{H}_f$ respectively. First, there is the three-dimensional subspace $\mathcal{H}_0$ comprised of the normalized zero-energy ground states

$$|z^1\rangle = \frac{1}{\sqrt{2}}|x_{2,1} - x_{3,1}\rangle, \tag{4.14}$$

$$|z^2\rangle = \frac{1}{\sqrt{2}}|x_{2,2} - x_{3,2}\rangle, \tag{4.15}$$

$$|z^3\rangle = \frac{1}{\sqrt{2}}|x_{2,3} - x_{3,3}\rangle. \tag{4.16}$$

We introduce the fermion number operator F as

$$F = x_{2,2} + x_{3,3}. \tag{4.17}$$

Clearly, this has eigenvalue 1 upon acting on the states in $\mathcal{H}_0$, so that the ground states are all fermionic. This makes $\mathcal{H}_0 \subset \mathcal{H}_f$. Second, there is the three-dimensional subspace consisting of the excited fermionic states

$$|f^1\rangle = \frac{1}{\sqrt{2}}|x_{2,1} + x_{3,1}\rangle, \tag{4.18}$$

$$|f^2\rangle = \frac{1}{\sqrt{2}}|x_{2,2} + x_{3,2}\rangle, \tag{4.19}$$

$$|f^3\rangle = \frac{1}{\sqrt{2}}|x_{2,3} + x_{3,3}\rangle. \tag{4.20}$$

[7] Such possibilities and their consequences for many-body systems are further discussed in [24].

We denote this space by $\mathcal{H}_{ef} \subset \mathcal{H}_f$, where the label stands for "excited fermionic". Finally, there is the three-dimensional subspace $\mathcal{H}_b$, consisting of bosonic states (the fermion number operator F acting on these states gives zero). These states are given by

$$|b^1\rangle = |x_{1,1}\rangle, \tag{4.21}$$

$$|b^2\rangle = |x_{1,2}\rangle, \tag{4.22}$$

$$|b^3\rangle = |x_{1,3}\rangle. \tag{4.23}$$

The supercharges $\mathfrak{q}, \mathfrak{q}^\dagger$ pair up bosonic states in $\mathcal{H}_b$ and excited fermionic states in $\mathcal{H}_{ef}$, as dictated by the product rules of the underlying SIS. They are excited states with positive energy eigenvalues. Note that

$$M^2 = M, \qquad P^2 = P, \qquad H^2 = H, \tag{4.24}$$

so the M, P act as projection operators on bosonic and fermionic subspaces, respectively. Correspondingly, the energy eigenvalue of the excited states is 1. The fermionic zero-energy ground states are unpaired. Summing up, we have $\mathcal{H} = \mathcal{H}_f \oplus \mathcal{H}_b$ and $\mathcal{H}_f = \mathcal{H}_0 \oplus \mathcal{H}_{ef}$.

The Witten index Δ is computed as

$$\Delta = \mathrm{Tr}_{\mathcal{H}(\mathcal{S}_1^3)}\,(-1)^F = \mathrm{Tr}_{\mathcal{H}(\mathcal{S}_1^3)}\,(e^{i\pi F}) = \mathrm{Tr}_{\mathcal{H}(\mathcal{S}_1^3)}\,(1-2F) = -3, \tag{4.25}$$

thus counting correctly the three fermionic zero-energy states in $\mathcal{H}_0$.

The $\mathbb{Z}_2$ grading of $\mathcal{H}(\mathcal{S}_1^3)$ is provided by the Klein operator $(-1)^F$. It is easy to check that $[(-1)^F, H] = 0$ and $\{\mathfrak{q}, (-1)^F\} = 0 = \{\mathfrak{q}^\dagger, (-1)^F\}$, satisfying the usual properties of the fermionic number operator in a supersymmetric theory.

As a remark we only consider operators that are even under the $\mathbb{Z}_2$ grading, they then form *superselection sectors* of the theory which are essentially the "bosons" and the "fermions". We cannot have physical states that are a superposition of the two sectors, as they do not have a well defined fermion number[8].

4.2.3 Supersymmetric deformations and Witten index

We are interested in classifying deformations of the hamiltonian H while preserving supersymmetry. We do not expect these deformations to mix different zero-energy ground states nor to lift them to excited states. As such, we require the Witten index to be invariant under supersymmetry preserving deformations added to the hamiltonian.

[8] However, it is possible to construct many-body supersymmetric systems with the above grading where entangled states exist, a subject discussed in [24].

We will classify the supersymmetry preserving deformations into two parts, those that are obtained by deforming the supercharges $\mathfrak{q}$ to $\mathfrak{q}_d$ resulting in deformed supersymmetric hamiltonians, H_d, and those that are added to the original supersymmetric hamiltonian H as just perturbations that can possibly lift the ground state degeneracy. We show that the Witten index is left invariant by both these types of deformations.

Deformed supercharges

Consider deformed supercharges of the form

$$\mathfrak{q}_d = \frac{1}{\sqrt{|a|^2+|b|^2}}\left[a x_{1,2} + b x_{1,3}\right], \qquad \mathfrak{q}_d^\dagger = \frac{1}{\sqrt{|a|^2+|b|^2}}\left[a^* x_{2,1} + b^* x_{3,1}\right], \tag{4.26}$$

with $a, b \in \mathbb{C}$.

The resulting deformed hamiltonian is given by

$$H_d = M_d + P_d, \tag{4.27}$$

with

$$M_d = M, \qquad P_d = \frac{1}{|a|^2+|b|^2}\left[|a|^2 x_{2,2} + |b|^2 x_{3,3} + a^* b x_{2,3} + b^* a x_{3,2}\right], \tag{4.28}$$

with both M_d, P_d being orthogonal projectors as in the undeformed hamiltonian, which is recovered with $a = b = 1$. Now we can compute the zero modes for this deformed system and we find them to be precisely

$$|z^1\rangle_d = \frac{1}{\sqrt{|a|^2+|b|^2}}|b x_{2,1} - a x_{3,1}\rangle, \tag{4.29}$$

$$|z^2\rangle_d = \frac{1}{\sqrt{|a|^2+|b|^2}}|b x_{2,2} - a x_{3,2}\rangle, \tag{4.30}$$

$$|z^3\rangle_d = \frac{1}{\sqrt{|a|^2+|b|^2}}|b x_{2,3} - a x_{3,3}\rangle. \tag{4.31}$$

These are fermionic ground states under the old fermion number operator, F (4.17), and the corresponding Klein operator, $(-1)^F$. Thus we see that we again have -3 as the Witten index for the deformed supersymmetric hamiltonian.

Supersymmetry preserving perturbations

The simplest class of supersymmetry preserving deformations corresponds to local perturbations that can be added to the hamiltonian while at the same time preserving the supercharges, $\mathfrak{q}$ and $\mathfrak{q}^\dagger$, and commuting with the Klein operator, $(1-2F)$. The only operator that preserves the supercharges in Equation (4.11) and the Klein operator is provided by the $M+P$, which is the hamiltonian itself.

Clearly this does neither mix the three zero modes in Equations (4.14)-(4.16) nor does it create an energy gap among these states.

We could ask for nontrivial deformations which do not preserve the supercharges but still keep the Witten index unchanged. It turns out that the system is stable to any perturbation built as a linear combination of $x_{1,1}$, $x_{1,2}$ and $x_{1,3}$ and their hermitian conjugates. This can be seen by their action on the zero-energy ground states in Equations (4.14)-(4.16). Accordingly, the system keeps the Witten index intact. Such deformation extends to more nontrivial partial symmetries.

For $\mathcal{S}_1^n$, with arbitrary n, we find that the Witten index Δ is given by

$$\Delta = -n(n-2), \tag{4.32}$$

and remains invariant under the class of deformations specified above.

This number for the Witten index can be seen by considering the following supercharge for an arbitrary $\mathcal{S}_1^n$

$$\mathfrak{q} = \frac{1}{\sqrt{n-1}} \left[x_{1,2} + \cdots + x_{1,n} \right], \tag{4.33}$$

and its conjugate, $\mathfrak{q}^\dagger$. The zero modes are now given by

$$|z^j\rangle = \frac{1}{\sqrt{n-1}} |x_{2,j} + \omega x_{3,j} + \cdots + \omega^{n-1} x_{n,j}\rangle, \qquad j \in \{1, \cdots, n\}, \tag{4.34}$$

which counts n of the zero modes and for each of them we have $n-2$ choices in cyclic permutations of $\omega, \omega^2, \cdots, \omega^{n-1}$. Here $\omega = e^{\frac{2\pi i}{n}}$ is the n-th root of unity. Thus we have $n(n-2)$ zero modes which are all fermionic.

This index is again left invariant by deformed supercharges of the form

$$\mathfrak{q} = \frac{1}{\sqrt{\sum_{i=1}^{n-1} |a_i|^2}} \left[a_1 x_{1,2} + \cdots + a_{n-1} x_{1,n} \right]. \tag{4.35}$$

The argument goes just as in the case of $n = 3$. Apart from these deformed supercharges, the system is also invariant under the local perturbations which are a linear combination of $x_{1,1}$, $x_{1,2}, \cdots, x_{1,n}$ and their hermitian conjugates, as these operators do not lift the degeneracy of the ground states just as in the $n = 3$ case.

4.3 Supersymmetric systems on a chain

So far, we constructed a system whose supercharge is defined on a single site, so it could be thought of as a one-particle supersymmetric quantum mechanics. Our next step is to extend the construction to a many-body supersymmetric system on a chain, described by a globally defined supercharge. For simplicity, we will choose the homogenous chain such that all sites are equivalent. The Hilbert

space of the N-site lattice is $\mathcal{H} = \bigotimes_{i=1}^{N} \mathcal{H}_i$, where each site supports one and the same Hilbert space spanned by the partial symmetries of $\mathcal{S}_1^3$. In total, $\dim(\mathcal{H}) = 9^N$. The hamiltonian is determined once the supercharges are specified.

We will first need to choose the grading of $\mathcal{H}$, which again can be chosen from many possibilities. We continue adopting the convention that, locally, the sector I is "bosonic" and the sectors II+III are "fermionic". We will now present several examples of many-body systems that can be obtained by selecting different supercharges for this choice of grading.

4.3.1 Non-interacting supersymmetric chain

As a warm-up, we start by considering a simple system in which different lattice sites do not interact with one another. This corresponds to taking the supercharge as

$$\mathfrak{Q} = \sum_i a_i \theta_i \,, \qquad a_i \in \mathbb{C}, \tag{4.36}$$

where, by definition, θ's are anticommuting and nilpotent variables, $\{\theta_i, \theta_j\} = 0$, that are built out of $\mathfrak{q}$'s and $\mathfrak{q}^\dagger$'s. We can concretely realize these variables using the $\mathfrak{q}$'s in Equation (4.11) as follows

$$\theta_i = \prod_{1 \le j < i} e^{i\pi F_j} \mathfrak{q}_i = \prod_{1 \le j < i} \left(1 - 2F_j\right) \mathfrak{q}_i, \qquad i = 1, \ldots, N \tag{4.37}$$

where the fermion number operator F_j was defined in Equation (4.17). The variable (4.37) can be thought of as the well-known non-local Jordan-Wigner transformation of the local $\mathfrak{q}_i$ variables. The purpose of this procedure is to ensure that the θ_i's on adjacent sites anticommute. We will use these variables repeatedly in the rest of this chapter.

The hamiltonian defined by the supercharge (4.36) is

$$H = \{\mathfrak{Q}, \mathfrak{Q}^\dagger\} = \sum_{i=1}^{N} |a_i|^2 \, H_i, \qquad \text{where} \qquad H_i = \{\mathfrak{q}_i, \mathfrak{q}_i^\dagger\} = M_i + P_i. \tag{4.38}$$

The total fermion number operator F in this case is given by $F = \sum_{j=1}^{N} F_j$. Therefore, the $\mathbb{Z}_2$-grading operator is given by

$$(-1)^F = e^{i\pi \sum_{j=1}^{N} F_j} = \prod_{j=1}^{N} (1 - 2F_j). \tag{4.39}$$

It is easy to see that this operator commutes with the hamiltonian H, thus forming superselection sectors as in the one-particle case. It also anticommutes with the supercharges $\mathfrak{Q}$ and $\mathfrak{Q}^\dagger$ only when N is odd. Henceforth we assume that N is odd.

Clearly, the N-site chain hamiltonian (4.38) describes a non-interacting many-body system. Since $[H_i, H_j] = 0$ for all i, j, the system is easily solved by labeling the eigenstates of H with the eigenvalues

of the H_i operators on each of the N sites. The spectrum of the one-site hamiltonian, H_i, was studied in the previous section. The states can be thought of as being bosonic or fermionic and the operators M_i and P_i project onto the bosonic and fermionic subspaces at site i, respectively. For example, we can label the N-site eigenstates in the following way

$$|b_1, f_2, f_3, b_f, \cdots, b_N\rangle\,, \qquad \text{where} \qquad b_i \in \text{sector I and } f_j \in \text{sector II+III}\,. \tag{4.40}$$

For simplicity, we assume the chain to be homogeneous and set $a_i = 1$ for all sites $i = 1, \cdots, N$. The form of H_i in terms of commuting orthogonal projectors, M_i and P_i (recall that $M_i^2 = M_i$ and $P_i^2 = P_i$), results in integer eigenvalues between 0 and N. Then, we can write the energy spectrum of the chain as

$$E_j = N - j\,, \qquad j = 0, \ldots, N\,, \qquad \text{Degeneracy}\,(E_j) = \begin{pmatrix} N \\ j \end{pmatrix} 3^j\, 6^{N-j}. \tag{4.41}$$

These spectra exhaust all the possible states of $\mathcal{H}$ as

$$\sum_{j=0}^{N} \text{Degeneracy}\,(E_j) = 9^N = \dim\,\mathcal{H}, \tag{4.42}$$

which, as we have seen, is the dimension of the total Hilbert space $\mathcal{H}$.

The ground states of H_i are given by (4.14)-(4.16). There are 3^N of them for the chain, all fermionic, matching the Witten index $\Delta = \text{Tr}_{\mathcal{H}}(-1)^F$. These zero-energy ground states have the form

$$|g\rangle = |z_1^{i_1}, z_2^{i_2}, z_3^{i_3}, \cdots, z_N^{i_N}\rangle\,, \qquad \{i_1, i_2, \cdots, i_N\} \in \{1, 2, 3\}. \tag{4.43}$$

The local excited states include both bosonic and fermionic ones. The three bosonic states on every site i are given by (4.21)-(4.23) and the normalized fermionic ones are given by (4.18)-(4.20). The many-body excited states are then built by filling up the sites with these local bosonic and fermionic excited states. Consequently, the system is fully solved.

At finite temperature β^{-1}, the partition function is given by

$$Z = \text{Tr}_{\mathcal{H}}\, e^{-\beta H} = \left(6e^{-\beta} + 3\right)^N. \tag{4.44}$$

4.3.2 Long-range interacting supersymmetric chain

We now demonstrate how a model of an interacting N-site system can be constructed. The model is associated with long-ranged supercharges and hamiltonian, which we study for the simplicity of computations[9].

Consider the following choice of supercharge

$$\mathfrak{Q} = \mathfrak{q}_1\mathfrak{q}_2\cdots\mathfrak{q}_N, \tag{4.45}$$

which is just a product of the local supercharges at each site. This is clearly a nilpotent operator and hence generates a supersymmetry algebra. The resulting hamiltonian is given by

$$H = \{\mathfrak{Q}, \mathfrak{Q}^\dagger\} = M_1M_2\cdots M_N + P_1P_2\cdots P_N. \tag{4.46}$$

Though interacting, the resulting hamiltonian is integrable; there are N local integrals of motion given by $H_i = M_i + P_i$.

We can organize the Hilbert space in terms of the cohomologies of nilpotent $\mathfrak{Q}$ and $\mathfrak{Q}^\dagger$. The subspace $\mathcal{H}_0$ of zero-energy states is spanned by solutions of $\mathfrak{Q}|Z\rangle = \mathfrak{Q}^\dagger|Z\rangle = 0$. We see that they are labelled by the product states of the following types. The first type of ground states have at least one local zero-energy state on an individual site:

$$\begin{aligned}
&|\cdots, z_{i_1}, \cdots\rangle\,, && \binom{N}{1}\cdot 3^1\cdot 6^{N-1}\text{ states},\\
&|\cdots, z_{i_1}, z_{i_2}, \cdots\rangle\,, && \binom{N}{2}\cdot 3^2\cdot 6^{N-2}\text{ states},\\
&\vdots && \\
&|z_{i_1}, z_{i_2}, \cdots, z_{i_{N-1}}, .\rangle\,, && \binom{N}{N-1}\cdot 3^{N-1}\cdot 6^1\text{ states},\\
&|z_1, z_2, \cdots, z_{N-1}, z_N\rangle\,, && \binom{N}{N}\cdot 3^N\cdot 6^0\text{ states},
\end{aligned} \tag{4.47}$$

where the ellipses denote any of single-site boson or fermion excited states. There are $9^N - 6^N$ many such states. The second type of ground states is built from the mixture of single-site boson and fermion excited states with at least one local fermion excited state:

[9] Interacting models with local supercharges and hamiltonians can be found in [24]. We emphasize that the MBL property studied for the supercharges in this section is also shared by the supercharges in [24], as those systems continue to possess the local integrals of motion that are possessed by the long-range interacting supercharges.

$$
\begin{aligned}
&|\cdots, f_{i_1}, \cdots\rangle\,, && \begin{pmatrix} N \\ 1 \end{pmatrix} \cdot 3^1 \cdot 3^{N-1} \text{ states,} \\
&\vdots && \\
&|f_{i_1}, f_{i_2} \cdots, f_{i_{N-1}}, .\,\rangle\,, && \begin{pmatrix} N \\ N-1 \end{pmatrix} \cdot 3^{N-1} \cdot 3^1 \text{ states}\,.
\end{aligned}
\tag{4.48}
$$

The ellipses are occupied by single-site bosons and there are $6^N - 2 \cdot 3^N$ such states. Combining the two types of ground states, the Hilbert subspace $\mathcal{H}_0$ has the dimension dim $\mathcal{H}_0 = 9^N - 2 \cdot 3^N$.

The excited states belonging to $\mathcal{H}_b, \mathcal{H}_f$ are all of the form

$$
|f_1, f_2, \cdots, f_N\rangle \pm |b_1, b_2, \cdots, b_N\rangle. \tag{4.49}
$$

The number of such states is precisely $3^N + 3^N$ for $\mathcal{H}_b$ and $\mathcal{H}_f$, all with eigenvalue 1. Although they are entangled eigenstates of the operator $\mathfrak{Q} + \mathfrak{Q}^\dagger$, note that they are not entangled as eigenstates of the hamiltonian. This can be understood as arising due to the fact that Equation (4.49) is a superposition of a bosonic and a fermionic state (except in the even N case, when this state is an eigenstate of the fermion number operator). The hamiltonian of this long-range interacting system then has only product states as eigenstates[10].

The total number of eigenstates is the number of ground states plus the number of excited states, which is equal to 9^N, the total dimension of the Hilbert space, dim $\mathcal{H} = 9^N$. Note that the spectrum of this system is independent of N and is given by the two eigenvalues 0 and 1.

The partition function can be easily computed for this system and is found to be

$$
Z = \left(9^N - 2 \cdot 3^N\right) + e^{-\beta}\left(2 \cdot 3^N\right). \tag{4.50}
$$

4.3.3 Supersymmetric deformations and Witten index

The $\mathbb{Z}_2$-grading Klein operator W is

$$
W = \prod_{j=1}^{N} e^{i\pi F_j} = \prod_{j=1}^{N} \left(1 - 2F_j\right), \qquad W^2 = \mathbb{I}. \tag{4.51}
$$

The supercharges $\mathfrak{Q}$ and $\mathfrak{Q}^\dagger$ anticommute with W.

The Witten index Δ is defined as the trace of the Klein operator. We can count this index from the ground states we identified above and find precisely -3^N for arbitrary N. This can be easily seen

[10] It is however possible to construct supercharges resulting in supersymmetric hamiltonians that do preserve the Klein operator, have entangled eigenstates and a Witten index different from -3^N [24].

by considering the form of the states enumerated in Equations (4.47) and (4.48). In each of these product states, there are an equal number of bosonic and fermionic states. The only state which is unpaired is the product state $|z_1, z_2, \cdots z_{N-1}, z_N\rangle$ made of one-particle ground state at every site. As each of these local zero modes are fermionic (recall from Equations (4.14)-(4.16)), all these states are fermionic. One can easily confirm that the excited states are paired between bosonic and fermionic states, with multiplicity one.

As in the one-particle case, we are interested in classifying supersymmetry preserving deformations in the many-body setting. Such deformations are defined by continuous perturbations of the hamiltonian that commute with the supercharge $\mathfrak{Q}$ given by Equation (4.45), its adjoint $\mathfrak{Q}^\dagger$, and the $\mathbb{Z}_2$ grading Klein operator W in (4.51). We split these up into those that can be added as perturbations to the supersymmetric hamiltonian and those that are obtained by deforming the supercharge $\mathfrak{Q}$ as in the one particle case.

Local and quasi-local supersymmetry preserving perturbations

On a chain, we can deform the system in a variety of manners. First, we can deform the system on each site. Such deformations are given by

$$\Delta_1 H = \sum_{i=1}^{N} C_1(i)(M_i + P_i), \tag{4.52}$$

where $C(i)$ is a site-dependent function. Obviously, the system is invariant under these single-site deformations as they do not change the Witten index Δ.

Next, we can also deform the system over two sites. These deformations take the form

$$\Delta_2 H = \sum_{i=1}^{N} \sum_{j=1}^{N} C_2(|i-j|)(e^{\alpha_i} M_i + P_i)(e^{-\alpha_i} M_j + P_j), \tag{4.53}$$

where the two-site coefficient function $C_2(|i-j|)$ decreases sufficiently fast when the two-site distance $|i-j|$ becomes large and α is a real parameter characterizing such deformations. Such deformations commute with the Klein operator and preserve supersymmetry. It is easily seen that this quasi-local operator does not mix the eigenstates of this system and, in fact, it is diagonal in this basis. Thus, the Witten index is clearly left invariant under the deformation of quasi-local operators. Note that these are deformations that are added to the original supersymmetric hamiltonian and are not obtained from a deformed supersymmetry algebra.

Continuing in a similar manner, we can also deform the system over multiple sites; these deformations are supported on several sites and take the form,

$$\Delta_k H = \sum_{i_1=1}^{N} \cdots \sum_{i_k=1}^{N} C_k(i_1, \cdots, i_k)(e^{\alpha_1} M_{i_1} + P_{i_1}) \cdots (e^{\alpha_k} M_{i_k} + P_{i_k}), \tag{4.54}$$

where $\sum_{i=1}^{k} \alpha_i = 0$ and the site-dependent coefficient function $C_k(i_1, \cdots, i_k)$ is taken to be suitably quasi-local. Such operators are again diagonal in the eigenbasis of this system and hence the Witten index is left invariant. These operators account for all the allowed deformations to this system.

Deformed supercharges

We can introduce a deformation of the supercharge as follows

$$\mathfrak{Q}_d = (\mathfrak{q}_d)_1 (\mathfrak{q}_d)_2 \cdots (\mathfrak{q}_d)_N \tag{4.55}$$

where each of the local deformed supercharges are given by Equation (4.26) with the coefficients in these supercharges being now site dependent. The deformed hamiltonian resulting from this has the same kind of spectrum as the undeformed supersymmetric hamiltonian in Equations (4.47)-(4.48). The only difference is that the local zero modes, bosons and fermions are replaced by the deformed counterparts like those given in (4.29)-(4.31). These states maintain their grading under the Klein operator and thus it is clear that the Witten index stays unchanged to these deformations.

4.4 The spreading of quantum information

So far, we focused on the spectrum and Witten index of the supersymmetric system on a chain. Here, we dwell on the time evolution of many-body entanglement. This is captured by correlations functions of various time-orderings. More specifically, we will compute out-of-time-order correlators (OTOC) and study whether the system scrambles and equilibrates, and, if so, how it does it. We do this for a prototype model, consisting of an interacting disordered system built from Equation (4.45) that exhibits a many-body localized phase which is supersymmetric. The solvability of this model, as we have seen for the spectral analysis in the previous section, is a remarkable feature brought by the supersymmetric nature of the SIS we utilized in the construction. This will allow us to proceed with analytic computations for the OTOC.

4.4.1 Slow scrambling

First of all, we introduce a quenched disorder in the system by dressing the supercharge in Equation (4.45) as

$$\mathfrak{Q} = \prod_{i=1}^{N} \mathcal{J}_i \theta_i, \tag{4.56}$$

where $\mathcal{J}_i$ are real-valued time-independent random variables that can be thought of as analogous to a static random on-site potential[11].

The many-body interacting hamiltonian built out of this supercharge is

$$H = \prod_{i=1}^{N} \mathcal{J}_i M_i + \prod_{i=1}^{N} \mathcal{J}_i P_i. \tag{4.57}$$

To probe scrambling behavior of this model, we should compute the correlator in Equation (4.4) and study its time dependence, as discussed in the Introduction. We choose local supercharges as local operators, $W(t) = \mathfrak{q}_i(t)$ and $V = \mathfrak{q}_j(0)$, with $i \neq j$. Moreover, we will set $\beta = 0$ for simplicity, since we are primarily interested in highly excited states,

$$C(t) = \langle [\mathfrak{q}_i(t), \mathfrak{q}_j]^\dagger [\mathfrak{q}_i(t), \mathfrak{q}_j] \rangle_{\beta=0}. \tag{4.58}$$

We prefer to compute $C(t)$ rather than the OTOC (usually considered in this context), but of course the results are independent of this choice.

It is possible to show that the time evolved operator $\mathfrak{q}_i(t)$ is given by

$$\mathfrak{q}_i(t) = \mathfrak{q}_i + \left[\exp\left(i \prod_k \mathcal{J}_k^2 t\right) - 1\right] \mathfrak{q}_i \prod_{k \neq i} M_k + \left[\exp\left(-i \prod_k \mathcal{J}_k^2 t\right) - 1\right] \mathfrak{q}_i \prod_{k \neq i} P_k \,, \tag{4.59}$$

and, consequently,

$$C(t) = \langle [\mathfrak{q}_i(t), \mathfrak{q}_j]^\dagger [\mathfrak{q}_i(t), \mathfrak{q}_j] \rangle_{\beta=0} = 4 \cdot 3^N \left[1 - \cos\left(\prod_k \mathcal{J}_k^2 t\right)\right]. \tag{4.60}$$

All the information about disorder is contained in the argument of the cosine, as a result of the "on-site disorder". In such circumstances, it is reasonable to absorb the effect of randomness into a single variable, defined with its probability measure as

$$\mathcal{J} = \prod_{k=1}^{N} \mathcal{J}_k^2, \qquad \mathrm{d}\mu_{\mathcal{J}} \equiv \frac{1}{\sqrt{4\pi J^2}} \exp\left(-\frac{\mathcal{J}^2}{4J^2}\right) \mathrm{d}\mathcal{J}, \tag{4.61}$$

where J is a constant. Performing the disorder average leads to

$$\langle C(t) \rangle_{\mathcal{J}}^{\mathrm{G}} \equiv \int \mathrm{d}\mu_{\mathcal{J}} C(t) = 4 \cdot 3^N \left[1 - \exp\left(-J^2 t^2\right)\right]. \tag{4.62}$$

The usual hamiltonian employed in the study of many-body localization is the one for a system of qubits that contains, among other contributions, on-site magnetic fields given by static random

[11] One could generalize this choice by restricting the product to subsets of sites, rather than including all sites (see [24]). The results should not depend on this choice.

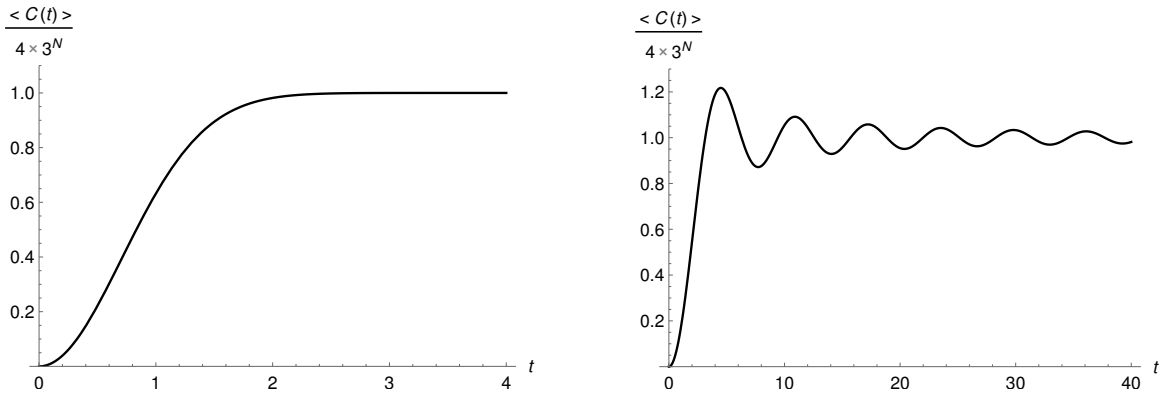

Figure 4.6: Normalized $\langle C(t)\rangle_{\mathcal{J}}$ for both Gaussian (left) and uniform (right) ensembles in the unit $J = 1$.

variables which are uniformly distributed. With this in mind, we also average $\mathcal{J}$ over a uniform ensemble between $[-J, J]$ for comparison, leading to

$$\langle C(t)\rangle_{\mathcal{J}}^{\text{unif}} \equiv \frac{1}{2J}\int_{-J}^{J} \mathrm{d}\mathcal{J}\, C(t) = 4\cdot 3^N\left[1-\frac{\sin(Jt)}{Jt}\right]. \qquad (4.63)$$

The behavior of Equation (4.62) and (4.63) are shown in Figure 4.6. Notice that no N-dependence appears in the time-dependence, apart from the trivial one in the normalization factor of the commutator.

Instead of the quenched quantity we have computed, $\langle C(t)\rangle_{\mathcal{J}}$, one could first average over realizations of the couplings and then take the expectation value. While the two procedures generally lead to different results, one can readily perform the computation on the reverse order and see that in this simple case they provide the same answer, that is, the averages commute. Under what conditions the two procedures are (in)equivalent is an interesting question.

In both choices of the ensemble, the early-time behavior is given by

$$\langle C(t)\rangle_{\mathcal{J}} \quad \propto \quad t^2 + \mathcal{O}(t^4), \qquad (4.64)$$

which is valid for any nonzero disorder. While we have shown this result for Gaussian and uniform distributions, it seems to hold for more general choices as well, with different proportionality constants set by the random disorder coupling. We discuss the meaning of this behavior in Section 4.4.3.

4.4.2 OTOC-EE theorem from partial symmetries

Recently, a connection between the decay of the OTOC taken in a thermal equilibrium state and the growth of a certain entanglement entropy was proposed for a system quenched by an arbitrary

operator [215]. To formulate the exact statement, assume a system described by a hamiltonian H initially in thermal equilibrium at temperature β^{-1} and split it into two regions, A and B. Let $S_A^{(2)}$ be the second Rényi entropy of A, $\mathcal{O}$ a quench operator that acts on the system at time $t = 0$ with the property $\mathrm{Tr}\left(\mathcal{O}\mathcal{O}^\dagger\right) = 1$, $V = \mathcal{O}e^{-\beta H}\mathcal{O}^\dagger$, and $\{W\}$ a complete set of operators for B. In this setup, the theorem of [215] establishes the following equality

$$\exp\left(-S_A^{(2)}\right) = \sum_{W\in B} \mathrm{Tr}\left[W^\dagger(t)VW(t)V\right]. \tag{4.65}$$

We can state a modified result in terms of our formalism that will supply the story we are developing with further insights. This is accomplished by requiring the quench operator $\mathcal{O}$ to act only on the subspace spanned by the partial symmetries of $\mathcal{S}_1^3$. In other words, we demand $\{x_{i,j}\}$ to form a complete set for the quench operators we may consider. This is certainly a restriction, since an arbitrary operator acting on the full Hilbert space cannot in general be expressed in terms of partial symmetries. However, this restriction will also provide hints for expecting slow scrambling in any supersymmetric model constructed out of SIS algebras.

As an example, we will verify the partial symmetry version of the OTOC-EE theorem for Equation (4.57). To this end, we assume again, for simplicity, that the system is at infinite temperature such that the right-hand side of Equation (4.65) is reduced to

$$\sum_{W\in B} \langle W^\dagger(t)\mathcal{O}\mathcal{O}^\dagger W(t)\mathcal{O}\mathcal{O}^\dagger\rangle_{\beta=0}. \tag{4.66}$$

As a first step, suppose the initial state to be a maximally mixed state, where $\rho(0) \propto \mathbb{1}$. We then quench the system at the first site with

$$\mathcal{O} = \sqrt{\frac{3}{4\cdot 9^N}}(\mathbb{1} + \mathfrak{q}_1), \qquad \text{such that} \qquad \mathrm{Tr}\left(\mathcal{O}\mathcal{O}^\dagger\right) = 1, \tag{4.67}$$

which amounts to sending $\rho(0) \mapsto \mathcal{O}\rho(0)\mathcal{O}^\dagger$. Then, let the system evolve for a time t under H, leading to $\rho(t) = U(t)\mathcal{O}\rho(0)\mathcal{O}^\dagger U^\dagger(t)$. Next, we write the Hilbert space as a bipartite decomposition, $\mathcal{H} = \mathcal{H}_A \otimes \mathcal{H}_B$, where we take the B-subsystem as a single site, $j \neq 1$ for definiteness. The second Rényi entropy on region A is defined by

$$S_2^{(A)} = -\log \mathrm{Tr}\,\rho_A^2, \qquad \rho_A = \mathrm{Tr}_B\,\rho. \tag{4.68}$$

To trace out B, we first need to compute the eigenvectors of the local hamiltonian $h_j \propto (P_j + M_j)$. Recall from previous sections that these are given by

$$|x_{1,k}\rangle_{k=1,2,3}, \qquad \frac{1}{\sqrt{2}}|x_{2,k} \pm x_{3,k}\rangle_{k=1,2,3}. \tag{4.69}$$

With this in mind, it is straightforward to show that

$$S_A^{(2)} = -\log\left[\frac{1}{3^{3N-3}}\left(\cos\left(\mathcal{J}t\right)-1\right)+\frac{1}{2\cdot 3^{2N-3}}\right]. \tag{4.70}$$

In order to compute the OTOCs in Equation (4.66), we use the hypothesis that the partial symmetries form a complete set on B, *i.e.* any quench operator in our model can be expressed in terms of $\{(x_{k,\ell})_j\}_{k,\ell=1}^{3}$ at site j. Thus, it is a straightforward, albeit tedious, exercise to show that

$$\begin{aligned}
\langle (x_{1,1})_j(t)\mathcal{O}\mathcal{O}^\dagger (x_{1,1})_j(t)\mathcal{O}\mathcal{O}^\dagger\rangle &= \frac{1}{2\cdot 3^{2N}}\,,\\
\langle (x_{2,1})_j(t)\mathcal{O}\mathcal{O}^\dagger (x_{1,2})_j(t)\mathcal{O}\mathcal{O}^\dagger\rangle &= \langle (x_{1,2})_j(t)\mathcal{O}\mathcal{O}^\dagger (x_{2,1})_j(t)\mathcal{O}\mathcal{O}^\dagger\rangle = \langle (x_{3,1})_j(t)\mathcal{O}\mathcal{O}^\dagger (x_{1,3})_j(t)\mathcal{O}\mathcal{O}^\dagger\rangle\\
&= \langle (x_{1,3})_j(t)\mathcal{O}\mathcal{O}^\dagger (x_{3,1})_j(t)\mathcal{O}\mathcal{O}^\dagger\rangle = \frac{(\cos\left(\mathcal{J}t\right)-1)}{16\cdot 3^{3N-3}}+\frac{1}{2\cdot 3^{2N}}\,,\\
\langle (x_{3,2})_j(t)\mathcal{O}\mathcal{O}^\dagger (x_{2,3})_j(t)\mathcal{O}\mathcal{O}^\dagger\rangle &= \langle (x_{2,3})_j(t)\mathcal{O}\mathcal{O}^\dagger (x_{3,2})_j(t)\mathcal{O}\mathcal{O}^\dagger\rangle = \langle (x_{2,2})_j(t)\mathcal{O}\mathcal{O}^\dagger (x_{2,2})_j(t)\mathcal{O}\mathcal{O}^\dagger\rangle\\
&= \langle (x_{3,3})_j(t)\mathcal{O}\mathcal{O}^\dagger (x_{3,3})_j(t)\mathcal{O}\mathcal{O}^\dagger\rangle = \frac{(\cos\left(\mathcal{J}t\right)-1)}{16\cdot 3^{3N-2}}+\frac{1}{2\cdot 3^{2N}}.
\end{aligned}$$

Adding all the above contributions,

$$\sum_{x\in B}\langle x^\dagger(t)\mathcal{O}\mathcal{O}^\dagger x(t)\mathcal{O}\mathcal{O}^\dagger\rangle = c\exp\left(-S_A^{(2)}\right),$$

where the constant c can be set equal to one by choosing a convenient normalization for the partial symmetries. This completes the check of the theorem.

4.4.3 Discussion: a supersymmetric MBL phase

We now present a heuristic explanation for the results encountered above. First of all, we should remark that, by a localized phase, we mean that decoherence does not occur, that is, long time dynamics does not hide all the information about the initial state. This implies that out-of-equilibrium "atypical" initial states do not evolve into equilibrium "typical" states. The possibility of keeping coherence is determined by the partial freeze on the process of scrambling, induced by the disorder in all sites of the chain.

The localization phenomenon is clearly a breakdown or violation of the ETH [211, 219, 220, 221, 222], which asserts that all many-body eigenstates of a given system are thermal if all its initial states are able to thermalize, which is supposed to provide a quantum version of thermalization. Since our hamiltonian is integrable, it was expected to violate the ETH due to the existence of many local integrals of motion [145, 223, 224, 225, 226], therefore defining a (supersymmetric) many-body localized phase. We stress that, as our system is finite-dimensional and hence does not allow mean field approximation, the localization is the MBL driven by many-particle effects, not the Anderson localization driven by single-particle effects.

Moreover, the supersymmetric many body system we consider is an example of a full-MBL (FMBL) phase, which is a term reserved for a system where all the initial states fail the ETH. By the statement of ETH, we require that

$$\langle \mathcal{O}(t) \rangle = \langle \mathcal{O} \rangle_{eq} = \langle \mathcal{O} \rangle_{C} = \langle \mathcal{O} \rangle_{MC},$$

where $\mathcal{O}$ is a local operator, $\langle \cdot \rangle_{eq}$ denotes the equilibrium value, and the labels C and MC denote the expectation value in a canonical and a microcanonical ensemble, respectively. By choosing the local operator to be M_1 in our setup, we can easily verify that the equilibrium value is not the same as the average in a canonical or a microcanonical ensemble for any initial state, $\rho = |\psi\rangle\langle\psi|$. This ratifies our claim that the SUSY many body systems we consider are an example of FMBL systems.

It is instructive to analyze the situation from other points of view. In Section 4.4.1, the power-law decay of the OTOC or, alternatively, the growth of $C(t)$ being faster than t in Equations (4.62) and (4.63), is a feature encountered in models that present a many-body localized phase [214, 215, 216, 217, 218]. The absence of a term linear in time slows down the growth of local operators, preventing the system from achieving thermalization.

It is also worth noting that, as observed in [215], the OTOC can distinguish between MBL and AL phases. For Anderson localization, the OTOC is constant, a feature that can be easily seen in our setup: the non-interacting hamiltonian in Equation (4.38) commutes with any local supercharge, hence $\mathfrak{q}_i(t) = \mathfrak{q}_i$ and $[\mathfrak{q}_i(t), \mathfrak{q}_j]$ is independent of time, leading to a constant OTOC.

To complete the picture, we try to give a heuristic explanation for the absence of fast scrambling in our models. From the analysis on Section 4.4.2, it was possible to relate the Rényi entropy with correlators involving partial symmetries, a fact that came from the restriction of $\mathcal{O}$ to be written out of the $\{x_{i,j}\}$. Notice that a generic operator acting on the Hilbert space of the system has many more degrees of freedom, by which we mean that the space of linear operators on a local Hilbert space cannot be generated or spanned using only the elements of the partial symmetries, $\mathcal{S}_1^3$. Nevertheless, the supersymmetric hamiltonians we can consider are ultimately written in terms of partial symmetries, which form a closed algebra. This means that the entanglement between all possible degrees of freedom one could generally have is largely reduced due to the presence of partial symmetries, which results in the possibility to retain all the information about the initial state as time evolution goes on. The net result is a many-body localized phase as we would naturally expect in this setting.

Finally, we want to address the question of supersymmetry breaking due to finite temperature and quenched disorder effects. To avoid confusion, we stress that, although we are borrowing the terminology of equilibrium physics, the concept of temperature is not well-defined since the system does not achieve thermal equilibrium. Thus, β^{-1} should be considered as a characteristic energy scale such that $\beta = \infty$ probes the ground state and $\beta = 0$ probes highly excited states. As discussed in the Introduction, the ground state energy can be thought of as an order parameter of spontaneous super-

symmetry breaking, since after eliminating auxiliary components, it results in a vanishing vacuum expectation value for the hamiltonian if supersymmetry is unbroken, or a positive value if supersymmetry is broken. At finite β, in analogy to equilibrium statistical mechanics, we may define a "thermal" vacuum by utilizing the thermo field double formalism in such a way that the vacuum expectation value of an operator is equal to its thermal average. For a good overview on this subject, we refer to [227]. We computed the vacuum expectation value of the hamiltonian (4.57) at finite β to be given by

$$\langle 0,\beta|H|0,\beta\rangle \equiv \langle H\rangle_\beta = Z^{-1}(\beta)\,\mathrm{Tr}\left(e^{-\beta H}H\right) = \frac{2\cdot 3^N e^{-\beta\mathcal{J}}\mathcal{J}}{9^N + 2\cdot 3^N(e^{-\beta\mathcal{J}}-1)}. \tag{4.71}$$

This quantity is nonzero for any finite β, showing the typical behavior of supersymmetric theories, namely, supersymmetry breaks at finite temperature. Note that, in the limit $\beta^{-1}\to 0$, the supersymmetry is unbroken, as one expects, since $\langle H\rangle_\infty = 0$. Note also that, in the limit $\mathcal{J}\to 0$, the supersymmetry is unbroken.

At quenched disorder, however, $\mathcal{J}$ is a random variable and so physical observables should be averaged over the disorder ensemble. Since we are interested in highly excited states, we will consider the case where β is small enough, which leads to

$$\int \mathrm{d}\mu_{\mathcal{J}}\langle H\rangle_\beta \;\propto\; \beta J^2 + \mathcal{O}(\beta^3 J^4). \tag{4.72}$$

This result is valid for both measures we considered previously. It is clear that the disorder effects also contribute to supersymmetry breaking along with the finite temperature effects. Nonetheless, this consideration shows that supersymmetry is unbroken at infinite temperature, like what happens at zero temperature.

All of these discussions point to the picture that the many-body system we constructed is a slow scrambler and can be used for studying MBL phases. In addition, we emphasize that this localized phase is also supersymmetric and protected by the corresponding Witten index that is independent of β due to the finite-dimensionality of Hilbert space: [12]

$$\Delta_\beta = \mathrm{Tr}\left((-1)^F e^{-\beta H}\right) = -3^N\,. \tag{4.73}$$

4.5 Discussion and Outlook

In this chapter, we have introduced how symmetric inverse semigroups can be used to realize supersymmetric algebras by constructing supercharges out of their elements. By choosing the SIS to be $\mathcal{S}_1^2$,

[12] Recall that N was chosen to be odd.

the simplest example, we recover the usual fermions and the supersymmetric many-body systems constructed in [200, 207][13]. Other choices of SIS lead to non-trivial, novel models. The elements of the SIS algebra allowed to consider graded Hilbert spaces and, for a given SIS other than $\mathcal{S}_1^2$, there are several choices for this grading. For a given grading, the many-body system constructed is integrable and characterized by an invariant Witten index protected by supersymmetry.

The fact that these many-body systems are integrable provides a favorable hunting ground for non-thermal states. In this spirit, by introducing disorder we find many-body localized states, which were diagnosed by the behavior of an out-of-time order correlator of local operators. The supersymmetry helped us to compute the OTOC analytically and establish the MBL property, as opposed to the usual MBL literature where most of the computations are numerical.

The supersymmetry algebras and hence the supersymmetric many-body systems constructed here are made up from the elements of $\mathcal{S}_1^3$. We can build a whole class of models by using the elements of other SISs, namely $\mathcal{S}_p^n$ with $n > p$. By going to higher n, we increase the dimension of the Hilbert space as the dimension of the algebra made from the elements of $\mathcal{S}_p^n$ is given by $\begin{pmatrix} n \\ p \end{pmatrix}^2 \cdot p!$. This makes the computations tedious but could nevertheless yield surprising results.

We would like to see if these systems have anything to do with quasicrystals. This can be especially seen once we have a hold on the specific inverse semigroups that describe a chosen quasicrystal. Given that our system models MBL phases by exhibiting slow scrambling, we could ask the question if this paves a way to experimentally realize MBL phases on quasicrystals[14]. This problem, however, requires a more systematic study where we construct a system that is invariant under the relevant inverse semigroup corresponding to the quasicrystal. The fact that this system describes the dynamics of a graded Hilbert space and thus a supersymmetric phase, and the fact that it is built very much like a spin system, makes us think of a possible way to realize such a system in the lab. This would account for a table-top experiment for graded Hilbert spaces and a phase of matter characterized by the Witten index and protected by supersymmetry.

Another question to be explored in this setting is whether there is a way to introduce chaotic behavior in such systems and possibly turn it into a toy model for holography *à la* SYK model [17] (or its supersymmetric version [231, 232]). Toward this end, we are currently looking at introducing open systems or considering subsystems inside a closed system in this setup to induce a linear growth in the OTOC's for early times and an exponential decay for later times.

[13] This is shown in [24].

[14] MBL phases on quasi-periodic systems have been studied recently [228, 229]. This is an extension of a long list of papers about the emergence of localization on quasi-periodic potentials on the one-dimensional chain [230]

The supercharge we worked with in this chapter is a very simple one which allowed for simple computations. However, as shown in [24], there are a number of non-trivial supercharges that produce local interactions and are non-integrable. The study of the OTOCs in these systems could show signatures of thermalization. Such considerations can also help us study the transition from localized to thermalized phases in this setting.

Integrability features frequently in the construction of these supercharges using the SIS algebras. We can ask the question if it is possible to find a Lax pair to describe this system as it is done for the Heisenberg spin chain systems [233]. This will possibly give us solutions to the Yang-Baxter equation and shed more light on these systems.

We could also explore higher-dimensional versions of the models presented in this chapter to find more interesting features. The robustness of MBL states to decoherence make them good candidates for engineering quantum memory devices, which might mark a testing ground for supersymmetry, partial symmetries, and SIS.

5

Essay on emergent geometries

"Damn good coffee!"

— Special Agent Dale Cooper in *Twin Peaks*.

A QUANTUM CRITICAL POINT is described by a conformal field theory. Section 1.2 walks through this process revealing the universal qualities common to the family of theories forming a class. The sequence to this movement, Section 1.4, outlines how the AdS spacetime can be conjured up from a CFT by a reinterpretation of the renormalization group. Recall that the argument to get the actual AdS metric relies on symmetry.

The above findings invite us to trace a parallel with the story for quantum phase transitions, where the symmetry analysis was elevated to a geometrical one, as delineated in Section 1.2.2. One may be inspired by this fact to look for an analogous process in order to determine an emergent metric out of the concepts defined in the CFT.

The present chapter deals with an example where it is indeed possible to realize the ideas in question. The setting is the one of two-dimensional conformal field theories. We will carry out a geometrical analysis of the Hilbert space of the CFT_2 using the metric induced by the Fubini-Study distance (1.34). Its direct evaluation for several cases will provide us hints of how the three-dimensional space is hidden in the CFT, adding to the interpretation of the AdS/CFT correspondence from an emergent point of view.

5.1 Introduction

Nonperturbative quantum gravity in asymptotically anti-de-Sitter spacetime can be defined in terms of a conformal field theory. This definition is motivated from the AdS/CFT correspondence [12] and it is strongly supported by explicit constructions and a myriad of tests with various degrees of precision. The wider notion of holography is conceived by assuming the duality to hold beyond the examples that are known.

The results invoking the holographic duality appear themselves as collections of observables computed either on the bulk side or on the boundary side, and sometimes on both, when their match is necessary for consistency. The underlying principle governing this approach is an isomorphism between the Hilbert spaces of the two different theories, also known as 'the AdS/CFT dictionary', which has driven more than two decades of unabated studies. However, the necessary and sufficient conditions for the duality to exist are yet unknown. While there is evidence for a sufficiency criterion – at the technical level, a CFT with (at least) a semiclassical dual is expected to be gapped and to have a large-N limit [74][1] – the existence of such a semiclassical dual is not enough to easily account for all phenomena that can happen in the bulk. For instance, excited states of the CFT that are far away from the vacuum can give rise to black hole geometries in AdS spacetime and, by definition, processes that take place behind the black hole horizon cannot reach the boundary. The description of such situation in terms of local correlation functions is therefore unavailable from the CFT perspective, and then it requires a deeper comprehension of the mechanism behind holography.

The aforementioned circumstances pose the question of how to describe bulk operators containing useful information about physics behind the horizon or, in general terms, which are not close to the boundary. The answer to this inquiry goes under the name of bulk reconstruction. One of the first steps in this program is to understand the reconstruction, or emergence, of the bulk spacetime itself, that is, when spacetime is a classical solution of gravity. Together with the representation of AdS fields in terms of boundary operators, this problem is well-understood at least near the vacuum: one can solve bulk equations of motion for the fields perturbatively as operator equations in the CFT using the dictionary to set boundary conditions. This was initiated in the early days of the AdS/CFT correspondence [234] and developed more rigorously by Hamilton, Kabat, Lifschytz and Lowe (HKLL) in a series of papers [235, 236, 237]. Much progress has been achieved since then, triggered in particular by the investigation of the quantum entanglement structure of quantum field theory states – as well as their counterpart in gravity – and due to the increasing introduction of ideas from quantum information science in holography.

[1] This was explained in Section 1.4.2. To avoid confusion, of course CFTs are gapless. Here the word 'gapped' refers to a gap in the spectrum of primary operators from the multi-trace ones. More precisely, the properties 1-5 listed in 1.4.2

Another major step towards the realization of bulk reconstruction through quantum computing language was given in [238] by identifying an apparent paradox in the HKLL reconstruction scheme. Roughly, it was pointed out that multiple regions on the boundary could be employed to define the same bulk operator, raising the question of where exactly the information about the operator was encoded in the CFT, which amounts to a tension with locality in the quantum field theory. The proposal of resolution to the paradox given by the authors relies in interpreting the AdS/CFT correspondence as a quantum error correcting code, though we will not delve into the meaning of this statement here. In reality, the subject is still controversial and the idea of incorporating gauge invariance in the boundary theory into the program of bulk reconstruction to explain the non-uniqueness of bulk fields, along the lines suggested by [239], seems more natural. All in all, the attempts to solve this problem rely on specific toy models, thus so far they appear to be inconclusive.

We will now depart from with the chronological enumeration of some advances in bulk reconstruction and start to expose some criticism. While the realization of spacetime from CFT data works near the vacuum, it is not as successful for more general states. There is no reason to believe that the HKLL analysis, or the one by Faulkner *et al.* [87], holds beyond the perturbative expansion. As a piece of evidence that we cannot trust them, it was argued by Berenstein and Miller in [240] that the reconstruction program fails to hold, generically, beyond the perturbative arguments, requiring trans-planckian physics. The appeal to reconstruct more general states, for instance, corresponding to black hole geometries followed by operators inside the horizon is teleological. As mentioned before, this is a major question. It might lead to a possible resolution of Hawking's information paradox [8] and, until the answer is ignored, we will not achieve a complete understanding of the mechanism behind holography and, consequently, any theory of quantum gravity in AdS spacetime is incomplete.

Henceforward, we will head the discussion to the reconstruction paradigm for AdS_3 space, that is to say, by means of CFT_2 machinery. Since the customary approach to hard problems relies in capitalizing the symmetries in toy models or ideal systems, the reconstruction in the two-dimensional case, where the conformal theory has an infinite dimensional symmetry group, turns out to be an implementation of this rule of thumb. Many faces of this proposal were elaborated in [241, 242, 243, 244, 245, 246] at different instances. The mutual agreement is the use of boundary states[2] to define operators at a point in the bulk. While in this proposal bulk operators are non-local at the boundary, it is possible to show they coincide with the HKLL construction at leading order in the large central charge expansion, though they are gravitationally dressed at non-perturbative level [248].

At this point, an important observation is that pure three-dimensional gravity is a topological theory. This fact raises puzzling issues in the reconstruction program, since it implies that pure AdS_3 space and the Bañados-Teitelboim-Zanelli (BTZ) black hole are related by a diffeomorphism, though

[2] These are either twisted Ishibashi states or cross-cap states that appear in certain boundary CFTs (cf. [247] for instance).

they differ in topology. Concretely, the former geometry should correspond to the vacuum state in the CFT while the later is the putative dual of a highly excited state. How are we supposed to accommodate these facts in reconstructing the bulk? The work of [245] claims to have a description of operators in the BTZ background – based on the aforementioned boundary states – nonetheless, the equivalence between their proposal and HKLL prescription, which at least in principle is expected to be valid only near the vacuum, seems a contradiction at first glance. Still, the study of the interior structure was not fully addressed and it remains unclear whether this approach is suitable or useful to tackle this question.

The brief review of the recent research exposed so far was intended to give a reference frame to the reader, but it certainly does not exhaust the branches of the topic at all. Most of the reasoning behind the description presented was based on [249, 250, 73], where an extensive amount of related material is available. The tension between emergent geometries vs. topology within the AdS_3/CFT_2 correspondence poses a challenge to the bulk reconstruction approach. Our script heads towards a distinct approach to obtain a holographic geometry using different principles relying in the geometrical description of the Hilbert space pointed out in Section 1.2.2. In particular, we will study the Riemannian metric derived from the Fubini-Study distance (1.34) for boundary states of a CFT_2. In the context of quantum information, this metric is sometimes named quantum information metric and it is related to the so-called fidelity susceptibility, which finds many application in condensed matter theory, e. g. in the study of phase transitions [62], as exposed in Section 1.2.2.

More recently, the quantum information metric has also been considered in holography where it may be seen as an emergent metric from the continuous multi-scale entanglement renormalization ansatz (cMERA) [242, 251]. Its gravity dual was computed for a particular construction, where the corresponding CFT was deformed by a marginal operator, and it was conjectured to measure a certain amount of complexity [252].

An interesting observation was made in [242]. By considering the distance between two Ishibashi-like states within a timeslice of a two-dimensional CFT, the authors have shown that the quantum information metric takes the form of the metric on the hyperbolic plane, $\mathbb{H}_2$. As we will show in Section 5.4.2, it is possible to go one step further and extend this analysis to reconstruct more general locally AdS_3 geometries.

5.2 Gravity in asymptotically AdS_3 spaces

Pure Euclidean gravity in $d = 3$ with a negative cosmological constant, $\Lambda = -\ell_{\mathrm{AdS}}^{-2}$, where ℓ_{AdS} is the AdS radius, is described by the action

$$8\pi G^{(3)} S[g] = -\frac{1}{2}\int_{\mathcal{M}} \mathrm{d}^3x\sqrt{g}\left(R - \frac{2}{\ell_{\mathrm{AdS}}^2}\right) - \int_{\partial\mathcal{M}} \mathrm{d}^2x\sqrt{\gamma}K + S_{\mathrm{ct}}[\gamma]. \tag{5.1}$$

The first term is the same as in (1.60). The second piece which involves the induced metric, γ, at the boundary of $\mathcal{M}$ – called the Gibbons-Hawking term – is required in order to establish a well-defined variational principle[3]. In view of the AdS/CFT correspondence, the counterterm part, $S_{\mathrm{ct}}[\gamma]$, is required to render the boundary stress tensor finite. This term will not affect the equations of motion, since it depends only on the boundary metric.

One solution to the Einstein equations that are derived from $S[g]$ is the AdS_3 space in Euclidean signature, or EAdS_3 for short,

$$\mathrm{d}s^2 = \left(1 + \frac{r^2}{\ell_{\mathrm{AdS}}^2}\right)\mathrm{d}\tau^2 + \frac{\mathrm{d}r^2}{\left(1 + \frac{r^2}{\ell_{\mathrm{AdS}}^2}\right)} + r^2\mathrm{d}\phi^2. \tag{5.2}$$

This is a homogeneous, maximally symmetric space with isometry group $\mathrm{SL}(2,\mathbb{R})_L \times \mathrm{SL}(2,\mathbb{R})_R$, as we review in Appendix 5.5. The metric (5.2) is written in global coordinates, meaning that they cover the entire manifold. There is another global coordinate system that will be useful later, defined by

$$r = \ell_{\mathrm{AdS}}\sinh\rho, \qquad \hat{\tau} = \ell_{\mathrm{AdS}}\tau, \tag{5.3}$$

which leads to

$$\mathrm{d}s^2 = \ell_{\mathrm{AdS}}^2\left(\cosh^2\rho\,\mathrm{d}\hat{\tau}^2 + \mathrm{d}\rho^2 + \sinh^2\rho\,\mathrm{d}\phi^2\right). \tag{5.4}$$

A more general one-parameter family of solutions is the BTZ black hole,

$$\mathrm{d}s^2 = \frac{(r^2 - r_+^2)}{\ell_{\mathrm{AdS}}^2}\mathrm{d}\tau^2 + \frac{\ell_{\mathrm{AdS}}^2}{(r^2 - r_+^2)}\mathrm{d}r^2 + r^2\mathrm{d}\phi^2. \tag{5.5}$$

Actually, by setting $r_+ = \mathrm{i}\,\ell_{\mathrm{AdS}}$, one recovers the metric for EAdS_3 (5.2). To see that r_+ is a genuine event horizon, we can Wick rotate to Lorentzian time, $\tau \to \mathrm{i}\,t$, and move to the so-called Eddington-Fikelstein coordinates, defined by

$$\mathrm{d}v = \mathrm{d}t + \frac{1}{f^2(r)}\mathrm{d}r, \qquad f(r) = \frac{(r^2 - r_+^2)}{\ell_{\mathrm{AdS}}^2}, \tag{5.6}$$

[3] C.f. Appendix E.1 of [253].

in terms of which the metric becomes

$$ds^2 = -f^2(r)dv^2 + 2dvdr + r^2 d\phi^2. \tag{5.7}$$

Now it becomes evident that $r = r_+$, that is $f(r_+) = 0$ is a null surface. The BTZ geometry (5.5) is asymptotically AdS for large r,

$$ds^2 \simeq \frac{\ell_{\text{AdS}}^2}{r^2}dr^2 + \frac{r^2}{\ell_{\text{AdS}}^2}\left(d\tau^2 + d\varphi^2\right), \qquad \varphi = \ell_{\text{AdS}}\,\phi. \tag{5.8}$$

The above metric is the so-called Poincaré patch in Euclidean signature. In contrast to (5.2), it covers only part of EAdS_3. Finally, let us register that with the following change of coordinates,

$$r = r_+ \cosh\rho, \qquad \hat{\tau} = \frac{r_+}{\ell_{\text{AdS}}}\phi, \qquad \hat{\phi} = \frac{r_+}{\ell_{\text{AdS}}^2}\tau, \tag{5.9}$$

the Euclidean BTZ metric becomes

$$ds^2 = \ell_{\text{AdS}}^2\left(\cosh^2\rho\, d\hat{\tau}^2 + d\rho^2 + \sinh^2\rho\, d\hat{\phi}^2\right). \tag{5.10}$$

The same form of geometry was derived for the EAdS_3 case, (5.4), with the roles of $\hat{\tau}$ and $\hat{\phi}$ interchanged[4].

The temperature of the black hole can be obtained by analyzing (5.10) near $r = r_+$, corresponding to $\rho \simeq 0$,

$$ds^2 \simeq \ell_{\text{AdS}}^2\left(d\hat{\tau}^2 + d\rho^2 + \rho^2 d\hat{\phi}^2\right). \tag{5.11}$$

The $(\rho, \hat{\phi})$ part of the geometry looks like a copy of $\mathbb{R}^2$ in the neighborhood of the origin, in polar coordinates. Regularity of the coordinate system demands that $\hat{\phi} \simeq \hat{\phi} + 2\pi$, which implies

$$\tau \simeq \tau + \frac{2\pi\ell_{\text{AdS}}^2}{r_+}. \tag{5.12}$$

As a result, τ parametrizes a thermal circle, S^1_β, with inverse temperature

$$\beta = \frac{2\pi\ell_{\text{AdS}}^2}{r_+}. \tag{5.13}$$

Note that when $\rho \to 0$ (or, alternatively, $r \to r_+$) the thermal circle shrinks to zero at the horizon, such that one of the homology cycles of the (solid) torus is contractible. In other words, the Euclidean BTZ is a solid torus with its boundary topologically equivalent to a torus $\text{S}^1_\beta \times \text{S}^1_{2\pi}$. That is, the thermal circle S^1_β is filled in to make the solid torus. By taking $\rho \to 0$ in Equation (5.4) one has a thermal circle

[4] This fact is the analogue of a modular transformation that arises for a CFT_2 defined on a torus.

that is is not contractible, as opposed to the $S^1_{2\pi}$ one.

The above content ends the review on AdS_3 geometries that will suffice for our purposes. For completeness, and in order to make contact with Section 1.4, we now move on and ask the following question: under what conditions a metric can be asymptotically AdS_3 space? To answer it, consider the so-called ADM-like decomposition of the metric[5],

$$ds^2 = N^2 dr^2 + \gamma_{\mu\nu}\left(dx^\mu + N^\mu dr\right)\left(dx^\nu + N^\nu dr\right), \tag{5.14}$$

where $\gamma = \gamma(x, r)$. This has the interpretation of foliating $\mathcal{M}$ by a collection of 2-dimensional timelike surfaces homeomorphic to $\partial\mathcal{M}$. In these terms, at some fixed r, we define $\mathcal{M}_r = \cup_r \partial\mathcal{M}_r$. Such decomposition gives a way to compute the stress tensor for the region $\mathcal{M}_r$. By varying (5.1), the on-shell contribution contains only boundary terms,

$$\delta S = \int_{\partial\mathcal{M}_r} d^2x \pi^{\mu\nu}\delta\gamma_{\mu\nu} + \frac{1}{8\pi G^{(3)}}\int_{\partial\mathcal{M}_r} d^2x \frac{\delta S_{\text{ct}}}{\delta\gamma_{\mu\nu}}\delta\gamma_{\mu\nu}, \tag{5.15}$$

where the momentum conjugate to γ evaluated at r is

$$\pi^{\mu\nu} = \frac{1}{16\pi G^{(3)}}\sqrt{\gamma}\left(K^{\mu\nu} - K\gamma^{\mu\nu}\right) \tag{5.16}$$

and the extrinsic curvature is given by

$$K^{\mu\nu} = -\nabla^{(\mu}n^{\nu)}, \qquad n \perp \partial\mathcal{M}_r \quad \text{(outward)}. \tag{5.17}$$

We then arrive at the quasilocal stress tensor,

$$T^{\mu\nu} \equiv \frac{2}{\sqrt{\gamma}}\frac{\delta S}{\delta\gamma_{\mu\nu}} = \frac{1}{8\pi G^{(3)}}\left(K^{\mu\nu} - K\gamma^{\mu\nu} + \frac{2}{\sqrt{\gamma}}\frac{\delta S_{\text{ct}}}{\delta\gamma_{\mu\nu}}\right). \tag{5.18}$$

The counterterm action must be chosen to cancel the divergences that show up when $\partial\mathcal{M}_r \to \partial\mathcal{M}$. We will take it to be a local functional of the intrinsic geometry of the boundary. For AdS_3, we need to cancel the infinite volume of AdS space,

$$S_{\text{ct}} = -\frac{1}{\ell_{\text{AdS}}}\int_{\partial\mathcal{M}_r} d^2x\sqrt{\gamma}. \tag{5.19}$$

Note that the stress tensor is not traceless,

$$T^\mu{}_\mu = -\frac{1}{8\pi G^{(3)}}\left(K + \frac{2}{\ell_{\text{AdS}}}\right). \tag{5.20}$$

[5] ADM stands for Arnowitt, Deser and Misner who developed a hamiltonian formalism for general relativity in [254].

To compute K, we first choose a suitable coordinate system,

$$ds^2 = \frac{\ell_{\text{AdS}}^2}{r^2} dr^2 + \gamma_{\mu\nu} dx^\mu dx^\nu, \tag{5.21}$$

where

$$K_{\mu\nu} = -\frac{r}{2\ell_{\text{AdS}}} \partial_r \gamma_{\mu\nu}. \tag{5.22}$$

This will give us the result at the boundary. We will skip the details of the calculation, which involves using the Fefferman-Graham theorem to write

$$\gamma_{\mu\nu} = r^2 \gamma_{\mu\nu}^{(0)} + \gamma_{\mu\nu}^{(2)} + \mathcal{O}(r^{-1}) + \mathcal{O}(\log r), \tag{5.23}$$

valid whenever γ obeys Einstein equations. Then, one can show that [255]

$$T^\mu{}_\mu = -\frac{1}{16\pi G^{(3)}} R\left[\gamma^{(0)}\right]. \tag{5.24}$$

Recall Section 1.3.2. Equation (5.24) agrees with the trace anomaly of a CFT_2 (1.55) if one sets the central charge as

$$c = \frac{3\ell_{\text{AdS}}}{2G^{(3)}}. \tag{5.25}$$

This relation between the central charge and the parameters of the gravity theory in AdS space illustrates our discussion of Section 1.4. In particular, it is clear that the condition for a consistent description within general relativity ignoring quantum effects (1.62) will hold for $c \gg 1$, as claimed in Footnote 28.

5.3 Boundary states in two-dimensional CFTs

The next step in our short review is to set up some notation regarding conformal field theories and to introduce the notion of boundary states. First, we will do it by means of the simplest example of a free boson in two dimensions. Then, we will discuss more general interpretations to boundary states that will be useful in what follows.

5.3.1 The free boson

This section is mainly based on [247]. Let us start with a real massless scalar field $X(\tau, \phi)$ defined on a cylinder, that is, $\phi \simeq \phi + 2\pi$. Its action is

$$\begin{aligned} S[X] &= \frac{1}{4\pi\kappa} \int d\tau\, d\sigma \left[(\partial_\tau X)^2 + (\partial_\phi X)^2\right] \\ &= \frac{1}{4\pi\kappa} \int d\tau\, d\sigma \sqrt{h} h^{\alpha\beta} \partial_\alpha X \partial_\beta X, \quad h = \mathbb{1}. \end{aligned} \tag{5.26}$$

where κ is a constant. Mapping the cylinder to the complex plane via $z = e^{\tau+i\phi}$, the new fields $X(z,\bar{z})$ are now described by

$$S[X] = \frac{1}{4\pi\kappa}\int dz d\bar{z}\sqrt{g}g^{\alpha\beta}\partial_\alpha X\partial_\beta X, \qquad g^{\alpha\beta} = 2\begin{pmatrix} 0 & z\bar{z} \\ z\bar{z} & 0 \end{pmatrix}.$$

The equation of motion reads

$$\partial\bar{\partial}X(z,\bar{z}) = 0\,. \tag{5.27}$$

The energy-momentum tensor is defined as

$$T_{ab} \equiv 4\pi\kappa\gamma\frac{1}{\sqrt{|g|}}\frac{\delta S}{\delta g^{ab}}, \tag{5.28}$$

where γ is a constant to be determined. Explicitly,

$$T_{zz} = \gamma\,\partial X\partial X, \qquad T_{\bar{z}\bar{z}} = \gamma\,\bar{\partial}X\bar{\partial}X, \qquad T_{z\bar{z}} = 0. \tag{5.29}$$

In order to guarantee that the vacuum expectation value of the energy-momentum tensor vanishes, we have to take the normal order expression,

$$T(z) \equiv \ :T_{zz}: \ \equiv \gamma : jj : (z), \tag{5.30}$$

where the currents are given by

$$j(z) \ = \ i\partial X(z,\bar{z})\,, \tag{5.31}$$

$$\bar{j}(z) \ = \ i\bar{\partial}X(z,\bar{z})\,. \tag{5.32}$$

The constant γ can be fixed by requiring $j(z)$ to be a primary field with conformal dimension $h = 1$, which amounts to the definition of a chiral field. First, we make an expansion,

$$T(z) = \sum_{n\in\mathbb{Z}} z^{-n-2}L_n\,, \qquad j(z) = \sum_{n\in\mathbb{Z}} z^{-n-1}j_n\,, \tag{5.33}$$

where the Laurent modes are related through

$$L_n = \gamma\sum_{k>-1} j_{n-k}j_k + \gamma\sum_{k\leq -1} j_k j_{n-k}\,. \tag{5.34}$$

This relation leads to the following commutation relation $[L_m, j_n] = -2\gamma\kappa n j_{m+n}$, which corresponds to $h = 1$ if $\gamma = (2\kappa)^{-1}$.

One can integrate the currents in terms of their mode expansions to find out

$$X(z,\bar{z}) = x_0 - \mathrm{i}\left(j_0 \log z + \bar{j}_0 \log \bar{z}\right) + \mathrm{i}\sum_{n\neq 0}\frac{1}{n}\left(j_n z^{-n} + \bar{j}_n \bar{z}^{-n}\right). \tag{5.35}$$

At the $z = \bar{z}$ surface, we have $\bar{z} = z^*$ and X must be invariant under rotation $z \mapsto e^{2\pi\mathrm{i}}z$. This relation implies that

$$j_0 = \bar{j}_0. \tag{5.36}$$

On the cylinder, Equation (5.35) reads

$$X(\tau,\phi) = x_0 - \mathrm{i}\left(j_0 + \bar{j}_0\right)\tau + \left(j_0 - \bar{j}_0\right)\phi + \mathrm{i}\sum_{n\neq 0}\frac{1}{n}\left(j_n e^{-n(\tau+\mathrm{i}\phi)} + \bar{j}_n e^{-n(\tau-\mathrm{i}\phi)}\right). \tag{5.37}$$

The action (5.3.1) is invariant under conformal transformations provided X has conformal dimension $(h,\bar{h}) = (0,0)$. Moreover, the same calculation shows that $(h,\bar{h})_j = (1,0)$ while $(h,\bar{h})_{\bar{j}} = (0,1)$. Thus, X itself is not a conformal field, though it can be used to define the so-called vertex operators $V(z,\bar{z})$ with non-vanishing conformal weights,

$$V_\alpha(z,\bar{z}) \equiv \ :e^{\mathrm{i}\alpha X(z,\bar{z})}: \ . \tag{5.38}$$

One can show that

$$[j_0, V_\alpha] = \alpha V_\alpha, \qquad j_0|\alpha\rangle = \alpha|\alpha\rangle, \tag{5.39}$$

where

$$|\alpha\rangle = \lim_{z,\bar{z}\to 0} V_\alpha(z,\bar{z})|0\rangle \tag{5.40}$$

is an asymptotic in-state obtained by the map between the plane and the cylinder, where $z = \bar{z} = 0$ corresponds to $\tau = -\infty$. Given that $j(z)$ is conserved with an associated conserved charge

$$Q = \oint \frac{\mathrm{d}z}{2\pi\mathrm{i}} j(z) = \int_0^{2\pi} \mathrm{d}\phi\, j_\tau = j_0, \tag{5.41}$$

we can interpret α as the charge of the vertex operator. With a bit more work, one can also obtain

$$L_0|\alpha\rangle = \alpha|\alpha\rangle, \tag{5.42}$$

proving that V_α is a primary field with $(h,\bar{h})_{V_\alpha} = \left(\frac{\alpha^2}{2}, \frac{\alpha^2}{2}\right)$. Notice that $\alpha = \sqrt{2}$ corresponds to currents. We therefore focus on the holomorphic part of $V_{\sqrt{2}}$ and define

$$j^\pm \equiv \ :e^{\pm\mathrm{i}\sqrt{2}X}: \ . \tag{5.43}$$

With the following identifications,

$$j^1 \equiv \frac{1}{\sqrt{2}}(j^+ + j^-), \qquad j^2 \equiv \frac{1}{\sqrt{2}\mathrm{i}}(j^+ - j^-), \qquad j^3 = j, \tag{5.44}$$

one discovers an $\mathfrak{su}(2)$ Kăc-Moody algebra at level $k = 1$, usually denoted by $\widehat{\mathfrak{su}}(2)_1$.

The Hilbert space of the theory is

$$\mathcal{H} = \{\text{Fock space generated by } j_{-n}, \bar{j}_{-m}, \quad n, m \geq 1\}\,. \tag{5.45}$$

For example, on the chiral sector we have

$$\begin{array}{lcl} \text{level 1} & : & j_{-1}|0\rangle \\ \text{level 2} & : & j_{-2}|0\rangle, \qquad j_{-1}j_{-1}|0\rangle \\ \text{level 3} & : & j_{-1}|0\rangle, \qquad j_{-2}j_{-1}|0\rangle, \qquad j_{-1}j_{-1}j_{-1}|0\rangle \\ & \vdots & \end{array} \tag{5.46}$$

The degeneracy at each level N is the number of partitions of N, $P(N)$. For the chiral sector, this is given by

$$\prod_{n\geq 1} \frac{1}{1-q^n} = \sum_{N=0}^{\infty} P(N) q^N. \tag{5.47}$$

5.3.2 Free boson with boundaries

The variation of (5.3.1) contains a boundary term which can be written as

$$\frac{1}{\pi} \int \mathrm{d}\tau (\partial_\phi X) \delta X\,. \tag{5.48}$$

Two possibilities of boundary conditions could be specified at $\phi = 0$ and $\phi = \pi$, namely,

$$\partial_\phi X|_0^\pi = 0, \qquad \text{Neumann condition} \tag{5.49}$$

$$\delta X|_0^\pi = \partial_\tau X|_0^\pi = 0, \qquad \text{Dirichlet condition.} \tag{5.50}$$

The translation of such conditions at $\phi = 0$ in terms of Laurent modes reads

$$j_n - \bar{j}_n = 0, \qquad \text{Neumann condition} \tag{5.51}$$

$$j_n + \bar{j}_n = 0, \quad (\pi_0 = 0), \qquad \text{Dirichlet condition.} \tag{5.52}$$

The above equations mean that the $\mathrm{U}(1) \times \mathrm{U}(1)$ symmetry associated with each of the $\mathrm{U}(1)$ currents, $j(z)$ and $\bar{j}(\bar{z})$, breaks down to a diagonal $\mathrm{U}(1)$. Since the energy-momentum tensor can be expressed

in terms of the currents, the boundary conditions also lead to constraints on the Virasoro operators,

$$L_n - \bar{L}_n = 0 \iff T(z) = \overline{T}(\bar{z}). \tag{5.53}$$

At last, we define a boundary state as one that respects the so-called gluing conditions,

$$(L_n - \bar{L}_{-n})|B\rangle = 0\,. \tag{5.54}$$

5.3.3 Boundary states as maximally entangled states

In the last section we have developed the notion of a boundary state for the free boson CFT. Nonetheless, a Lagrangian formulation is not always available for a general CFT, meaning that in general we cannot count with boundary terms arising from a variation principle. Although it is possible to develop an inherent formulation of a boundary and its states[6], we will not get into the details here and just use Equation (5.54) as a practical definition of a boundary state.

One solution to (5.54) is provided by the so-called Ishibashi states,

$$|I_h\rangle = \sum_{\vec{k}} |\vec{k}, h\rangle_L \otimes |\vec{k}, h\rangle_R\,, \tag{5.55}$$

where the descendant at level $N = \sum_i k_i$ is given by $|h,k\rangle = \cdots L_{-2}^{k_2} L_{-1}^{k_1}|h\rangle$, such that $k = (k_1, k_2, \ldots)$ and $\langle h, k'|h,k\rangle = \delta_{kk'}$. Equation (5.55) expresses a class of maximally entangled states between the left and right-moving sectors of the CFT. Boundary states that correspond to physical boundary conditions are called Cardy states, which are superposition of the Ishibashi states. We can therefore write the full Hilbert space of the CFT as

$$\mathcal{H} = \bigoplus_{h,\bar{h}} n_{h,\bar{h}} \mathcal{V}_h \otimes \mathcal{V}_{\bar{h}}\,, \tag{5.56}$$

where $n_{h,\bar{h}}$ are non-negative integers that specify how many distinct primaries $(h, \bar{h})$ there exist in the CFT and $\mathcal{V}, \bar{\mathcal{V}}$ are the Verma-moduli – the set of all states of the form $|h\rangle$ and $|\bar{h}\rangle$, respectively. This implies that $|B\rangle$ is some linear superposition of states belonging to $\mathcal{V}_h \otimes \mathcal{V}_{\bar{h}}$. The Ishibashi states, as we have written, are solutions for $n_{h,\bar{h}} = \delta_{h,\bar{h}}$, corresponding to a diagonal CFT.

The Ishibashi states have infinite norm. In order to regularize them, we perform an Euclidean time evolution, $e^{-\epsilon H}$, during an infinitesimal amount of time, ϵ, where

$$H = L_0 + \bar{L}_0 - \frac{c}{12} \tag{5.57}$$

[6] For a complete account of this approach, we refer to [256].

is the hamiltonian on the cylinder with energy $E(\vec{k})$. Thus, the normalized state can be written as

$$|I_h\rangle_\epsilon = \frac{1}{\mathcal{Z}_\epsilon^{1/2}} \sum_{\vec{k}} e^{-\epsilon E(\vec{k})} |\vec{k}, h\rangle_L \otimes |\vec{k}, \bar{h}\rangle_R, \tag{5.58}$$

with

$$\mathcal{Z}_\epsilon = \sum_{\vec{k}} e^{-2\epsilon E(\vec{k})}. \tag{5.59}$$

As an interesting observation, note that the reduced state on just one side looks thermal,

$$\rho_L(h, \epsilon) = \mathrm{tr}_R\, |I_h\rangle_\epsilon\, {}_\epsilon\langle I_h| = \frac{1}{\mathcal{Z}_\epsilon} \sum_{\vec{k}} e^{-2\epsilon E(\vec{k})} |\vec{k}, h\rangle_L\, {}_L\langle \vec{k}, h|, \tag{5.60}$$

which is exactly a Gibbs state if we set $\beta = 2\epsilon$.

5.4 Quantum information metric

We finished the excursion into basic topics and now we turn to the next goal, which will be the computation of the quantum information metric in a fixed timeslice of a two-dimensional conformal field theory. As mentioned before, Section 5.4.1 mainly includes the results of [242], though with a somewhat complementary point of view. Then, in Sections 5.4.2 and 5.4.3 we will advance one step further and present new results.

5.4.1 The hyperbolic plane

Let us start with a boundary conformal field theory in two dimensions, BCFT_2 for short, defined on $\mathbb{R} \times \mathrm{S}^1$. The presence of the boundary breaks half of the conformal symmetries: from $\mathrm{SL}(2,\mathbb{R})_L \times \mathrm{SL}(2,\mathbb{R})_R$ down to a (by assumption) diagonal $\mathrm{SL}(2,\mathbb{R})$. Some properties of this group are reviewed in Appendix 5.5. The generators obey the following algebra,

$$[\ell_0, \ell_{\pm 1}] = \mp \ell_{\pm 1}, \qquad [\ell_1, \ell_{-1}] = 2\ell_0 \tag{5.61}$$

where the relation between ℓ_a and the previous generators L_a is

$$\ell_0 = L_0 - \tilde{L}_0\,, \qquad \ell_{-1} = \tilde{L}_1 - L_{-1}\,, \qquad \ell_1 = \tilde{L}_{-1} - L_1\,. \tag{5.62}$$

A general $\mathrm{SL}(2,\mathbb{R})$ element, g, can be put in the form of Euler-like rotations,

$$g(\rho, \phi, \theta) = e^{\phi \Lambda_0} e^{\rho \Lambda_1} e^{-\theta \Lambda_0}, \qquad \rho \geq 0. \tag{5.63}$$

using the $\Lambda_{0,\pm 1}$ generators that are introduced in (5.115).

Next, consider the $\mathrm{SL}(2,\mathbb{R})$ highest weight state, $|h\rangle$, defined by

$$\ell_0|h\rangle = h|h\rangle, \qquad \ell_1|h\rangle = 0. \tag{5.64}$$

The stabilizer of $|h\rangle$ is the $\mathrm{SO}(2)$ generated by ℓ_0. We can therefore construct a family of states achieved by inequivalent $\mathrm{SL}(2,\mathbb{R})$ transformations, that is, with parameters living in the hyperbolic plane

$$\frac{\mathrm{SL}(2,\mathbb{R})}{\mathrm{SO}(2)} \simeq \mathbb{H}^2. \tag{5.65}$$

In other words, the $\mathrm{SL}(2,\mathbb{R})$ transformation takes the origin of $\mathbb{H}^2$ to the point (ρ,ϕ) defining a section of the $\mathrm{U}(1)$ bundle $\mathrm{SL}(2,\mathbb{R}) \to \mathbb{H}^2$,

$$|h(\rho,\phi)\rangle \equiv g(\rho,\phi)|h\rangle\,, \qquad g(\rho,\phi) = e^{\mathrm{i}\ell_0\phi}e^{\frac{\rho}{2}(\ell_1-\ell_{-1})}\,. \tag{5.66}$$

Likewise, we construct a family of boundary states that mimic Equation (5.66),

$$|\Psi_h(\rho,\phi)\rangle = g(\rho,\phi)|\Psi_h\rangle\,, \tag{5.67}$$

where

$$|\Psi_h\rangle \equiv e^{\mathrm{i}\frac{\pi}{2}H}|I_h\rangle \tag{5.68}$$

is a twisted Ishibashi state, meaning that it satisfies the following "twisted" gluing conditions

$$(L_0 - \tilde{L}_0)|\Psi_h\rangle = (L_1 + \tilde{L}_{-1})|\Psi_h\rangle = (L_{-1} + \tilde{L}_1)|\Psi_h\rangle = 0 \tag{5.69}$$

instead of the usual ones (5.54). Similarly to the untwisted version, twisted Ishibashi states also have an infinite norm. Then, we can proceed in the same way as in Equation (5.58) to regularize them,

$$|\Psi_h\rangle \to \frac{1}{\sqrt{Z_\delta}}e^{-\delta H}e^{\mathrm{i}\frac{\pi}{2}H}|I_h\rangle, \qquad Z_\delta = \sum_k e^{-2\delta E_k}. \tag{5.70}$$

Now, we apply the machinery of Section 1.2.2 to this situation. First, we note that the Berry connection (1.30) for the states (5.67) vanishes

$$A_\rho = \mathrm{i}\langle\Psi_h(\rho,\phi)|\partial_\rho\Psi_h(\rho,\phi)\rangle = \frac{\mathrm{i}}{2}\langle\Psi_h|\ell_1 - \ell_{-1}|\Psi_h\rangle = 0, \tag{5.71}$$

where we have used that

$$\langle k,h|L_{-1}|h,k\rangle \propto \langle(k_1,k_2,\ldots)|(k_1+1,k_2,\ldots)\rangle = \delta_{k_1,k_1+1}\,. \tag{5.72}$$

The same is true along the ϕ-direction,

$$A_\phi = \mathrm{i}\langle\Psi_h(\rho,\phi)|\partial_\phi\Psi_h(\rho,\phi)\rangle = \langle\Psi_h|e^{-\frac{\rho}{2}(\ell_1-\ell_{-1})}\ell_0 e^{\frac{\rho}{2}(\ell_1-\ell_{-1})}|\Psi_h\rangle = 0\,, \tag{5.73}$$

since

$$e^{-\frac{\rho}{2}(\ell_1-\ell_{-1})}\ell_0 e^{\frac{\rho}{2}(\ell_1-\ell_{-1})} = (\cosh\rho)\ell_0 - \frac{1}{2}(\sinh\rho)(\ell_1+\ell_{-1}) \tag{5.74}$$

and

$$\langle\Psi_h|\ell_0|\Psi_h\rangle = 0\,, \qquad \langle\Psi_h|\ell_1-\ell_{-1}|\Psi_h\rangle = 0\,. \tag{5.75}$$

In the absence of the connection term, the non-vanishing components of the quantum information metric are simply given by

$$g_{\rho\rho} = \langle\partial_\rho\Psi_h(\rho,\phi)|\partial_\rho\Psi_h(\rho,\phi)\rangle = \frac{1}{4}\langle\Psi_h|\{\ell_1,\ell_{-1}\}|\Psi_h\rangle\,, \tag{5.76}$$

and

$$g_{\phi\phi} = \frac{1}{2}\langle\Psi_h|\ell_1\ell_{-1}|\Psi_h\rangle\sinh^2\rho\,. \tag{5.77}$$

To compute such expectation values, note that

$$\tilde{L}_1|\Psi_h\rangle = \frac{1}{\sqrt{Z_\delta}}e^{(-2\delta+\mathrm{i}\pi)L_0}L_{-1}|I_h\rangle = -e^{-2\delta}L_{-1}|\Psi_h\rangle\,. \tag{5.78}$$

Similarly,

$$\tilde{L}_{-1}|\Psi_h\rangle = -e^{2\delta}L_1|\Psi_h\rangle\,. \tag{5.79}$$

Then, it follows that

$$\ell_{\pm1}|\Psi_h\rangle = -\left(e^{\pm2\delta}+1\right)L_{\pm1}|\Psi_h\rangle\,, \qquad \langle\Psi_h|\ell_{\mp1} = -\langle\Psi_h|\left(e^{\pm2\delta}+1\right)L_{\mp1}\,, \tag{5.80}$$

leading to

$$\langle\Psi_h|\ell_{-1}\ell_1|\Psi_h\rangle = (e^{2\delta}+1)^2\langle\Psi_h|L_{-1}L_1|\Psi_h\rangle = \langle\Psi_h|\ell_1\ell_{-1}|\Psi_h\rangle\,. \tag{5.81}$$

Using the above relation, one readily shows that

$$\langle\Psi_h|L_{-1}L_1|\Psi_h\rangle \;\;=\;\; \frac{2}{e^{4\delta}-1}\langle\Psi_h|L_0|\Psi_h\rangle\,, \tag{5.82}$$

where the expectation value can be evaluated as

$$\langle\Psi_h|L_0|\Psi_h\rangle = \frac{e^{\frac{c\delta}{6}}}{Z_\delta}\sum_k e^{-4\delta(h+N(k))}\,(h+N(k)) = \frac{1}{4\delta}+\left(h-\frac{1}{2}\right)+\mathcal{O}(\delta)\,. \tag{5.83}$$

Collecting the above results, we can finally obtain

$$\langle\Psi_h|\ell_{-1}\ell_1|\Psi_h\rangle = \frac{2(e^{2\delta}+1)^2}{e^{4\delta}-1}\langle\Psi_h|L_0|\Psi_h\rangle = \frac{1}{2\delta^2}+\frac{2h-1}{\delta}+\frac{5}{6}+\mathcal{O}(\delta)\,, \tag{5.84}$$

which fixes the form of $g_{\rho\rho}$ and $g_{\phi\phi}$. Thus, the quantum information metric up to $\mathcal{O}(\delta^{-2})$,

$$\mathrm{d}s^2 = \frac{1}{4\delta^2}\left(\mathrm{d}\rho^2+\sinh^2\rho\,\mathrm{d}\phi^2\right)\,. \tag{5.85}$$

which is the hyperbolic plane.

5.4.2 The BTZ black hole

Let us perform an Euclidean evolution of the boundary state

$$|\Psi_h(\rho,\phi,\tau)\rangle = e^{-H\tau}|\Psi_h(\rho,\phi)\rangle\,. \tag{5.86}$$

The Berry connection is no longer zero for this case,

$$\begin{aligned} A_\tau &= \langle\Psi_h(\rho,\phi)|H|\Psi_h(\rho,\phi)\rangle = \langle\Psi_h|e^{-\frac{\rho}{2}(\ell_1-\ell_{-1})}He^{\frac{\rho}{2}(\ell_1-\ell_{-1})}|\Psi_h\rangle \\ &= \cosh\rho\,\langle\Psi_h|\left(L_0+\tilde{L}_0-\frac{c}{12}\right)|\Psi_h\rangle \\ &= \frac{2(\cosh\rho)e^{\frac{\delta c}{6}}}{Z_\delta}\sum_k e^{-4\delta(h+N(k))}\left(h+N(k)-\frac{c}{24}\right) \\ &= \frac{\cosh(\rho)}{2\delta}-\frac{1}{12}(c-24h+12)\cosh(\rho)+\mathcal{O}(\delta)\,. \end{aligned} \tag{5.87}$$

Due to the inclusion of Euclidean time in the parametrization of the state, there will be a corresponding metric component. Taking similar steps as the ones in the above calculation, one has

$$g_{\tau\tau} = \langle\Psi_h|g^\dagger(\rho,\phi)H^2g(\rho,\phi)|\Psi_h\rangle - A_\tau^2 = \frac{\cosh^2\rho}{4\delta^2}+\mathcal{O}(\delta^{-1})\,. \tag{5.88}$$

Thefore, the quantum information metric now reads

$$\mathrm{d}s^2 = \frac{1}{4\delta^2}\left(\cosh^2\rho\,\mathrm{d}\tau^2+\mathrm{d}s^2_{\mathbb{H}^2}\right)\,. \tag{5.89}$$

As we have seen in Section 5.2, this is the metric of either thermal AdS space or the BTZ black hole, depending on the temperature. The difference between the two spaces lies in the topology, such that we can diagnose the global behavior by means of the Berry connection:

$$\oint_\gamma A = \oint_\gamma A_\tau\,\mathrm{d}\tau = \frac{\beta\cosh\rho}{2\delta}-\frac{\beta}{12}(c-24h+12)\cosh(\rho)+\mathcal{O}(\delta),\quad \text{for}\quad \gamma=\mathrm{S}^1_\tau \tag{5.90}$$

while

$$\oint_\gamma A = 0, \quad \text{for} \quad \gamma = \mathrm{S}^1_\phi \,. \tag{5.91}$$

These cycles agree with the case of thermal AdS space. However, in terms of $(\hat{\tau}, \varphi)$ coordinates,

$$\begin{aligned} \oint_\gamma A &= 0, \quad \text{for} \quad \gamma = \mathrm{S}^1_{\hat{t}} \\ \oint_\gamma A &= 2\pi r_+ \cosh\rho - \frac{\pi\delta r_+}{6}(c - 24h + 12)\cosh(\rho) + \mathcal{O}(\delta^2), \quad \text{for} \quad \gamma = \mathrm{S}^1_\varphi \,, \end{aligned} \tag{5.92}$$

that correctly captures the topology of the BTZ black hole.

5.4.3 The rotating BTZ

Despite of being another change of coordinates from the point of view of $3d$ gravity, it is worthy to point out the possibility of deriving the metric for the BTZ black hole with a nonzero angular momentum as well. To do that, let us consider a deformation of the family of twisted boundary states as follows

$$|\Omega_h(\rho,\phi)\rangle \equiv e^{\mathrm{i}a\phi L_0}|\Psi_h(\rho, b\phi)\rangle \,, \tag{5.93}$$

where $a, b \in \mathbb{R}$, and also its Euclidean time evolved version,

$$|\Omega_h(\rho,\phi,\tau)\rangle = e^{-H\tau}|\Omega_h(\rho,\phi)\rangle \,. \tag{5.94}$$

The A_τ component remains unchanged for this class of states. Nonetheless, now there will be a A_ϕ term,

$$A_\phi = -\langle\Psi_h|e^{-\frac{\rho}{2}(\ell_1-\ell_{-1})}(aL_0 + b\ell_0)e^{\frac{\rho}{2}(\ell_1-\ell_{-1})}|\Psi_h\rangle = -a\cosh\rho\left[\frac{1}{4\delta} + \left(h - \frac{1}{2}\right) + \mathcal{O}(\delta)\right]. \tag{5.95}$$

which reflects on a $g_{\phi\phi}$ component,

$$\begin{aligned} g_{\phi\phi} &= \langle\Psi_h|e^{-\frac{\rho}{2}(\ell_1-\ell_{-1})}(b\ell_0 + aL_0)^2 e^{\frac{\rho}{2}(\ell_1-\ell_{-1})}|\Psi_h\rangle - A_\phi^2 \\ &= \frac{b^2}{4\delta^2}\sinh^2\rho + a^2\cosh^2\rho\langle\Psi_h|L_0^2|\Psi_h\rangle - A_\phi^2 = \frac{b^2}{4\delta^2}\sinh^2\rho + \frac{a^2}{16\delta^2}\cosh^2\rho + \mathcal{O}\left(\frac{1}{\delta}\right). \end{aligned}$$

and also on a nonzero off-diagonal entry,

$$\begin{aligned} g_{\tau\phi} &= \langle\partial_\tau\Omega_h(\rho,\phi)|\partial_\phi\Omega_h(\rho,\phi)\rangle - A_\tau A_\phi = -\langle\Psi_h|e^{-\frac{\rho}{2}(\ell_1-\ell_{-1})}H(b\ell_0 + aL_0)e^{\frac{\rho}{2}(\ell_1-\ell_{-1})}|\Psi_h\rangle - A_\tau A_\phi \\ &= -2a\cosh^2\rho\,\langle\Psi_h|L_0^2|\Psi_h\rangle - A_\tau A_\phi = -\frac{a\cosh^2\rho}{8\delta^2} + \mathcal{O}\left(\frac{1}{\delta}\right). \end{aligned} \tag{5.96}$$

Collecting the results and re-scaling $a \to -2a$, we obtain

$$ds^2 = \frac{1}{4\delta^2}\left[\cosh^2\rho\, d\tau^2 + d\rho^2 + \left(a^2\cosh^2\rho + b^2\sinh^2\rho\right) d\phi^2 + 2a\cosh^2\rho\, d\tau d\phi\right],$$

which is proportional to the Euclidean BTZ metric in global coordinates. This can be seen by considering the following change of coordinates,

$$\rho = \sinh^{-1}\left(\frac{r}{b}\right), \qquad \tau = b\hat{\tau}, \tag{5.97}$$

resulting in

$$ds^2 = \frac{1}{4\delta^2}\left[(r^2+b^2)\left(d\hat{\tau} + \frac{a}{b}d\phi\right)^2 + r^2 d\phi^2 + \frac{dr^2}{r^2+b^2}\right]. \tag{5.98}$$

One can also take one step further and formally Wick rotate to Minkowski space by taking $\tau = it$ and $b \to -ib$[7]. To put the metric in a conventional form, define

$$\hat{r} = b\sqrt{\frac{r^2-a^2}{b^2-a^2}}, \qquad \phi = \varphi + \frac{a}{b}t, \qquad \hat{t} = t\frac{b^2-a^2}{b^2}, \tag{5.99}$$

such that (dropping the hats)

$$ds^2 = \frac{1}{4\delta^2}\left[-f(r)dt^2 + f(r)^{-1}dr^2 + r^2\left(d\varphi - \frac{ab}{r^2}d\tau\right)^2\right], \tag{5.100}$$

$$f(r) = \frac{(r^2-a^2)(r^2-b^2)}{r^2}. \tag{5.101}$$

This geometry is proportional to the usual Lorentzian BTZ with $M = a^2 + b^2$ and $J = 2ab$.

5.5 Appendix: $\mathrm{SL}(2,\mathbb{R})$

Any real 2×2 matrix can be written as

$$g = \frac{1}{\ell}\begin{pmatrix} -X^0 + X^1 & X^2 + X^3 \\ -X^2 + X^3 & X^0 + X^1 \end{pmatrix} \tag{5.102}$$

This will be an element of $\mathrm{SL}(2,\mathbb{R})$ if and only if $\det g = 1$, which implies

$$-(X^0)^2 + (X^1)^2 + (X^2)^2 - (X^3)^2 = -\ell^2 \tag{5.103}$$

[7] The need to rotate the outer radius in addition to the time coordinate is due to the fact that $J_{\text{Euclidean}} = iJ$.

which defines a hyperboloid with topology $\mathbb{R}^2 \times \mathrm{S}^1$, where S^1 corresponds to timelike circles $(X^0)^2 + (X^3)^2 =$ constant. This hyperboloid is embedded in $\mathbb{R}^{2,2}$ with the group invariant metric

$$\mathrm{d}s^2 = -\frac{1}{2}\mathrm{tr}\, g^{-1}\mathrm{d}g g^{-1}\mathrm{d}g = -(\mathrm{d}X^0)^2 + (\mathrm{d}X^1)^2 + (\mathrm{d}X^2)^2 - (\mathrm{d}X^3)^2. \tag{5.104}$$

One can solve Equation (5.103) by parametrizing the X^a coordinates in terms of a new set (t, ρ, ϕ),

$$\begin{aligned} X^0 &= \ell \cosh\rho \cos t \qquad X^1 = \ell \sinh\rho \sin\phi \\ X^2 &= \ell \sinh\rho \cos\phi \qquad X^3 = \ell \cosh\rho \sin t\,, \end{aligned} \tag{5.105}$$

which induces the following metric on the hyperboloid

$$\mathrm{d}s^2 = \ell^2(-\cosh^2\rho\, \mathrm{d}t^2 + \mathrm{d}\rho^2 + \sinh^2\rho\, \mathrm{d}\phi^2). \tag{5.106}$$

This is the universal cover of the AdS_3 space in global coordinates if we unwind the circle. The isometry group of AdS_3 is the subgroup of the isometry group of (5.104) which leaves (5.106) invariant, that is, $\mathrm{SO}(2,2)$, where the rotations along (X^0, X^3) that differ by $2\pi n$, $n \in \mathbb{Z}$, are not identified. In the representation furnished by (5.102), the $\mathrm{SO}(2,2)$ isometries are induced by the two-fold cover $\mathrm{SL}(2,\mathbb{R})_L \times SL(2,\mathbb{R})_R$,

$$g \to g_L g g_R\,, \qquad g_L, g_R \in \mathrm{SL}(2,\mathbb{R})\,. \tag{5.107}$$

This is two-fold since $(g_L, g_R) \to (-g_L, -g_R)$ leads to the same element $g \in \mathrm{SO}(2,2)$.

A general $\mathfrak{sl}(2,\mathbb{R})$ element is traceless and, therefore, we can chose the following matrices as generators,

$$L_{-1} = \begin{pmatrix} 0 & 1 \\ 0 & 0 \end{pmatrix}, \qquad L_0 = \frac{1}{2}\begin{pmatrix} 1 & 0 \\ 0 & -1 \end{pmatrix}, \qquad L_1 = \begin{pmatrix} 0 & 0 \\ -1 & 0 \end{pmatrix}. \tag{5.108}$$

This basis elements obey $[L_n, L_m] = (n-m)L_{m+n}$.

Since Anti-de-Sitter space inherits the isometries of its embedding, one can find all its Killing vectors using the embedding space formalism. That is, consider the boost vectors in $\mathbb{R}^{2,2}$,

$$K = X^1\partial_{X^0} + X^0\partial_{X^1}\,, \qquad \bar{K} = X^3\partial_{X^2} + X^2\partial_{X^3}\,. \tag{5.109}$$

We can project these 4-vectors on the hyperboloid by means of the following tensor

$$\Pi^A_\mu = \frac{\partial X^A}{\partial x^\mu}\,, \qquad A = 0,1,2,3\,, \qquad x^\mu = (t,\rho,\phi)\,. \tag{5.110}$$

Then, the Killing vectors are given by

$$\xi_\mu = \Pi^A_\mu K_A\,, \qquad \bar{\xi}_\mu = \Pi^A_\mu \bar{K}_A\,. \tag{5.111}$$

Explicitly,

$$\begin{aligned}
\xi_{-1} &= \frac{1}{2}e^{-\mathrm{i}(t+\phi)}\left(\tanh\rho\,\partial_t + \coth\rho\,\partial_\phi + \mathrm{i}\partial_\rho\right)\\
\xi_0 &= \frac{1}{2}\left(\partial_t + \partial_\phi\right)\\
\xi_1 &= \frac{1}{2}e^{\mathrm{i}(t+\phi)}\left(\tanh\rho\,\partial_t + \coth\rho\,\partial_\phi - \mathrm{i}\partial_\rho\right)\\
\bar{\xi}_{-1} &= \frac{1}{2}e^{-\mathrm{i}(t-\phi)}\left(\tanh\rho\,\partial_t - \coth\rho\,\partial_\phi + \mathrm{i}\partial_\rho\right)\\
\bar{\xi}_0 &= \frac{1}{2}\left(\partial_t - \partial_\phi\right)\\
\bar{\xi}_1 &= \frac{1}{2}e^{\mathrm{i}(t-\phi)}\left(\tanh\rho\,\partial_t - \coth\rho\,\partial_\phi - \mathrm{i}\partial_\rho\right)\,. \qquad (5.112)
\end{aligned}$$

The Killing vectors obey the $\mathrm{SL}(2,\mathbb{R})_L \times \mathrm{SL}(2,\mathbb{R})_R$ under the Lie brackets,

$$\mathrm{i}\{\xi_i, \xi_j\} = (i-j)\xi_{i+j}. \qquad (5.113)$$

We may also define the coordinates $z = e^{\tau+\mathrm{i}\phi}$, $\bar{z} = e^{\tau-\mathrm{i}\phi}$ at the boundary $\rho = \infty$, where the basis vector fields of the Lie algebra become

$$L_n = -z^{n+1}\partial_z\,, \qquad L_n = -\bar{z}^{n+1}\partial_{\bar{z}}\,. \qquad (5.114)$$

These are Killing vectors that preserve the metric of the upper-half complex plane. Instead, if we choose them to preserve the unit disk $|z| < 1$, we can use the Cayley map, $z \mapsto \dfrac{z-\mathrm{i}}{z+\mathrm{i}}$ to write,

$$\Lambda_0 = \frac{1}{2}\begin{pmatrix}\mathrm{i} & 0\\ 0 & -\mathrm{i}\end{pmatrix} = \mathrm{i}L_0\,,\ \Lambda_1 = \frac{1}{2}\begin{pmatrix}0 & 1\\ 1 & 0\end{pmatrix} = \frac{L_{-1}-L_1}{2},\ \Lambda_2 = \frac{1}{2}\begin{pmatrix}0 & \mathrm{i}\\ -\mathrm{i} & 0\end{pmatrix} = \mathrm{i}\frac{L_{-1}+L_1}{2}, \qquad (5.115)$$

which obey

$$[\Lambda_0, \Lambda_1] = \Lambda_2, \qquad [\Lambda_0, \Lambda_2] = -\Lambda_1, \qquad [\Lambda_1, \Lambda_2] = -\Lambda_0. \qquad (5.116)$$

6

Closing remarks

"Essa preocupação com o fim ou os resultados, como também com as diversidades e apreciações dos mesmos, é, pois, uma tarefa mais fácil do que pareça. Com efeito, tal [modo de] agir, em vez de se ocupar com a Coisa mesma, passa sempre por cima. Em vez de nela demorar-se e esquecer a si mesmo, prende-se sempre a algo distinto; prefere ficar em si mesmo a estar na Coisa e a abandonar-se a ela. Nada mais fácil do que julgar o que tem conteúdo e solidez; apreendê-lo é mais difícil; e o que há de mais difícil é produzir sua exposição, que unifica a ambos."

— Hegel, *Fenomenologia do Espírito*

The bridge between many-body quantum systems and quantum gravity – in the form of the AdS/CFT correspondence – has occupied our attention in Chapter 1. After that, we provided several studies along the subsequent chapters with regard to the diversity of concepts that allowed us to build such a connection.

Complexity, the main concept of Chapter 2, was employed in the description of nonequilibrium quantum phase transitions that turn up after one periodically drives the transverse field Ising model. Further evidence was provided that the circuit complexity carries information on universal features out of equilibrium and that it can also diagnose different types of critical phenomena, including equilibrium, topological and dynamical quantum phase transitions.

Entanglement, the main concept of Chapter 3, was considered from a dynamical point of view in a class of quantum circuits with Floquet dynamics. A bound on its rate of spreading was derived and an example of an integrable system that saturates this maximal rate was given. Abstracting particularities of the example – a circuit of parallel SWAP gates acting on entangled pairs – but retaining its qualitative aspects – a quasiparticle picture for the propagation of entanglement – we were able to suggest that chaos tends to reduce the speed at which two subregions become entangled by a corresponding increase of multipartite entanglement among the degrees of freedom. Deepening our argument might help in the understanding of the interplay between multiparty entanglement, chaos and information spread.

Integrability, not the main, but one central concept of Chapter 4, was an output of the class of supersymmetric many-body systems we have constructed out of the partial symmetries described by symmetric inverse semigroups. The consequences of integrability were crucial for identifying examples of supersymmetric phases of matter and for the appearance of a many-body localized phase upon the introduction of disorder in one particular toy model.

Geometry, the main concept of Chapter 5, was studied under an emergent perspective in the context of the AdS_3/CFT_2 correspondence, where a Riemannian structure introduced in the CFT Hilbert space was the key element mediating the field theory side to the gravity one.

Taken separately, the above concepts were sufficient to extract several lessons for the systems where they were independently applied. Resuming the opening words in the Introduction and the course of Chapter 1, taken together – with the caveat on integrability, that should be replaced by nonintegrability – those concepts appear to be fundamental for the development of an indirect probe of quantum gravity through the manipulation of quantum many-body systems.

Bibliography

[1] M. Cheneau, P. Barmettler, D. Poletti, M. Endres, P. Schauß, T. Fukuhara, C. Gross, I. Bloch, C. Kollath, and S. Kuhr, *Light-cone-like spreading of correlations in a quantum many-body system*, *Nature* **481** (2012), no. 7382 484–487.

[2] E. H. Lieb and D. W. Robinson, *The finite group velocity of quantum spin systems*, *Comm. Math. Phys.* **28** (1972), no. 3 251–257.

[3] M. Greiner, O. Mandel, T. Esslinger, T. Haensch, and I. Bloch, *Quantum phase transition from a superfluid to a mott insulator in a gas of ultracold atoms*, *Nature* **415** (2002) 39–44.

[4] L. Landau and E. Lifshitz, *Statistical Physics*. Butterworth-Heinemann, 1980.

[5] S. Sachdev, *Quantum Phase Transitions*. Cambridge University Press, 1999.

[6] B. Zeng, X. Chen, D.-L. Zhou, and X.-G. Wen, *Quantum information meets quantum matter – from quantum entanglement to topological phase in many-body systems*, arXiv:1508.02595.

[7] M. H. Freedman, A. Kitaev, M. J. Larsen, and Z. Wang, *Topological Quantum Computation*, quant-ph/0101025.

[8] S. Hawking, *Particle Creation by Black Holes*, *Commun. Math. Phys.* **43** (1975) 199–220. [Erratum: Commun.Math.Phys. 46, 206 (1976)].

[9] S. W. Hawking, *Breakdown of predictability in gravitational collapse*, *Phys. Rev. D* **14** (1976) 2460–2473.

[10] G. 't Hooft, *Dimensional reduction in quantum gravity*, *Conf. Proc. C* **930308** (1993) 284–296, [gr-qc/9310026].

[11] L. Susskind, *The World as a hologram*, *J. Math. Phys.* **36** (1995) 6377–6396, [hep-th/9409089].

[12] J. M. Maldacena, *The Large N limit of superconformal field theories and supergravity*, *Int. J. Theor. Phys.* **38** (1999) 1113–1133, [hep-th/9711200].

[13] S. Ryu and T. Takayanagi, *Holographic derivation of entanglement entropy from the anti–de sitter space/conformal field theory correspondence*, *Phys. Rev. Lett.* **96** (2006) 181602.

[14] S. Ryu and T. Takayanagi, *Aspects of Holographic Entanglement Entropy*, *JHEP* **08** (2006) 045, [hep-th/0605073].

[15] M. V. Raamsdonk, *Comments on quantum gravity and entanglement*, arXiv:0907.2939.

[16] M. Van Raamsdonk, *Building up spacetime with quantum entanglement*, *Gen. Rel. Grav.* **42** (2010) 2323–2329, [arXiv:1005.3035].

[17] A. Kitaev, "A simple model of quantum holography." http://online.kitp.ucsb.edu/online/entangled15/kitaev/ http://online.kitp.ucsb.edu/online/entangled15/kitaev2/. Talks at KITP: April 7 and May 27 (2015).

[18] J. Maldacena and D. Stanford, *Remarks on the Sachdev-Ye-Kitaev model*, *Phys. Rev. D* **94** (2016), no. 10 106002, [arXiv:1604.07818].

[19] G. Sárosi, *AdS_2 holography and the SYK model*, *PoS* **Modave2017** (2018) 001, [arXiv:1711.08482].

[20] D. A. Trunin, *Pedagogical introduction to SYK model and 2D Dilaton Gravity*, arXiv:2002.12187.

[21] A. R. Brown, H. Gharibyan, S. Leichenauer, H. W. Lin, S. Nezami, G. Salton, L. Susskind, B. Swingle, and M. Walter, *Quantum Gravity in the Lab: Teleportation by Size and Traversable Wormholes*, arXiv:1911.06314.

[22] G. Camilo and D. Teixeira, *Complexity and Floquet dynamics: non-equilibrium Ising phase transitions*, *Phys. Rev. B* **102** (2020), no. 17 174304, [arXiv:2009.00069].

[23] D. Berenstein and D. Teixeira, *Maximally entangling states and dynamics in one dimensional nearest neighbor Floquet systems*, arXiv:1901.02944.

[24] P. Padmanabhan, S.-J. Rey, D. Teixeira, and D. Trancanelli, *Supersymmetric many-body systems from partial symmetries — integrability, localization and scrambling*, *JHEP* **05** (2017) 136, [arXiv:1702.02091].

[25] P. W. Anderson, *More is different*, *Science* **177** (1972), no. 4047 393–396.

[26] J. von Neumann, *On infinite direct products*, *Compositio Mathematica* **6** (1939) 1–77.

[27] E. H. Lieb, *The stability of matter*, *Rev. Mod. Phys.* **48** (1976) 553–569.

[28] B. Nachtergaele and R. Sims, *Lieb-robinson bounds in quantum many-body physics*, arXiv:1004.2086.

[29] M. B. Hastings and T. Koma, *Spectral gap and exponential decay of correlations*, *Commun. Math. Phys.* **265** (2006) 781–804, [math-ph/0507008].

[30] B. Nachtergaele and R. Sims, *Lieb-robinson bounds and the exponential clustering theorem*, *Communications in Mathematical Physics* **265** (2006), no. 1 119–130.

[31] S. Bravyi, M. Hastings, and F. Verstraete, *Lieb-Robinson Bounds and the Generation of Correlations and Topological Quantum Order*, *Phys. Rev. Lett.* **97** (2006) 050401, [quant-ph/0603121].

[32] M. B. Hastings, *Locality in quantum systems*, arXiv:1008.5137.

[33] M. Fannes, B. Nachtergaele, and R. F. Werner, *Finitely correlated states on quantum spin chains*, *Comm. Math. Phys.* **144** (1992), no. 3 443–490.

[34] F. Verstraete and J. Cirac, *Renormalization algorithms for quantum-many body systems in two and higher dimensions*, cond-mat/0407066.

[35] M. Cramer and J. Eisert, *Correlations, spectral gap and entanglement in harmonic quantum systems on generic lattices*, *New Journal of Physics* **8** (2006), no. 5 71.

[36] M. Cramer, J. Eisert, M. B. Plenio, and J. Dreißig, *Entanglement-area law for general bosonic harmonic lattice systems*, *Phys. Rev. A* **73** (2006) 012309.

[37] M. B. Plenio, J. Eisert, J. Dreißig, and M. Cramer, *Entropy, entanglement, and area: Analytical results for harmonic lattice systems*, *Phys. Rev. Lett.* **94** (2005) 060503.

[38] M. Cramer, J. Eisert, and M. B. Plenio, *Statistics dependence of the entanglement entropy*, *Phys. Rev. Lett.* **98** (2007) 220603.

[39] S. Farkas and Z. Zimborás, *The von neumann entropy asymptotics in multidimensional fermionic systems*, *Journal of Mathematical Physics* **48** (2007), no. 10 102110.

[40] D. Gioev and I. Klich, *Entanglement entropy of fermions in any dimension and the widom conjecture*, *Phys. Rev. Lett.* **96** (2006) 100503.

[41] M. M. Wolf, *Violation of the entropic area law for fermions*, *Phys. Rev. Lett.* **96** (2006) 010404.

[42] G. Refael and J. E. Moore, *Entanglement entropy of the random $s = 1$ heisenberg chain*, *Physical Review B* **76** (2007), no. 2.

[43] M. Hastings, *An area law for one-dimensional quantum systems*, *J. Stat. Mech.* **0708** (2007) P08024, [arXiv:0705.2024].

[44] X. Han and S. A. Hartnoll, *Quantum Scrambling and State Dependence of the Butterfly Velocity*, *SciPost Phys.* **7** (2019), no. 4 045, [arXiv:1812.07598].

[45] A. I. Larkin and Y. N. Ovchinnikov, *Quasiclassical Method in the Theory of Superconductivity*, *Soviet Journal of Experimental and Theoretical Physics* **28** (1969) 1200.

[46] A. Almheiri, D. Marolf, J. Polchinski, D. Stanford, and J. Sully, *An Apologia for Firewalls*, *JHEP* **09** (2013) 018, [arXiv:1304.6483].

[47] V. Khemani, D. A. Huse, and A. Nahum, *Velocity-dependent Lyapunov exponents in many-body quantum, semiclassical, and classical chaos*, *Phys. Rev. B* **98** (2018), no. 14 144304, [arXiv:1803.05902].

[48] S. Xu and B. Swingle, *Accessing scrambling using matrix product operators*, *Nature Phys.* **16** (2019), no. 2 199–204, [arXiv:1802.00801].

[49] R. J. Deissler, *One-dimensional strings, random fluctuations, and complex chaotic structures*, *Physics Letters A* **100** (1984), no. 9 451 – 454.

[50] K. Kaneko, *Lyapunov analysis and information flow in coupled map lattices*, *Physica D: Nonlinear Phenomena* **23** (1986), no. 1 436 – 447.

[51] R. J. Deissler and K. Kaneko, *Velocity-dependent lyapunov exponents as a measure of chaos for open-flow systems*, *Physics Letters A* **119** (1987), no. 8 397 – 402.

[52] D. A. Roberts and B. Swingle, *Lieb-robinson bound and the butterfly effect in quantum field theories*, *Physical Review Letters* **117** (2016), no. 9.

[53] C. G. Callan, *Broken scale invariance in scalar field theory*, *Phys. Rev. D* **2** (1970) 1541–1547.

[54] K. Symanzik, *Small distance behavior in field theory and power counting*, *Commun. Math. Phys.* **18** (1970) 227–246.

[55] L. P. Kadanoff, *Scaling laws for ising models near T_c*, *Physics Physique Fizika* **2** (1966) 263–272.

[56] K. G. Wilson, *The renormalization group: Critical phenomena and the kondo problem*, *Rev. Mod. Phys.* **47** (1975) 773–840.

[57] K. G. Wilson, *Renormalization group and critical phenomena. i. renormalization group and the kadanoff scaling picture*, *Phys. Rev. B* **4** (1971) 3174–3183.

[58] K. G. Wilson, *Renormalization group and critical phenomena. ii. phase-space cell analysis of critical behavior*, *Phys. Rev. B* **4** (1971) 3184–3205.

[59] K. G. Wilson and M. E. Fisher, *Critical exponents in 3.99 dimensions*, *Phys. Rev. Lett.* **28** (1972) 240–243.

[60] A. J. D. Chruscinski, *Geometric Phases in Classical and Quantum Mechanics*. Birhauser Basel, 2004.

[61] J. P. Provost and G. Valle, *Riemannian structure on manifolds of quantum states*, *Commun. Math. Phys.* **76** (1980) 289–301.

[62] S.-J. GU, *Fidelity approach to quantum phase transitions*, *International Journal of Modern Physics B* **24** (2010), no. 23 4371–4458.

[63] A. Carollo, D. Valenti, and B. Spagnolo, *Geometry of quantum phase transitions*, *Phys. Rept.* **838** (2020) 1–72, [arXiv:1911.10196].

[64] J. Eisert, M. Cramer, and M. Plenio, *Area laws for the entanglement entropy - a review*, *Rev. Mod. Phys.* **82** (2010) 277–306, [arXiv:0808.3773].

[65] A. Osterloh, L. Amico, G. Falci, and R. Fazio, *Scaling of entanglement close to a quantum phase transition*, *Nature* **416** (2002), no. 6881 608–610.

[66] G. Vidal, J. I. Latorre, E. Rico, and A. Kitaev, *Entanglement in quantum critical phenomena*, *Physical Review Letters* **90** (2003), no. 22.

[67] C. Holzhey, F. Larsen, and F. Wilczek, *Geometric and renormalized entropy in conformal field theory*, *Nucl. Phys. B* **424** (1994) 443–467, [hep-th/9403108].

[68] P. Calabrese and J. L. Cardy, *Entanglement entropy and quantum field theory*, *J. Stat. Mech.* **0406** (2004) P06002, [hep-th/0405152].

[69] Y. Nakayama, *Scale invariance vs conformal invariance*, *Phys. Rept.* **569** (2015) 1–93, [arXiv:1302.0884].

[70] P. M. P. Francesco and D. Sénéchal, *Conformal Field Theory*. Springer-Verlag New York, 1997.

[71] A. Zamolodchikov, *Renormalization Group and Perturbation Theory Near Fixed Points in Two-Dimensional Field Theory*, *Sov. J. Nucl. Phys.* **46** (1987) 1090.

[72] J. Cardy, *Scaling and Renormalization in Statistical Physics*. Cambridge University Press, 1996.

[73] D. Harlow, *TASI Lectures on the Emergence of Bulk Physics in AdS/CFT*, *PoS* **TASI2017** (2018) 002, [arXiv:1802.01040].

[74] I. Heemskerk, J. Penedones, J. Polchinski, and J. Sully, *Holography from Conformal Field Theory*, *JHEP* **10** (2009) 079, [arXiv:0907.0151].

[75] E. Witten, *Anti-de Sitter space and holography*, *Adv. Theor. Math. Phys.* **2** (1998) 253–291, [hep-th/9802150].

[76] S. H. Shenker and D. Stanford, *Multiple Shocks*, *JHEP* **12** (2014) 046, [arXiv:1312.3296].

[77] S. H. Shenker and D. Stanford, *Black holes and the butterfly effect*, *Journal of High Energy Physics* **2014** (2014), no. 3.

[78] D. A. Roberts, D. Stanford, and L. Susskind, *Localized shocks*, *JHEP* **03** (2015) 051, [arXiv:1409.8180].

[79] S. H. Shenker and D. Stanford, *Stringy effects in scrambling*, arXiv:1412.6087.

[80] J. Maldacena, S. H. Shenker, and D. Stanford, *A bound on chaos*, *Journal of High Energy Physics* **2016** (2016), no. 8.

[81] L. Bombelli, R. K. Koul, J. Lee, and R. D. Sorkin, *Quantum source of entropy for black holes*, *Phys. Rev. D* **34** (1986) 373–383.

[82] M. Srednicki, *Entropy and area*, *Phys. Rev. Lett.* **71** (1993) 666–669.

[83] R. Bousso, *The Holographic principle*, *Rev. Mod. Phys.* **74** (2002) 825–874, [hep-th/0203101].

[84] V. E. Hubeny, M. Rangamani, and T. Takayanagi, *A covariant holographic entanglement entropy proposal*, *Journal of High Energy Physics* **2007** (2007), no. 07 062–062.

[85] A. Lewkowycz and J. Maldacena, *Generalized gravitational entropy*, *JHEP* **08** (2013) 090, [arXiv:1304.4926].

[86] X. Dong, A. Lewkowycz, and M. Rangamani, *Deriving covariant holographic entanglement*, *JHEP* **11** (2016) 028, [arXiv:1607.07506].

[87] T. Faulkner, F. M. Haehl, E. Hijano, O. Parrikar, C. Rabideau, and M. Van Raamsdonk, *Nonlinear Gravity from Entanglement in Conformal Field Theories*, *JHEP* **08** (2017) 057, [arXiv:1705.03026].

[88] M. Botta-Cantcheff, P. Martínez, and G. A. Silva, *On excited states in real-time AdS/CFT*, *JHEP* **02** (2016) 171, [arXiv:1512.07850].

[89] D. Marolf, O. Parrikar, C. Rabideau, A. Izadi Rad, and M. Van Raamsdonk, *From Euclidean Sources to Lorentzian Spacetimes in Holographic Conformal Field Theories*, *JHEP* **06** (2018) 077, [arXiv:1709.10101].

[90] M. A. Nielsen, *A geometric approach to quantum circuit lower bounds*, quant-ph/0502070.

[91] M. A. Nielsen, *Quantum computation as geometry*, *Science* **311** (2006), no. 5764 1133–1135.

[92] T. Kibble, *Topology of Cosmic Domains and Strings*, *J. Phys. A* **9** (1976) 1387–1398.

[93] W. Zurek, *Cosmological Experiments in Superfluid Helium?*, *Nature* **317** (1985) 505–508.

[94] J. Dziarmaga, *Dynamics of a quantum phase transition: Exact solution of the quantum ising model*, *Phys. Rev. Lett.* **95** (2005) 245701.

[95] A. Polkovnikov, *Universal adiabatic dynamics in the vicinity of a quantum critical point*, *Phys. Rev. B* **72** (2005) 161201.

[96] W. H. Zurek, U. Dorner, and P. Zoller, *Dynamics of a quantum phase transition*, *Phys. Rev. Lett.* **95** (2005) 105701.

[97] F. Liu, S. Whitsitt, J. B. Curtis, R. Lundgren, P. Titum, Z.-C. Yang, J. R. Garrison, and A. V. Gorshkov, *Circuit complexity across a topological phase transition*, *Physical Review Research* **2** (2020), no. 1.

[98] Z. Xiong, D.-X. Yao, and Z. Yan, *Nonanalyticity of circuit complexity across topological phase transitions*, *Phys. Rev. B* **101** (2020) 174305.

[99] N. Jaiswal, M. Gautam, and T. Sarkar, *Complexity and information geometry in spin chains*, arXiv:2005.03532.

[100] D. Stanford and L. Susskind, *Complexity and Shock Wave Geometries*, *Phys. Rev. D* **90** (2014), no. 12 126007, [arXiv:1406.2678].

[101] A. R. Brown, D. A. Roberts, L. Susskind, B. Swingle, and Y. Zhao, *Holographic Complexity Equals Bulk Action?*, *Phys. Rev. Lett.* **116** (2016), no. 19 191301, [arXiv:1509.07876].

[102] R. Jefferson and R. C. Myers, *Circuit complexity in quantum field theory*, *JHEP* **10** (2017) 107, [arXiv:1707.08570].

[103] P. Caputa and J. M. Magan, *Quantum Computation as Gravity*, *Phys. Rev. Lett.* **122** (2019), no. 23 231302, [arXiv:1807.04422].

[104] V. Balasubramanian, M. Decross, A. Kar, and O. Parrikar, *Quantum Complexity of Time Evolution with Chaotic Hamiltonians*, *JHEP* **01** (2020) 134, [arXiv:1905.05765].

[105] A. Polkovnikov, K. Sengupta, A. Silva, and M. Vengalattore, *Colloquium: Nonequilibrium dynamics of closed interacting quantum systems*, *Reviews of Modern Physics* **83** (2011), no. 3 863–883.

[106] A. Mitra, *Quantum quench dynamics*, *Annual Review of Condensed Matter Physics* **9** (2018), no. 1 245–259.

[107] D. W. Alves and G. Camilo, *Evolution of complexity following a quantum quench in free field theory*, *JHEP* **06** (2018) 029, [arXiv:1804.00107].

[108] H. A. Camargo, P. Caputa, D. Das, M. P. Heller, and R. Jefferson, *Complexity as a novel probe of quantum quenches: universal scalings and purifications*, *Phys. Rev. Lett.* **122** (2019), no. 8 081601, [arXiv:1807.07075].

[109] S. Liu, *Complexity and scaling in quantum quench in* $1+1$ *dimensional fermionic field theories*, *JHEP* **07** (2019) 104, [arXiv:1902.02945].

[110] T. Ali, A. Bhattacharyya, S. S. Haque, E. H. Kim, and N. Moynihan, *Post-quench evolution of distance and uncertainty in a topological system: Complexity, entanglement and revivals*, arXiv:1811.05985.

[111] A. Eckardt, *Colloquium: Atomic quantum gases in periodically driven optical lattices*, *Reviews of Modern Physics* **89** (2017), no. 1.

[112] T. Oka and S. Kitamura, *Floquet engineering of quantum materials*, *Annual Review of Condensed Matter Physics* **10** (2019), no. 1 387–408.

[113] H. Lignier, C. Sias, D. Ciampini, Y. Singh, A. Zenesini, O. Morsch, and E. Arimondo, *Dynamical control of matter-wave tunneling in periodic potentials*, *Phys. Rev. Lett.* **99** (2007) 220403.

[114] N. H. Lindner, G. Refael, and V. Galitski, *Floquet topological insulator in semiconductor quantum wells*, *Nature Physics* **7** (2011), no. 6 490–495.

[115] G. Jotzu, M. Messer, R. Desbuquois, M. Lebrat, T. Uehlinger, D. Greif, and T. Esslinger, *Experimental realization of the topological haldane model with ultracold fermions*, *Nature* **515** (2014), no. 7526 237–240.

[116] V. Mukherjee and A. Dutta, *Effects of interference in the dynamics of a spin- 1/2 transversexychain driven periodically through quantum critical points*, *Journal of Statistical Mechanics: Theory and Experiment* **2009** (2009), no. 05 P05005.

[117] A. Das, *Exotic freezing of response in a quantum many-body system*, *Physical Review B* **82** (2010), no. 17.

[118] A. Russomanno, A. Silva, and G. E. Santoro, *Periodic steady regime and interference in a periodically driven quantum system*, *Physical Review Letters* **109** (2012), no. 25.

[119] V. M. Bastidas, C. Emary, G. Schaller, and T. Brandes, *Nonequilibrium quantum phase transitions in the ising model*, *Physical Review A* **86** (2012), no. 6.

[120] D. H. Dunlap and V. M. Kenkre, *Dynamic localization of a charged particle moving under the influence of an electric field*, *Phys. Rev. B* **34** (1986) 3625–3633.

[121] F. Grossmann, T. Dittrich, P. Jung, and P. Hänggi, *Coherent destruction of tunneling*, *Phys. Rev. Lett.* **67** (1991) 516–519.

[122] E. Kierig, U. Schnorrberger, A. Schietinger, J. Tomkovic, and M. K. Oberthaler, *Single-Particle Tunneling in Strongly Driven Double-Well Potentials*, *Phys. Rev. Lett.* **100** (2008), no. 19 190405, [arXiv:0803.1406].

[123] A. Eckardt, C. Weiss, and M. Holthaus, *Superfluid-Insulator Transition in a Periodically Driven Optical Lattice*, *Phys. Rev. Lett.* **95** (2005), no. 26 260404, [cond-mat/0601020].

[124] M. Sillanpää, T. Lehtinen, A. Paila, Y. Makhlin, and P. Hakonen, *Continuous-Time Monitoring of Landau-Zener Interference in a Cooper-Pair Box*, *Phys. Rev. Lett.* **96** (2006), no. 18 187002, [cond-mat/0510559].

[125] E. Lieb, T. Schultz, and D. Mattis, *Two soluble models of an antiferromagnetic chain*, *Annals of Physics* **16** (1961), no. 3 407 – 466.

[126] S. Bhattacharyya, A. Das, and S. Dasgupta, *Transverse ising chain under periodic instantaneous quenches: Dynamical many-body freezing and emergence of slow solitary oscillations*, *Physical Review B* **86** (2012), no. 5.

[127] G. Floquet, *Sur les équations différentielles linéaires à coefficients périodiques*, *Annales scientifiques de l'École Normale Supérieure* **2e série, 12** (1883) 47–88.

[128] J. H. Shirley, *Solution of the schrödinger equation with a hamiltonian periodic in time*, *Phys. Rev.* **138** (1965) B979–B987.

[129] S. Ashhab, J. R. Johansson, A. M. Zagoskin, and F. Nori, *Two-level systems driven by large-amplitude fields*, *Physical Review A* **75** (2007), no. 6.

[130] Q. Xie and W. Hai, *Analytical results for a monochromatically driven two-level system*, *Phys. Rev. A* **82** (2010) 032117.

[131] T. Mikami, S. Kitamura, K. Yasuda, N. Tsuji, T. Oka, and H. Aoki, *Brillouin-wigner theory for high-frequency expansion in periodically driven systems: Application to floquet topological insulators*, *Phys. Rev. B* **93** (2016) 144307.

[132] E. Barouch, B. M. McCoy, and M. Dresden, *Statistical mechanics of the xy model. i*, *Phys. Rev. A* **2** (1970) 1075–1092.

[133] M. Heyl, *Dynamical quantum phase transitions: a review*, *Reports on Progress in Physics* **81** (2018), no. 5 054001.

[134] K. Yang, L. Zhou, W. Ma, X. Kong, P. Wang, X. Qin, X. Rong, Y. Wang, F. Shi, J. Gong, and et al., *Floquet dynamical quantum phase transitions*, *Physical Review B* **100** (2019), no. 8.

[135] V. Gritsev and A. Polkovnikov, *Integrable floquet dynamics*, *SciPost Physics* **2** (2017), no. 3.

[136] L. Zhang, V. Khemani, and D. A. Huse, *A floquet model for the many-body localization transition*, *Physical Review B* **94** (2016), no. 22.

[137] G. Camilo and D. Teixeira, *Complexity and dynamical quantum phase transitions*, *To appear soon* (2021).

[138] H. T. Quan, Z. Song, X. F. Liu, P. Zanardi, and C. P. Sun, *Decay of loschmidt echo enhanced by quantum criticality*, *Phys. Rev. Lett.* **96** (2006) 140604.

[139] G. Kells, D. Sen, J. K. Slingerland, and S. Vishveshwara, *Topological blocking in quantum quench dynamics*, *Phys. Rev. B* **89** (2014) 235130.

[140] M. Heyl, A. Polkovnikov, and S. Kehrein, *Dynamical quantum phase transitions in the transverse-field ising model*, *Phys. Rev. Lett.* **110** (2013) 135704.

[141] N. Sedlmayr, P. Jaeger, M. Maiti, and J. Sirker, *Bulk-boundary correspondence for dynamical phase transitions in one-dimensional topological insulators and superconductors*, *Phys. Rev. B* **97** (2018) 064304.

[142] H. Araki and E. H. Lieb, *Entropy inequalities*, *Communications in Mathematical Physics* **18** (1970), no. 2 160–170.

[143] A. Polkovnikov, K. Sengupta, A. Silva, and M. Vengalattore, *Colloquium: Nonequilibrium dynamics of closed interacting quantum systems*, *Rev. Mod. Phys.* **83** (2011) 863–883.

[144] T. Langen, R. Geiger, and J. Schmiedmayer, *Ultracold atoms out of equilibrium*, *Annual Review of Condensed Matter Physics* **6** (2015), no. 1 201–217, [https://doi.org/10.1146/annurev-conmatphys-031214-014548].

[145] R. Nandkishore and D. A. Huse, *Many-body localization and thermalization in quantum statistical mechanics*, *Annual Review of Condensed Matter Physics* **6** (2015), no. 1 15–38, [https://doi.org/10.1146/annurev-conmatphys-031214-014726].

[146] C. Gogolin and J. Eisert, *Equilibration, thermalisation, and the emergence of statistical mechanics in closed quantum systems*, *Reports on Progress in Physics* **79** (2016), no. 5 056001.

[147] P. Calabrese and J. Cardy, *Evolution of entanglement entropy in one-dimensional systems*, *Journal of Statistical Mechanics: Theory and Experiment* **2005** (2005), no. 04 P04010.

[148] J. Eisert and T. J. Osborne, *General entanglement scaling laws from time evolution*, *Phys. Rev. Lett.* **97** (2006) 150404.

[149] P. Calabrese and J. Cardy, *Quantum quenches in 1+1 dimensional conformal field theories*, *Journal of Statistical Mechanics: Theory and Experiment* **2016** (2016), no. 6 064003.

[150] E. A. Carlen and E. H. Lieb, *Bounds for entanglement via an extension of strong subadditivity of entropy*, *Letters in Mathematical Physics* **101** (2012), no. 1 1–11.

[151] D. N. Page, *Average entropy of a subsystem*, *Phys. Rev. Lett.* **71** (1993) 1291–1294.

[152] B. Bertini, P. Kos, and T. Prosen, *Entanglement spreading in a minimal model of maximal many-body quantum chaos*, *Physical Review X* **9** (2019), no. 2.

[153] D. Berenstein, *A toy model for time evolving qft on a lattice with controllable chaos*, arXiv:1803.02396.

[154] S. Gopalakrishnan and B. Zakirov, *Facilitated quantum cellular automata as simple models with nonthermal eigenstates and dynamics*, arXiv:1802.07729.

[155] H. Liu and S. J. Suh, *Entanglement tsunami: Universal scaling in holographic thermalization*, *Physical Review Letters* **112** (2014), no. 1.

[156] H. Casini, H. Liu, and M. Mezei, *Spread of entanglement and causality*, *Journal of High Energy Physics* **2016** (2016), no. 7.

[157] T. Hartman and N. Afkhami-Jeddi, *Speed limits for entanglement*, arXiv:1512.02695.

[158] J. S. Cotler, G. Gur-Ari, M. Hanada, J. Polchinski, P. Saad, S. H. Shenker, D. Stanford, A. Streicher, and M. Tezuka, *Black Holes and Random Matrices*, *JHEP* **05** (2017) 118, [arXiv:1611.04650]. [Erratum: JHEP 09, 002 (2018)].

[159] S. Sachdev, *Bekenstein-Hawking Entropy and Strange Metals*, *Phys. Rev. X* **5** (2015), no. 4 041025, [arXiv:1506.05111].

[160] R. A. Davison, W. Fu, A. Georges, Y. Gu, K. Jensen, and S. Sachdev, *Thermoelectric transport in disordered metals without quasiparticles: The Sachdev-Ye-Kitaev models and holography*, *Phys. Rev. B* **95** (2017), no. 15 155131, [arXiv:1612.00849].

[161] Y. Gu, X.-L. Qi, and D. Stanford, *Local criticality, diffusion and chaos in generalized Sachdev-Ye-Kitaev models*, *JHEP* **05** (2017) 125, [arXiv:1609.07832].

[162] D. J. Gross and V. Rosenhaus, *A Generalization of Sachdev-Ye-Kitaev*, *JHEP* **02** (2017) 093, [arXiv:1610.01569].

[163] W. Fu, D. Gaiotto, J. Maldacena, and S. Sachdev, *Supersymmetric Sachdev-Ye-Kitaev models*, *Phys. Rev. D* **95** (2017), no. 2 026009, [arXiv:1610.08917]. [Addendum: Phys.Rev.D 95, 069904 (2017)].

[164] E. Witten, *An SYK-Like Model Without Disorder*, *J. Phys. A* **52** (2019), no. 47 474002, [arXiv:1610.09758].

[165] E. P. Wigner, *Gruppentheorie und ihre Anwen-dung auf die Quanten mechanik der Atomspektren*. Friedrich Vieweg und Sohn, 1931.

[166] M. Lawson, *Inverse Semigroups: The Theory of Partial Symmetries*. World Scientific, 1998.

[167] J. Kellendonk and M. V. Lawson, *Tiling semigroups*, *Journal of Algebra* **224** (2000), no. 1 140 – 150.

[168] P. J. S. D. P. Di Vincenzo, *Quasicrystals: The State of Art*. World Scientific, 1991.

[169] C. Janot, *Quasicrystals - A Primer*. Clarendon, 1992.

[170] M. Senechal, *Quasicrystals and Geometry*. Cambridge University Press, 1995.

[171] B. Unal, V. Fournée, K. J. Schnitzenbaumer, C. Ghosh, C. J. Jenks, A. R. Ross, T. A. Lograsso, J. W. Evans, and P. A. Thiel, *Nucleation and growth of ag islands on fivefold al-pd-mn quasicrystal surfaces: Dependence of island density on temperature and flux*, *Phys. Rev. B* **75** (2007) 064205.

[172] R. Exel, D. G. calves, and C. Starling, *The tiling c*-algebra viewed as a tight inverse semigroup algebra*, arXiv:1106.4535.

[173] J. Kellendonk, *The local structure of tilings and their integer group of coinvariants*, *Communications in Mathematical Physics* **187** (1997), no. 1 115–157.

[174] J. Kellendonk, *Topological equivalence of tilings*, *Journal of Mathematical Physics* **38** (1997), no. 4 1823–1842.

[175] D. Damanik, A. Gorodetski, and W. Yessen, *The fibonacci hamiltonian*, *Inventiones mathematicae* **206** (2016), no. 3 629–692.

[176] J. Bellissard, A. Bovier, and J.-M. Ghez, *Gap labeling theorems for one-dimensional discrete Schrodinger operators*, *Rev. Math. Phys.* **4** (1992) 1–38.

[177] J. KELLENDONK, *Noncommutative geometry of tilings and gap labelling*, *Reviews in Mathematical Physics* **07** (1995), no. 07 1133–1180.

[178] V. V. Wager, *The theory of generalised heaps and generalised groups*, *Matematicheskii Sbornik* **32** 545–632.

[179] G. B. Preston, *Representations of inverse semi-groups*, *J. London Math. Soc.* **29** 411–419.

[180] Y. Golfand and E. Likhtman, *Extension of the Algebra of Poincare Group Generators and Violation of p Invariance*, *JETP Lett.* **13** (1971) 323–326.

[181] P. Ramond, *Dual Theory for Free Fermions*, *Phys. Rev. D* **3** (1971) 2415–2418.

[182] A. Neveu and J. Schwarz, *Factorizable dual model of pions*, *Nucl. Phys. B* **31** (1971) 86–112.

[183] D. Volkov and V. Akulov, *Is the Neutrino a Goldstone Particle?*, *Phys. Lett. B* **46** (1973) 109–110.

[184] J. Wess and B. Zumino, *Supergauge Transformations in Four-Dimensions*, *Nucl. Phys. B* **70** (1974) 39–50.

[185] M. Sohnius, *Introducing Supersymmetry*, *Phys. Rept.* **128** (1985) 39–204.

[186] E. Witten, *Dynamical Breaking of Supersymmetry*, *Nucl. Phys. B* **188** (1981) 513.

[187] F. Cooper and B. Freedman, *Aspects of Supersymmetric Quantum Mechanics*, *Annals Phys.* **146** (1983) 262.

[188] F. Cooper, A. Khare, and U. Sukhatme, *Supersymmetry and quantum mechanics*, *Physics Reports* **251** (1995), no. 5-6 267–385.

[189] E. Witten, *Constraints on Supersymmetry Breaking*, *Nucl. Phys. B* **202** (1982) 253.

[190] O. Buerschaper, J. M. Mombelli, M. Christandl, and M. Aguado, *A hierarchy of topological tensor network states*, *Journal of Mathematical Physics* **54** (2013), no. 1 012201.

[191] X. Chen, Z.-C. Gu, Z.-X. Liu, and X.-G. Wen, *Symmetry protected topological orders and the group cohomology of their symmetry group*, *Physical Review B* **87** (2013), no. 15.

[192] M. J. B. Ferreira, P. Padmanabhan, and P. Teotonio-Sobrinho, *2d quantum double models from a 3d perspective*, *Journal of Physics A: Mathematical and Theoretical* **47** (2014), no. 37 375204.

[193] M. F. Atiyah and I. M. Singer, *The index of elliptic operators on compact manifolds*, *Bull. Amer. Math. Soc.* **69** (1963), no. 3 422–433.

[194] M. Atiyah, R. Bott, and V. Patodi, *On the Heat equation and the index theorem*, *Invent. Math.* **19** (1973) 279–330.

[195] R. Melrose, *The Atiyah-Patodi-Singer Index Theorem*. Taylor and Francis, 1993.

[196] F. Gesztesy and B. Simon, *Topological invariance of the witten index*, *Journal of Functional Analysis* **79** (1988), no. 1 91–102.

[197] K. Aghababaei Samani and A. Mostafazadeh, *Quantum mechanical symmetries and topological invariants*, *Nuclear Physics B* **595** (2001), no. 1-2 467–492.

[198] S. M. Girvin, A. H. MacDonald, M. P. A. Fisher, S.-J. Rey, and J. P. Sethna, *Exactly soluble model of fractional statistics*, *Phys. Rev. Lett.* **65** (1990) 1671–1674.

[199] G. Junker, *Supersymmetric Methods in Quantum and Statistical Physics*. Springer-Verlag Berlin Heidelberg, 1996.

[200] H. Nicolai, *Supersymmetry and Spin Systems*, *J. Phys. A* **9** (1976) 1497–1506.

[201] H. Moriya, *On supersymmetric fermion lattice systems*, 2015.

[202] P. Dondi and H. Nicolai, *Lattice Supersymmetry*, *Nuovo Cim. A* **41** (1977) 1.

[203] C. Hagendorf, *Spin chains with dynamical lattice supersymmetry*, *Journal of Statistical Physics* **150** (2013), no. 4 609–657.

[204] N. Ilieva, H. Narnhofer, and W. Thirring, *Supersymmetric models for fermions on a lattice*, *Fortschritte der Physik* **54** (2006), no. 2-3 124–138.

[205] J. de Gier, G. Z. Feher, B. Nienhuis, and M. Rusaczonek, *Integrable supersymmetric chain without particle conservation*, arXiv:1510.02520.

[206] H. Saleur and N. Warner, *Lattice models and N=2 supersymmetry*, hep-th/9311138.

[207] P. Fendley, B. Nienhuis, and K. Schoutens, *Lattice fermion models with supersymmetry*, *Journal of Physics A: Mathematical and General* **36** (2003), no. 50 12399–12424.

[208] L. Huijse and B. Swingle, *Area law violations in a supersymmetric model*, *Physical Review B* **87** (2013), no. 3.

[209] P. Hosur, X.-L. Qi, D. A. Roberts, and B. Yoshida, *Chaos in quantum channels*, *Journal of High Energy Physics* **2016** (2016), no. 2.

[210] Y. Sekino and L. Susskind, *Fast scramblers*, *Journal of High Energy Physics* **2008** (2008), no. 10 065–065.

[211] M. Srednicki, *Chaos and quantum thermalization*, *Physical Review E* **50** (1994), no. 2 888–901.

[212] P. W. Anderson, *Absence of diffusion in certain random lattices*, *Phys. Rev.* **109** (1958) 1492–1505.

[213] R. Nandkishore and D. A. Huse, *Many-body localization and thermalization in quantum statistical mechanics*, *Annual Review of Condensed Matter Physics* **6** (2015), no. 1 15–38.

[214] B. Swingle and D. Chowdhury, *Slow scrambling in disordered quantum systems*, *Physical Review B* **95** (2017), no. 6.

[215] R. Fan, P. Zhang, H. Shen, and H. Zhai, *Out-of-time-order correlation for many-body localization*, *Science Bulletin* **62** (2017), no. 10 707–711.

[216] Y. Huang, Y.-L. Zhang, and X. Chen, *Out-of-time-ordered correlators in many-body localized systems*, *Annalen der Physik* **529** (2016), no. 7 1600318.

[217] Y. Chen, *Universal logarithmic scrambling in many body localization*, arXiv:1608.02765.

[218] X. Chen, T. Zhou, D. A. Huse, and E. Fradkin, *Out-of-time-order correlations in many-body localized and thermal phases*, *Annalen der Physik* **529** (2016), no. 7 1600332.

[219] J. M. Deutsch, *Quantum statistical mechanics in a closed system*, *Phys. Rev. A* **43** (1991) 2046–2049.

[220] H. Tasaki, *From quantum dynamics to the canonical distribution: General picture and a rigorous example*, *Physical Review Letters* **80** (1998), no. 7 1373–1376.

[221] M. Rigol, V. Dunjko, and M. Olshanii, *Thermalization and its mechanism for generic isolated quantum systems*, *Nature* **452** (2008), no. 7189 854–858.

[222] H. Kim, T. N. Ikeda, and D. A. Huse, *Testing whether all eigenstates obey the eigenstate thermalization hypothesis*, *Physical Review E* **90** (2014), no. 5.

[223] E. Altman and R. Vosk, *Universal dynamics and renormalization in many-body-localized systems*, *Annual Review of Condensed Matter Physics* **6** (2015), no. 1 383–409.

[224] M. Serbyn, Z. Papić, and D. A. Abanin, *Local conservation laws and the structure of the many-body localized states*, *Physical Review Letters* **111** (2013), no. 12.

[225] D. A. Huse, R. Nandkishore, and V. Oganesyan, *Phenomenology of fully many-body-localized systems*, *Phys. Rev. B* **90** (2014) 174202.

[226] R. Vosk and E. Altman, *Many-body localization in one dimension as a dynamical renormalization group fixed point*, *Physical Review Letters* **110** (2013), no. 6.

[227] A. Das, *Supersymmetry and finite temperature*, *Physica A: Statistical Mechanics and its Applications* **158** (1989), no. 1 1–21.

[228] S. Iyer, V. Oganesyan, G. Refael, and D. A. Huse, *Many-body localization in a quasiperiodic system*, *Physical Review B* **87** (2013), no. 13.

[229] S. Nag and A. Garg, *Many-body mobility edges in a one-dimensional system of interacting fermions*, *Physical Review B* **96** (2017), no. 6.

[230] S. Aubry and G. André, *Analyticity breaking and anderson localization in incommensurate lattices*, 1980.

[231] W. Fu, D. Gaiotto, J. Maldacena, and S. Sachdev, *Supersymmetric sachdev-ye-kitaev models*, *Physical Review D* **95** (2017), no. 2.

[232] T. Li, J. Liu, Y. Xin, and Y. Zhou, *Supersymmetric syk model and random matrix theory*, *Journal of High Energy Physics* **2017** (2017), no. 6.

[233] L. Faddeev, *How algebraic Bethe ansatz works for integrable model*, in *Les Houches School of Physics: Astrophysical Sources of Gravitational Radiation*, pp. 149–219, 1996. hep-th/9605187.

[234] T. Banks, M. R. Douglas, G. T. Horowitz, and E. J. Martinec, *AdS dynamics from conformal field theory*, hep-th/9808016.

[235] A. Hamilton, D. N. Kabat, G. Lifschytz, and D. A. Lowe, *Local bulk operators in AdS/CFT: A Boundary view of horizons and locality*, *Phys. Rev. D* **73** (2006) 086003, [hep-th/0506118].

[236] A. Hamilton, D. N. Kabat, G. Lifschytz, and D. A. Lowe, *Holographic representation of local bulk operators*, *Phys. Rev. D* **74** (2006) 066009, [hep-th/0606141].

[237] D. Kabat, G. Lifschytz, and D. A. Lowe, *Constructing local bulk observables in interacting AdS/CFT*, *Phys. Rev. D* **83** (2011) 106009, [arXiv:1102.2910].

[238] A. Almheiri, X. Dong, and D. Harlow, *Bulk Locality and Quantum Error Correction in AdS/CFT*, *JHEP* **04** (2015) 163, [arXiv:1411.7041].

[239] E. Mintun, J. Polchinski, and V. Rosenhaus, *Bulk-Boundary Duality, Gauge Invariance, and Quantum Error Corrections*, *Phys. Rev. Lett.* **115** (2015), no. 15 151601, [arXiv:1501.06577].

[240] D. Berenstein and A. Miller, *Reconstructing spacetime from the hologram, even in the classical limit, requires physics beyond the Planck scale*, *Int. J. Mod. Phys. D* **25** (2016), no. 12 1644012, [arXiv:1605.05288].

[241] H. Verlinde, *Poking Holes in AdS/CFT: Bulk Fields from Boundary States*, arXiv:1505.05069.

[242] M. Miyaji, T. Numasawa, N. Shiba, T. Takayanagi, and K. Watanabe, *Continuous Multiscale Entanglement Renormalization Ansatz as Holographic Surface-State Correspondence*, *Phys. Rev. Lett.* **115** (2015), no. 17 171602, [arXiv:1506.01353].

[243] Y. Nakayama and H. Ooguri, *Bulk Locality and Boundary Creating Operators*, *JHEP* **10** (2015) 114, [arXiv:1507.04130].

[244] Y. Nakayama and H. Ooguri, *Bulk Local States and Crosscaps in Holographic CFT*, *JHEP* **10** (2016) 085, [arXiv:1605.00334].

[245] K. Goto and T. Takayanagi, *CFT descriptions of bulk local states in the AdS black holes*, *JHEP* **10** (2017) 153, [arXiv:1704.00053].

[246] N. Anand, H. Chen, A. L. Fitzpatrick, J. Kaplan, and D. Li, *An Exact Operator That Knows Its Location*, *JHEP* **02** (2018) 012, [arXiv:1708.04246].

[247] E. P. R. Blumenhagen, *Introduction to Conformal Field Theory: With Applications to String Theory*. Springer-Verlag Berlin Heidelberg, 2009.

[248] A. Lewkowycz, G. J. Turiaci, and H. Verlinde, *A CFT Perspective on Gravitational Dressing and Bulk Locality*, *JHEP* **01** (2017) 004, [arXiv:1608.08977].

[249] T. T. M. Rangamani, *Holographic Entanglement Entropy*. Springer International Publishing, 2017.

[250] T. De Jonckheere, *Modave lectures on bulk reconstruction in AdS/CFT*, *PoS* **Modave2017** (2018) 005, [arXiv:1711.07787].

[251] M. Nozaki, S. Ryu, and T. Takayanagi, *Holographic Geometry of Entanglement Renormalization in Quantum Field Theories*, *JHEP* **10** (2012) 193, [arXiv:1208.3469].

[252] M. Miyaji, T. Numasawa, N. Shiba, T. Takayanagi, and K. Watanabe, *Distance between Quantum States and Gauge-Gravity Duality*, *Phys. Rev. Lett.* **115** (2015), no. 26 261602, [arXiv:1507.07555].

[253] R. Wald, *General Relativity*. University of Chicago Press, 1984.

[254] R. Arnowitt, S. Deser, and C. W. Misner, *Dynamical structure and definition of energy in general relativity*, *Phys. Rev.* **116** (1959) 1322–1330.

[255] V. Balasubramanian and P. Kraus, *A Stress tensor for Anti-de Sitter gravity*, *Commun. Math. Phys.* **208** (1999) 413–428, [hep-th/9902121].

[256] V. S. A. Recknagel, *Boundary Conformal Field Theory and the Worldsheet Approach to D-branes*. Cambridge University Press, 2013.